MicroRNA-30a Promotes Sprouting Angiogenesis

By Targeting *dll4* And Inhibiting Notch Signaling

Inaugural-Dissertation

to obtain the academic degree

Doctor rerum naturalium (Dr. rer. nat.)

submitted to the Department of Biology, Chemistry and Pharmacy

of Freie Universität Berlin

by

Qiu Jiang (蔣璆)

from Taicang, China

2013

I completed my doctorate studies from July 2010 to May 2013 under the supervision of Prof. Dr. F. le Noble at the Max Delbrück Center for Molecular Medicine, Berlin-Buch.

1st Reviewer: Prof. Dr. Ferdinand le Noble

2nd Reviewer: Prof. Dr. Udo Heinemann

Date of defense: November 21, 2013

Acknowledgements

Table of contents

1   Abstract

Endothelial tip cells in angiogenic sprouts direct branching of vascular networks. Specification of tip cells involves tight spatiotemporal control of Dll4-Notch signaling. MicroRNAs repress gene expression through binding with the 3'UTR of target mRNA. Computational analyses predict a highly conserved interaction of microRNA-30 (miR-30) family members with *dll4*-3'UTR but their contribution in regulating endothelial Dll4 and vascular branching morphogenesis is unknown. Through deep sequencing and functional screening in zebrafish model, we identified endothelial miR-30a as an essential regulator for angiogenesis. The miR-30 family consists of 5 members (miR-30a-e), and loss-of-function approaches in zebrafish embryos showed that only loss of miR-30a significantly reduced sprouting of intersegmental artery sprouts, and impaired tip cell filopodial extensions. Overexpression of miR-30a stimulated angiogenic cell behavior, and hyperbranching of intersegmental artery sprouts. *In vitro* and *in vivo* reporter assays demonstrated that miR-30a directly targets *dll4*, and co-administration of dll4 morpholino in miR-30a morphant embryos rescued branching deficits. Conversely, conditional overactivation of Notch signaling by overexpressing Notch-intracellular domain (NICD) restored vessel branching in miR-30a gain-of-function embryos. Furthermore, in human endothelial cells, loss of miR-30a increased DLL4 protein levels, overactivated NOTCH signaling as indicated in NOTCH reporter assays, and augmented expression of NOTCH downstream effectors *Hey2* and *EFNB2*. In spheroid assays, miR-30a loss-of-function and gain-of-function affected angiogenic cell behavior consistent with miR-30a targeting *DLL4*. Taken together, these findings uncover a novel molecular mechanism that endothelial miR-30a acts as an evolutionarily conserved positive regulator to control angiogenic cell behavior and vessel branching by targeting *dll4* and inhibiting Notch signaling.

2   Zusammenfassung

Die Sproßung von endothelialen Zellen wird durch sogenannte "tip cells" geleitet welche somit das Verzweigungsmuster des Gefäßnetzwerkes bestimmen. Die Spezifizierung der "tip cell" erfolgt durch eine räumliche und zeitliche Regulation des Dll4-Notch-Signalweges. "Micro-RNAs" inhibieren die Genexpression durch Bindung an die 3´-UTR der Ziel-mRNA. *In silico* Analysen weisen auf eine hoch konservierte Interaktion der "micro-RNA" (miR-30) Familie mit der Dll4-3´-UTR hin. Eine Beeinflussung von endothelialem Dll4 und damit einhergehender Regulation der Gefäßmorphogenese ist unbekannt. Durch "deep sequencing" und eines funktionalen Screens im Zebrafischmodel identifizierten wir endotheliale miR-30a als essentiellen Angiogeneseregulator. Die miR-30 Familie besteht aus fünf Mitgliedern (miR-30a-e). Die Depletion dieser zeigte, dass nur der Verlust von miR-30a zu einer signifikanten Reduktion der Sprossung von intersegmentalen Arterien (ISA) führte. Überexpression von miR-30a führte zu einer verstärkten Verzweigung von ISAs. *In vitro* und *in vivo* Reporterassays demonstrierten das miR-30a direkt *dll4* angreift. Eine gleichzeitige Administration von dll4 Morpholino mit miR-30a stellte das normale Verzweigunsmuster von ISAs wieder her. Die Aktivierung des Notchsignalweges durch eine Überexpression der Notch-intrazellulären Domäne stellte einen normalen Gefäßphenotyp in miR-30a überexprimierten Embryonen wieder her. Desweiteren konnte in humanen Endothelzellen gezeigt werden, dass eine miR-30a Defizienz zu erhöhten DLL4 Proteinleveln führt, den Notchsignalweg verstärkt aktiviert und dadurch die Notcheffektoren Hey2 und EFNB2 vermehrt exprimiert werden. In "spheroid-assays" führte miR-30a Überexpression und Depletion zu verändertem Gefäßwachstum, welches konsistent mit einer Interaktion von miR-30a mit DLL4 ist. Zusammengenommen konnten wir einen neuen molekularen Regulationsmechanismus aufzeigen: endotheliale miR-30a ist ein evolutionär konservierter positiver Regulator des Gefäßwachstums, speziell der Gefäßverzweigung, durch Interaktion mit *dll4* und damit einhergehender Inhibierung des Notchsignalweges.

3 Introduction

3.1 Functional role of angiogenesis

Extensive network of blood vessels arose during evolution to nurture almost all tissues by supplying oxygen and nutrients, to provide gateways for immune surveillance, and as well as to remove wastes. Its development and growth proceed via two distinct stages: vasculogenesis and angiogenesis (Figure 1) (Carmeliet and Jain, 2011; Poole and Coffin, 1989; Potente et al., 2011). Vasculogenesis involves the *de novo* formation of embryonic primary arteries and veins. Subsequently, the simple trunk-like vasculature becomes expanded into the elaborate hierarchical vascular network mainly through the angiogenic sprouting of smaller caliber vessels from pre-existing ones, a process named angiogenesis. Actually, the latter process occurs during the entire life of an organism. Furthermore, disruption of the balance in angiogenesis contributes to the pathogenesis of numerous diseases involving angiogenesis (Carmeliet and Jain, 2011). For example, tissue growth and regeneration benefit from new blood vessel formation, and tumor cell-mediated stimulation of angiogenesis fuels tumor growth and progression to metastasis, whereas insufficient angiogenesis limits tissue recovery in ischaemic ailments, such as ischaemic heart disease, stroke, and ischaemic colitis. Given the significant clinical benefits from the tight control of pathological angiogenesis, it is of importance and urgency to better understand the mechanisms underlying this process.

3.2 Cellular and molecular mechanisms of angiogenesis

Angiogenesis is a fundamental, dynamic, and multistep process in health and diseases, involving differentiation, proliferation, sprouting and migration of endothelial cells (ECs) (Potente et al., 2011). Sprouting angiogenesis requires strict orchestration of distinct EC behaviors between the leading tip cells and the trailing stalk cells (Gerhardt et al., 2003). To date, a number of seminal studies have begun to uncover the exquisite molecular mechanisms that regulate key signaling pathways (such as the vascular endothelial growth factor (VEGF) and Notch cascades) to coordinate this process (Herbert and Stainier, 2011; Phng and Gerhardt, 2009; Potente et al., 2011). Here I dissect and introduce the sequential multistep process of blood vessel branching, including sprout initiation, tip and stalk cell selection, sprout elongation, sprouts anastomosis and vascular network formation.
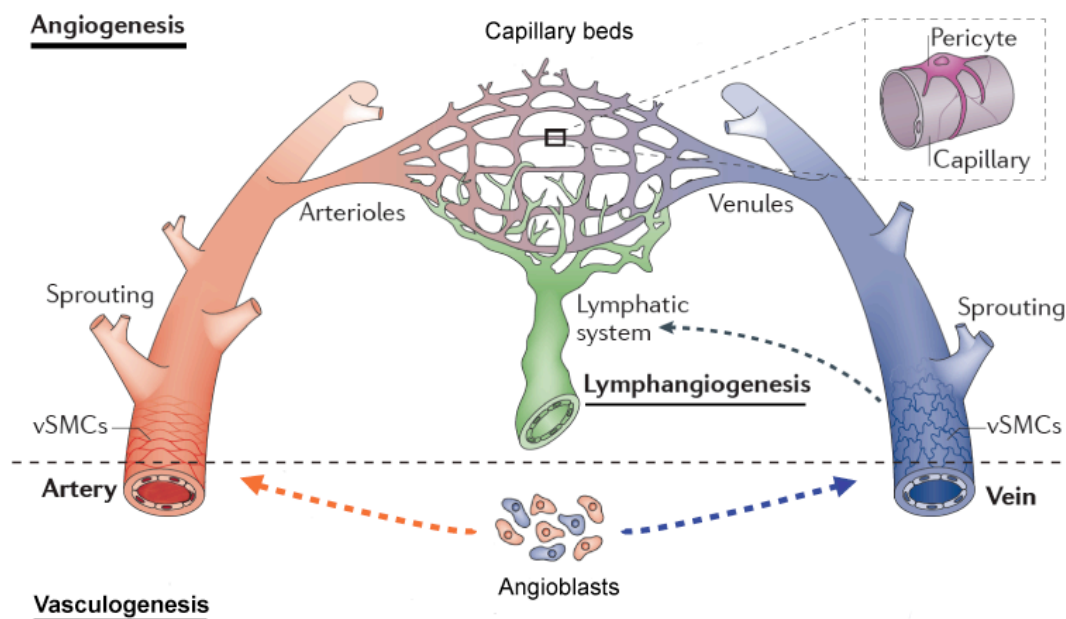
Figure 1. Assembly of the vasculature

Mesoderm-derived cells differentiate into angioblasts (endothelial precursor cells), coalesce to form the vascular cord, and then *de novo* form the embryonic primary arteries (in red) and veins (in blue) in a process termed vasculogenesis.

Subsequently, the simple trunk-like vasculature is progressively expanded into an elaborate hierarchical vascular network of arterioles, capillaries, and venules in a process named angiogenesis. During angiogenesis, endothelial cells (ECs) sprout and branch from pre-existing vessels in response to the pro-angiogenic factors around. Once the newly growing vessels are lumenized and the heart starts beating, blood circulation initiates to be established. Further steps of the vascular tree maturation is featured by the recruitment and attachment of arteries and veins with mural cells, including vascular smooth muscle cells (vSMCs) and pericytes. Similarly, lymphangiogenesis involves sprouting, branching, proliferation, differentiation and remodeling processes. Lymphatic ECs differentiate and sprout from the venous compartment to form the lymphatic network (in green). Adapted from Herbert and Stainier, 2011.

3.2.1 Sprout initiation

Stable blood vessels are lined with a cobblestone-like monolayer of inactive ECs at their luminal surface (Figure 2A) (Mazzone et al., 2009). ECs and mural cells, which include pericytes and vascular smooth muscle cells (vSMCs), share a basement membrane comprised of diverse extracellular matrix (ECM) proteins at the abluminal surface of blood vessels (Davis and Senger, 2005; Eble and Niland, 2009). The ECM scaffolds together with mural cells, take responsibility to prevent escape of resident ECs from blood vessels. Actually, the quiescent state of these ECs is maintained until they respond to pro-angiogenic factors such as VEGFs, which promote liberating ECs by loosening cell-cell junctional contacts and activating proteases that proteolytically break down the surrounding basement membrane (Figure 2B) (Adams and Alitalo, 2007; Carmeliet and Jain, 2011). Specifically, the degradation of basement membrane is tightly orchestrated by endothelial tip cell-enriched matrix metalloproteases (MMPs) and plasminogen activator inhibitors (PAIs) (Blasi and Carmeliet, 2002). During this process, another pro-angiogenic growth factor Angiopoietin 2 (ANG2) is rapidly released from ECs to activate the detachment of their surrounding mural cells by

antagonizing ANG1-Tie2 signaling (Augustin et al., 2009; Huang et al., 2010). Thereby, ECs are liberated from ECM and mural cells, and acquire extensively invasive and motile behavior to initiate angiogenesis.
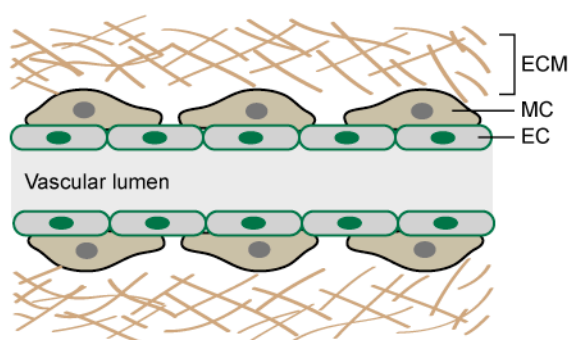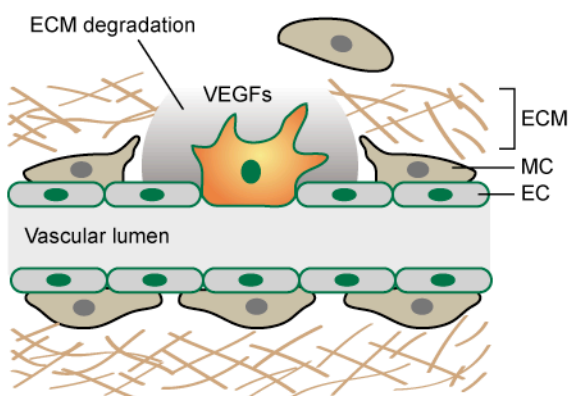
Figure 2. Sprout initiation

(A) Without the stimulation of pro-angiogenic factors, endothelial cells (ECs) are maintained in a quiescent state. The quiescent vessels are characterized by their coverage with mural cells (MCs, such as pericytes) and extracellular matrix (ECM). (B) During sprout initiation of the angiogenic process, a gradient of exogenous pro-angiogenic stimuli (such as VEGFA and VEGFC) and EC-specific VEGF receptors (such as VEGFR2 and VEGFR3) signaling select a subset of ECs (in yellow) for sprouting. Sprouting behavior is facilitated through loosening of EC-EC junctions, ECM degradation, and pericyte detachment.

3.2.2 Tip and stalk cell selection

Of the ECs that are exposed to pro-angiogenic stimuli, only a small fraction will be selected to become the leading cells that guide the newly sprouting vessels (Figure 3). These leading ECs, termed tip cells, display their default cellular behavior when exposed to pro-angiogenic signals, extending numerous dynamic filopodial protrusions that respond to attractive and repulsive guidance cues within the surrounding microenvironment (De Smet et al., 2009; Gerhardt et al., 2003). In contrast, ECs trailing the tip cells are named stalk cells, which exhibit less invasive and motile behavior but critically maintain the connection between the leading tip cell and the patent vascular system. Mechanistically, an exquisite feedback loop between VEGF signaling and Delta-like 4 (Dll4)-Notch signaling promotes the specification of ECs into tip and stalk cells in a single newly sprouting vessel (Figure 3) (Eilken and Adams, 2010; Phng and Gerhardt, 2009). Specifically, exposed to the principal attractive guidance factor VEGFA, a small proportion of ECs extend numerous filopodia and are activated via VEGFA-VEGFR2-mediated signaling. In these activated endothelial tip cells, VEGFR2 (also known as Flk1, or Kdr) activation induces the Notch ligand Dll4 expression, which activates Notch signaling in adjacent stalk cells. Subsequently, activated Notch signaling in stalk cells downregulates the VEGFR2 and VEGFR3 (also known as Flt4) expressions and expands the expression of VEGFR1 (also named Flt1), which acts as the VEGFA decoy receptor to re-shape the gradient of local VEGFA to suppress VEGFA-VEGFR2 interaction and function, and eventually blocks their tip cell behavior.

3.2.3 Sprout elongation

Tip cell, after its apical dominance has been temporarily confirmed, guides the newly sprouting vessel to grow towards a correct direction which is formed by a combination of gradients of attractive and repulsive guidance cues such as

VEGFs (Gerhardt et al., 2003). Sprout elongation involves a series of events including sprout guidance and EC proliferation of the newly growing vessels (Figure 4).
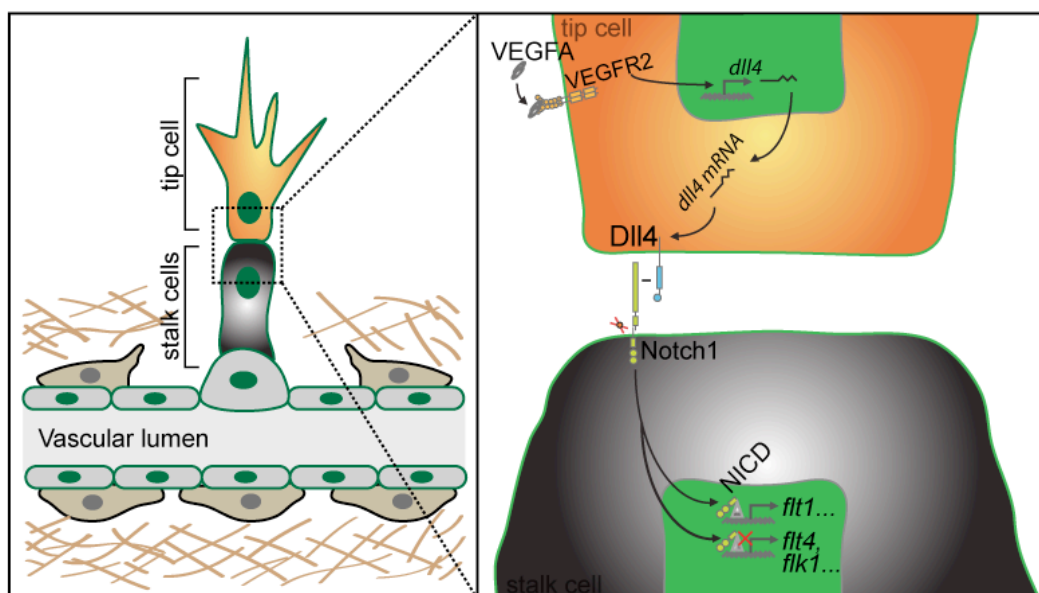
Figure 3. Tip and stalk cell selection

Endothelial cells (ECs) of the emerging sprout are hierarchically organized into the leading tip cell and the trailing stalk cells that assume distinct cell behaviors. The leading EC is induced by vascular endothelial growth factor (VEGF) signaling to form the tip cell exhibiting numerous filopodial extensions, whereas Dll4-Notch signaling suppresses VEGF signaling and tip cell behavior and fate in the following stalk cells. Specifically, activation of VEGF receptor 2 (VEGFR2, also known as Flk1) induces the Notch ligand Dll4 expression in tip cell, which activates Notch receptor on adjacent stalk cells. Notch activation in stalk cells downregulates VEGFR2 and VEGFR3 (also known as Flt4) expression and upregulates the expression of VEGFR1 (also named Flt1), which inhibits VEGFR2 function by competitively binding to VEGFA and represses tip cell behavior.

During the subsequent growth of new sprouts, the first important event is to tightly control the direction of angiogenic sprout elongation. Actually, the

8

VEGFA-VEGFR2 interaction level is considered to be the most efficient "positive energy" for sprout guidance. Previous findings described two strategies to control the level of VEGFA-VEGFR2 interaction. As mentioned above, activation of Notch signaling in stalk cells promotes the expression of membrane-associated VEGFR1 and soluble VEGFR1, which lead to a local reduction of VEGFA through membrane-bound VEGFR1-mediated trapping of VEGFA and soluble VEGFR1-mediated arresting of VEGFA locally outside of stalk cells (Geudens and Gerhardt, 2011). Thereby, an effective gradient of VEGFA-VEGFR2 interaction is created: much more VEGFA-VEGFR2 interaction happening on the tip cell membrane of the emerging vessel and relatively less interaction occurring on the adjacent stalk cells membrane (Figure 4). This pattern of VEGFA-VEGFR2 interaction efficiently optimizes the spreading of the vascular network, and successfully avoids the premature contact with nearby developing sprouts (Geudens and Gerhardt, 2011). However, the concept of stable tip and stalk cell selection was challenged by the recent time-lapse imaging studies indicating a dynamic shuffling of tip and stalk cells, which probably contributes to the real-time evaluation of the VEGF and Dll4-Notch signaling loop at the leading front of developing sprouts (Geudens and Gerhardt, 2011; Jakobsson et al., 2010). Neighboring ECs of growing vessels compete for the tip cell position based on their relative level of VEGFA-VEGFR2 interaction and the resulting expression level of Dll4. Specifically, differential levels of VEGFA-VEGFR2 activities between the neighboring ECs support an EC with higher VEGFA-VEGFR2 activities and Dll4 expression level to prevent its neighboring ECs with relatively lower VEGFA-VEGFR2 activities from becoming tip cells via Dll4-Notch signaling-mediated lateral inhibition.

In addition, EC proliferation and migration are essential for the sustained elongation of a newly growing sprout. Endothelial stalk cells assume much stronger proliferative behaviors than its neighboring tip cell does, and the sprouts grow through proliferation of the stalk cells as the tip cells guide and migrate

(Figure 4A) (Gerhardt et al., 2003). However, recent studies in zebrafish model demonstrated that the leading tip cells of intersegmental vessel (ISV) sprouts exhibit both migration and proliferation (Figure 4B) (Blum et al., 2008; Siekmann and Lawson, 2007).
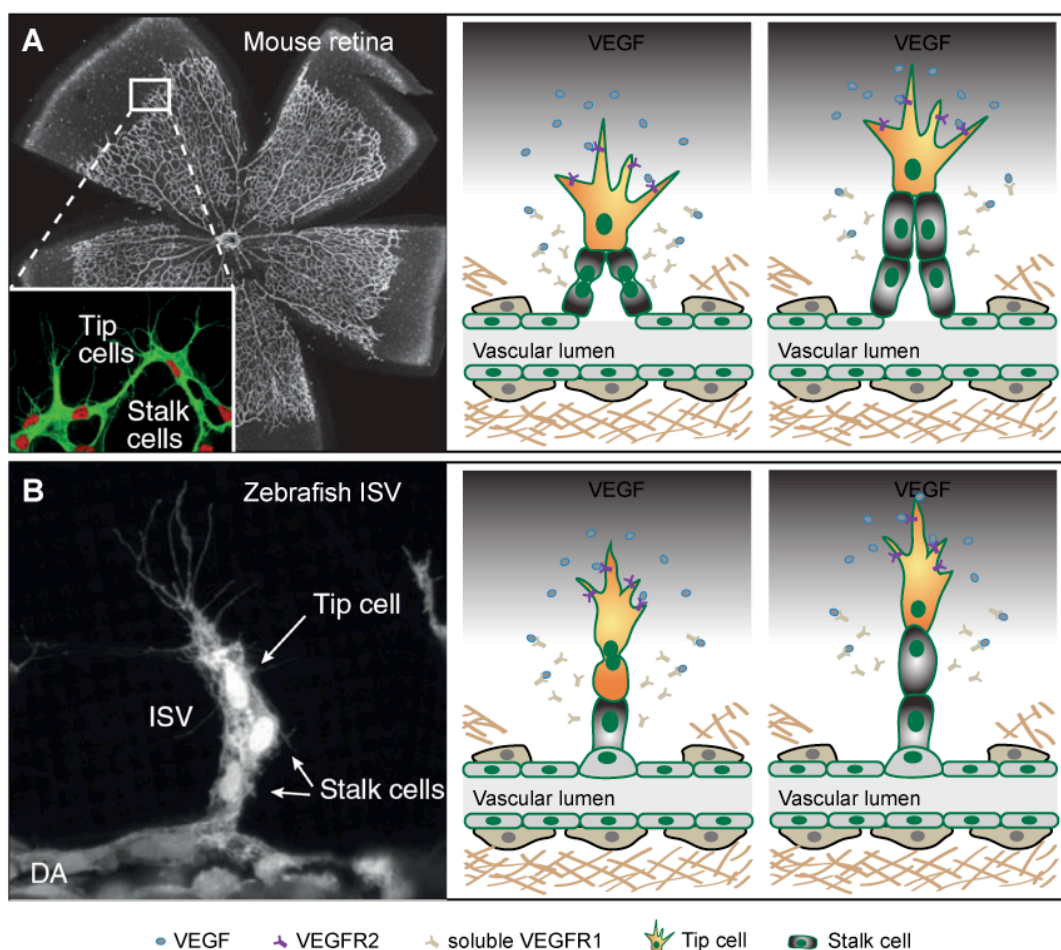
Figure 4. Sprout elongation

Endothelial tip cell sprout towards the VEGF gradient, and directs branching of the angiogenic sprout. Sprout elongation involves a series of events, such as sprout guidance and endothelial cell (EC) proliferation of the newly growing vessels. Soluble VEGFR1 secreted by the cells within and/or immediately next to the newly growing sprout neutralizes VEGF ligand molecules on either side of the sprout, thereby providing a ligand corridor for the emerging sprout. This corridor might effectively optimize spreading of the vascular network by pushing the emerging

sprout in the proper direction. (A) In mouse retinal vasculature, the vascular network grows via proliferation of stalk cells as tip cell migration. (B) In zebrafish intersegmental vessels (ISVs), tip cells assume both migration and proliferation behavior. Partially adapted from Geudens and Gerhardt, 2011.

3.2.4 Sprout anastomosis

Once the tip cell of a newly developing sprout contacts the adjacent sprout, these two sprouts become connected and undergo anastomosis, resulting in the fusion of the contacting vessels (Figure 5) (Herbert and Stainier, 2011). As a matter of fact, the mechanism underlying this process remains rather elusive, but recent studies indicate that VE-Cadherin-mediated EC-EC junction and macrophages as cellular chaperones might contribute to vascular anastomosis (Figure 5) (Almagro et al., 2010; Fantin et al., 2010). For example, VE-Cadherin was detected at the filopodial tips of endothelial tip cells, where it probably facilitates the establishment of new EC-EC junctions (Almagro et al., 2010). As for the aspects of macrophage-assisted sprout anastomosis, Fantin et al. (2010) demonstrated that recruitment of macrophages to the contacting field of adjacent tip cells might facilitate the EC-EC contact and stabilize the nascent vascular connections (Fantin et al., 2010). Macrophage secretion of soluble VEGFR1 might gradually decrease the motile ability of adjacent tip cells to increase the efficiency of their interaction by EC-EC junction but not work as an on/off switch of angiogenic anastomosis.

3.2.5 Network formation: remodeling and maturation

Immediately after or when nascent vascular network is established, a series of development events involving vascular remodeling and maturation take place,

including nascent vessel remodeling, recruitment of mural cells, and deposition of basement membrane at the abluminal surface of blood vessel.

During nascent vessel remodeling, oxygen and blood flow act as remodeling stimuli (Chen et al., 2012; Claxton and Fruttiger, 2005). Early studies demonstrated that increased oxygen levels activate vascular pruning to ensure that vascular density is correctly adapted to tissue oxygenation (Claxton and Fruttiger, 2005). Interestingly, a recent study in zebrafish indicates that extensive vessel pruning is also tightly driven by changes in blood flow (Chen et al., 2012). Specifically, changes of blood flow drive vascular pruning through lateral migration of ECs, leading to the simplification of the vasculature and possibly efficient routing of blood flow in the developing brain.
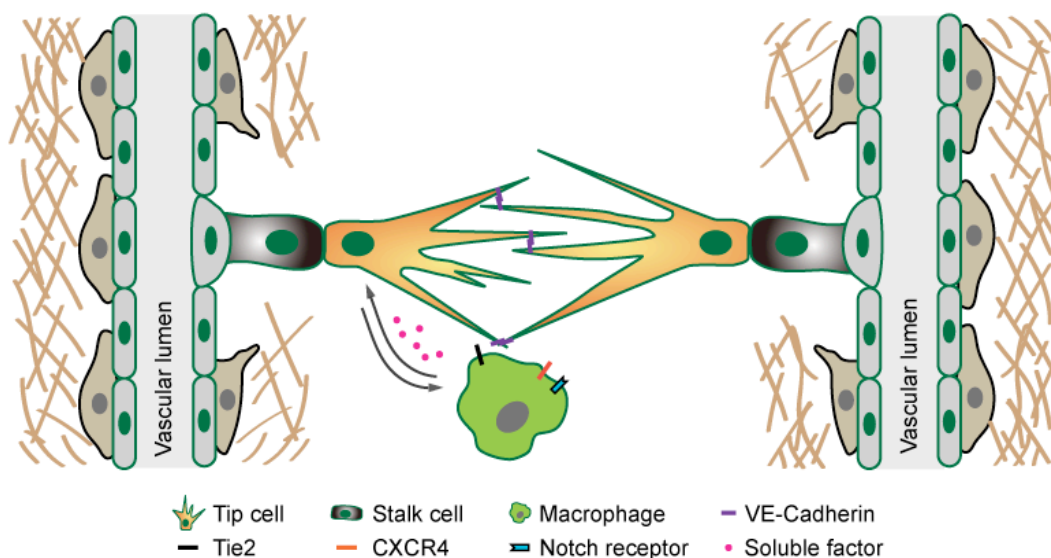
Figure 5. Sprout anastomosis

Tissue macrophage (in green) interaction with vessel facilitates the formation of new connections between growing sprouts by acting as cellular chaperones to promote filopodial contact between tip cells (in yellow). Upon contact with other vessels, VE-Cadherin-mediated adhesion junctions are established initially at the filopodial tips and later along the extending interface of the contacting cells. Candidate pathways involved in this process are the Notch, Tie2 and chemokine (C-X-C motif) receptor 4 (CXCR4) signaling pathways. Macrophages can express

the Notch receptors (in blue), the Tie2 receptors (in black) and the CXCR4 receptors (in brown), and tip cells can express their cognate ligands (not shown). An unknown soluble-factors-mediated bidirectional interaction between EC and macrophage has also been illustrated. For simplicity, vascular lumen of the emerging sprouts is not shown. Modified from Geudens and Gerhardt, 2011.
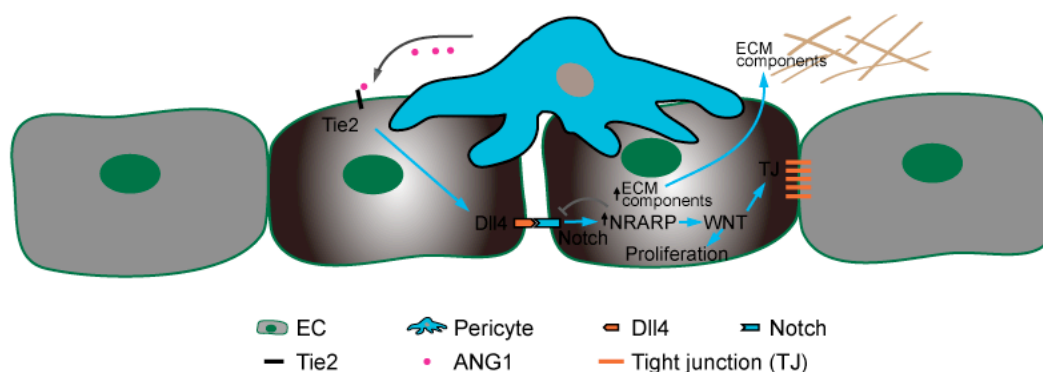
Figure 6. The stabilization of new vessels

Pericytes (in blue) recruitment is essential for vessel stabilization, possibly by the production and secretion of stabilizing factors such as ANG1. ANG1 ligand by binding to the Tie2 receptor promotes the stabilization of the vasculature, at least in part through inducing Dll4 expression in endothelial cells (ECs) and activating Notch signaling. Notch activation then downregulates the expression of VEGFR3 and upregulates the expression of membrane-bound and soluble VEGFR1, which inhibits VEGFR2 function, thereby preventing further sprouting (not shown). In addition, Notch activation induces the expression of Notch-regulated ankyrin repeat-containing protein (NRARP), which enhances WNT signaling leading to increased proliferation and EC-EC tight junction (TJ) stabilization. Modified from Geudens and Gerhardt, 2011.

In addition, numerous genetic factors modulate blood vessel maturation, such as ANG1-Tie2 signaling and Dll4-Notch signaling (Figure 6). As mentioned above for a role for ANG1-Tie2 signaling in this process, ANG1 released from pericytes binds to and activates the Tie2 receptor in ECs, with a series of downstream

regulatory events occurring including promotion of EC survival, maintenance of EC quiescence and pericytes attachment (Figure 6) (Augustin et al., 2009; Gaengel et al., 2009). Dll4-Notch signaling is also essential for vascular maturation. Activation of Dll4-Notch signaling in ECs suppresses angiogenic sprouting and further promotes vascular stabilization (Hellstrom et al., 2007; Leslie et al., 2007; Lobov et al., 2007; Lobov et al., 2011; Siekmann and Lawson, 2007; Suchting et al., 2007). Moreover, Notch signaling also supports vascular stabilization by inducing the expression of Notch-regulated ankyrin repeat protein (NRARP) and ECM components (Figure 6) (Phng et al., 2009; Trindade et al., 2008; Zhang et al., 2011). For example, Notch signaling-induced NRARP expression promotes feedback inhibition of Notch signaling and enhances WNT signaling in stalk cells, which supports vascular stability by maintaining EC-EC junctions and prevents EC retraction by promoting proliferation (Phng et al., 2009).

3.3 Key signaling pathways in angiogenesis

3.3.1 VEGF signaling in angiogenesis

The secreted growth factor VEGF is a family of homodimeric glycoproteins, consisting of placental growth factor (PlGF), VEGFA (initially known as vascular permeability factor, VPF), VEGFB, VEGFC, and VEGFD (Figure 7) (Coultas et al., 2005; Lohela et al., 2009). Their cognate receptors include three major tyrosine kinases VEGFR1, VEGFR2, VEGFR3, and two non-receptor tyrosine kinases Neuropilin1 (Nrp1) and Nrp2 (Figures 7 and 9) (Herbert and Stainier, 2011).
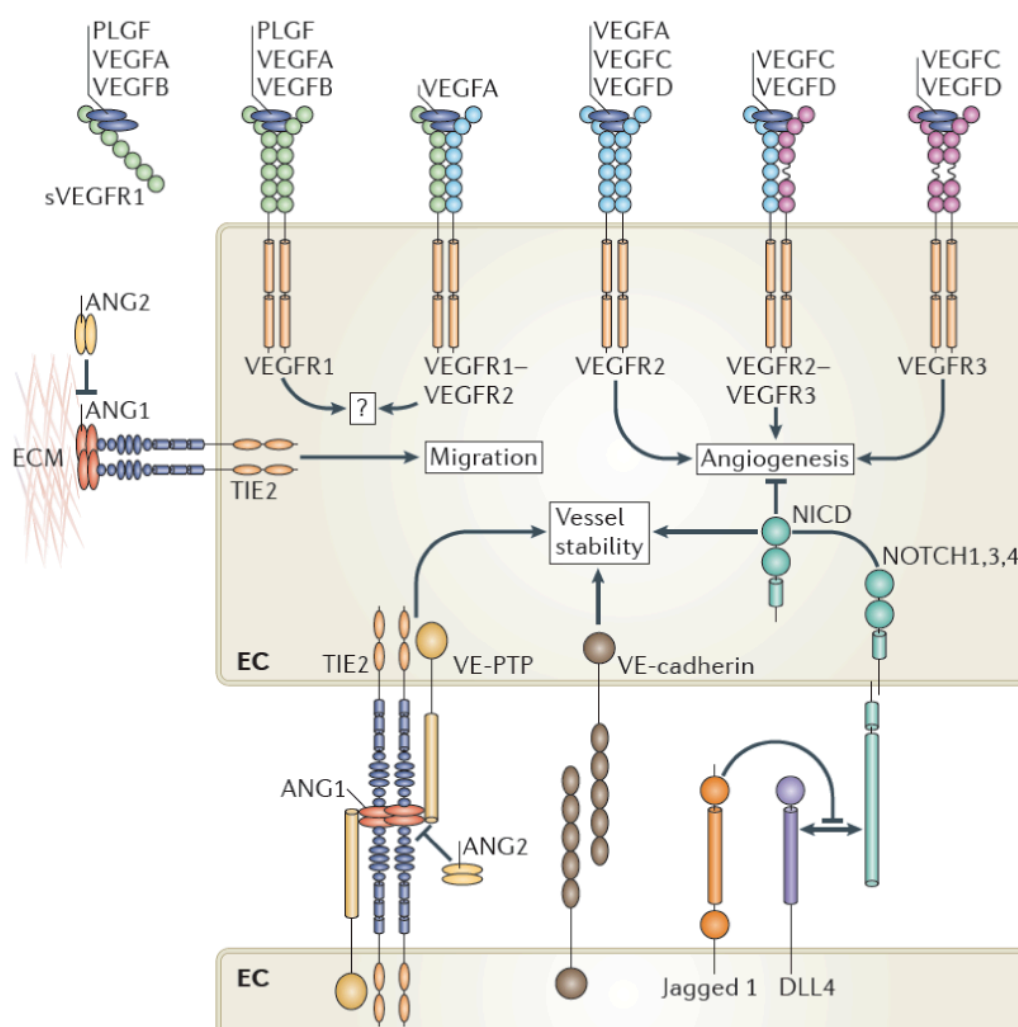
Figure 7. Key signaling pathways in angiogenesis

Main signalling pathways controlling endothelial cell (EC) behaviour. Vascular endothelial growth factors (VEGFs, including PlGF, VEGFA, VEGFB, VEGFC, and VEGFD) bind to the homodimers and heterodimers of three VEGF receptors (VEGFRs, including VEGFR1, VEGFR2, and VEGFR3). Signalling via VEGFR2, VEGFR3 or VEGFR2–VEGFR3 heterodimers promotes sprouting angiogenesis. VEGFA can bind to VEGFR1 and VEGFR2, wheras PlGF and VEGFB can only bind to VEGFR1. Membrane-bound VEGFR1 and soluble VEGFR1 (sVEGFR1) by binding VEGFA act as a sink for VEGFA that limits its availability to interact with VEGFR2. The bioactivity of VEGFC and VEGFD regulated by proteolytic processing is required for the permission of their interaction with VEGFR2, but mainly function through VEGFR3 on lymphatic ECs. The interaction of Tie2 receptor with extracellular matrix (ECM)-associated angiopoietin 1 (ANG1) at EC–ECM junction promotes EC migration. The ANG1–Tie2 interaction at EC–EC junction induces vascular quiescence upon the formation of trans-complex with Tie2 on adjacent ECs. ANG2 antagonizes the ANG1-Tie2 interaction to repress vessel stabilization and induce angiogenic remodelling. DLL4-mediated activation of NOTCH receptors by proteolytically releasing the NOTCH intracellular domain (NICD) blocks angiogenic cell behaviour to stabilize vessels. In certain contexts, Jagged1 by competing with DLL4 for NOTCH receptors represses the DLL4 –NOTCH signaling. Adapted from Herbert and Stainier, 2011.

VEGFA is the best-studied member in VEGF family and is the principal modulator of sprouting angiogenesis during development and disease (Coultas et al., 2005; Lohela et al., 2009). Given that tissue hypoxia is the main stimulator of VEGFA expression, VEGFA-mediated angiogenesis is quickly initiated in response to tissue oxygen deficiency (Pugh and Ratcliffe, 2003). As mentioned above, VEGFA binds its cognate receptor VEGFR2 to activate a series of angiogenic events (such as degradation of ECM and chemotaxis, EC proliferation, and filopodial extension) by eliciting multiple downstream pathways via intermediate signaling molecules, such as mitogen-activated protein kinases (MAPKs), phosphoinositide 3-kinases (PI3Ks), the protein serine/threonine kinase AKT (also known as PKB),

Src kinases, Smads, phospholipase C gamma (PLCγ) and small GTPases (Figure 7) (Coultas et al., 2005; Lohela et al., 2009). In accordance, targeted inactivation of a single *Vegfa* allele leads to severe vascular defects and embryonic lethality (Carmeliet et al., 1996; Ferrara et al., 1996). Moreover, VEGFR2-deficient mice also manifest deficient vascular assembly and early embryonic lethality (Shalaby et al., 1995).

VEGFA can also bind to VEGFR1, which has a higher affinity for VEGFA but weaker tyrosine kinase activity than VEGFR2 (Figure 7). Therefore, VEGFR1 is thought to be an efficient decoy receptor, competitively suppressing VEGFA-VEGFR2 interaction (Hiratsuka et al., 2005). In addition to the membrane-bound VEGFR1 with tyrosine kinase domain within the intracellular region, soluble VEGFR1, a splice variant of VEGFR1, lacks transmembrane region and intracellular region, thus becoming freely diffusible and lacking tyrosine kinase activity. Its features contribute to a significant reduction in free VEGFA level and tailoring its pattern for sprouting guidance. Consequently, a number of studies in mice and zebrafish indicate that VEGFR1 deficiency enhances angiogenic EC behavior (Fong et al., 1995; Fong et al., 1999; Hiratsuka et al., 2005; Krueger et al., 2011). Interestingly, heterodimerization between the membrane-bound VEGFR1 and VEGFR2 subunits (VEGFR1/2) has been found in ECs *in vitro* (Autiero et al., 2003; Huang et al., 2001; Kanno et al., 2000; Neagoe et al., 2005), and recent studies suggested that VEGFR1 regulates VEGF activity predominantly by forming heterodimers with VEGFR2, activation of which mediates EC migration and tube formation via the nitric oxide signaling (Ahmad et al., 2006; Cudmore et al., 2012).

A role for VEGFR3 in sprouting angiogenesis is supported by recent studies in mice and zebrafish indicating that VEGFR3 is dynamically enriched in endothelial tip cells and blockade of VEGFR3 signaling can normalize excessive blood vessel branching and endothelial proliferation in Dll4-deficient embryos (Hogan et al.,

2009; Siekmann and Lawson, 2007; Tammela et al., 2008). VEGFC, a cognate ligand for VEGFR2 and VEGFR3, can activate endothelial tip cells (Figure 7) (Tvorogov et al., 2010). Recent evidence suggested that VEGFA and VEGFC potently induce the formation of VEGFR2/3 heterodimers enriched in the tip cells of developing blood vessel, and enhance sprouting angiogenesis (Nilsson et al., 2010). Interestingly, two more recent findings indicated that Notch-dependent VEGFR3 upregulation promotes blood vessel growth in the absence of VEGFA-VEGFR2 signaling, and this vessel growth requires the kinase activity of VEGFR3 in a VEGFC-independent manner (Benedito et al., 2012; Tammela et al., 2011).

Other VEGF family members PlGF and VEGFB selectively bind to membrane-associated VEGFR1 and soluble VEGFR1, whereas VEGFD prefers VEGFR2 and VEGFR3 (Figure 7). Functional roles of these members during blood vessel development remain to be extensively elucidated, although there is emerging evidence to indicate their angiogenic effects (Fischer et al., 2008; Hedlund et al., 2013; Lahteenvuo et al., 2009). In addition, a number of recent studies reveal that alternative splicing produces numerous VEGFA variants with their divergent functions and bioavailablitities during angiogenesis, undoubtedly enhancing the complexity of VEGFA-VEGFR interaction (Adams and Alitalo, 2007; Carmeliet and Jain, 2011). For further reading on alternative splicing in angiogenesis, refer to these excellent reviews (Adams and Alitalo, 2007; Carmeliet and Jain, 2011).

3.3.2 Notch signaling in angiogenesis

Notch signaling is a highly conserved pathway for cell fate specification, involving interactions between adjacent Notch ligand- and receptor-expressing cells (Roca and Adams, 2007). Both Notch ligands and receptors are single-pass

transmembrane proteins, but the former lack a substantial intracellular domain (Figure 7). Notch ligand binding induces double cleavages of Notch receptor by ADAM-family protease ADAM10 (or ADAM17) and γ-secretase/ presenilin complex. Once the Notch intracellular domain (NICD) is released, it translocates to the nucleus and functions as a key transcriptional modulator during cell fate determination. To date, the identified endothelial Notch ligands and receptors are Dll1, Dll4, Jagged1, Jagged2, and Notch1, Notch3, Notch4, respectively. As described above, Dll4-Notch signaling is well investigated and has an essential role in tip and stalk cell fate determination during angiogenesis (Figure 3) (Phng and Gerhardt, 2009; Roca and Adams, 2007). VEGFA-induced Dll4 expression in tip cell activates Notch signaling in the neighboring stalk cell, which is prevented from exhibiting tip cell behavior. However, Notch signaling in tip cells is inhibited by stalk cell expression of Jagged1 (Figure 7) (Benedito et al., 2009). In particular, Jagged1 blocks Dll4-Notch interaction on tip cells once the extracellular domain of Notch receptor is glycosylated by Fringe family glycosyltransferases. Besides, a study on the NAD^+-dependent deacetylase sirtuin1 (SIRT1) in mice and zebrafish revealed that SIRT1 makes NICD unstable by deacetylating, thereby blocking Notch signaling and promoting vessel branching (Guarani et al., 2011).

In addition, the angiogenic role for Dll1 was supported by a recent study indicating that Dll1 serves as an extrinsic cue to regulate tip cell selection and vascular branching morphogenesis (Napp et al., 2012). Functional roles of other members such as Jagged2, Notch3 and Notch4 in angiogenesis remain unclear.

3.3.3 ANG-Tie signaling in angiogenesis

ANG-Tie signaling contributes greatly to vessel remodeling and maturation. A family of ANG ligands comprises three members ANG1, ANG2, and ANG4, and their corresponding receptor tyrosine kinases include Tie1 and Tie2 (Carmeliet

and Jain, 2011). Among the components of this signaling, the well-characterized ligands ANG1 and ANG2 both bind to Tie2 with similar affinities (Figure 7) (Maisonpierre et al., 1997). In general, ANG1 is released from mural and tumor cells, whereas ANG2 expressed by endothelial tip cells, functions at the angiogenic and vessel remodeling sites. As introduced above, ANG1-Tie2 signaling stimulates the recruitment of mural cells and deposition of basement membrane, thereby promoting vessel maturation (Figure 6) (Carmeliet and Jain, 2011). However, when exposed to angiogenic stimuli, sprouting tip cells express and secrete ANG2, which functions as an antagonist of ANG1-Tie2 signaling to induce mural cell detachment, vascular permeability and angiogenic sprouting (Figure 7) (Augustin et al., 2009).

To date, ligands for Tie1 haven't been identified. However, this orphan receptor-deficient mice manifest edema, microvascular fragility with hemorrhage, and embryonic lethality (Sato et al., 1995). In addition, ANG4 has not been well studied yet.

3.3.4 TGF-β signaling in angiogenesis

Transforming growth factor-β (TGF-β) family consists of three members TGF-β1, TGF-β2, and TGF-β3, showing partially overlapping as well as distinct functions (Lebrin et al., 2005). TGF-β is secreted in a biologically latent form and its activation is dependent on proteases or thrombospondin 1 (TSP1) (Lebrin et al., 2005). TGF-β-mediated signal transduction requires a series of TGF-β receptors, co-receptors, and Smad proteins (Figure 8) (Lebrin et al., 2005; Pardali et al., 2010). TGF-β receptors are serine/threonine kinases, including two distinct TGF-β type 1 receptors (activin receptor-like kinase 1 (ALK1, also known as ACVRL1) and ALK5 (also known as TGF-βR1, or TβR-1)) and one TGF-β type 2 receptor (TGF-βR2, or TβR-2). Co-receptors of TGF-β signaling consist of two structurally

related proteins Endoglin and Betaglycan, both of which are single-pass transmembrane receptors with short serine/threonine residues-containing intracellular domains that lack the enzymatic motif. Mechanistically, active TGF-β ligand by Endoglin-mediated binding to TGF-βR2 activates ALK1 or ALK5, which further phosphorylate their respective downstream Smad proteins (Figure 8) (Lebrin et al., 2005; Pardali et al., 2010). Interestingly, EC-specific ALK1 and ubiquitously expressed ALK5 control EC behaviors in opposite manners (Lebrin et al., 2005; Pardali et al., 2010). For example, activation of ALK1 promotes EC proliferation and migration by phosphorylating Smad1 and Smad5, whereas ALK5 via activation of Smad2 and Smad3 suppresses EC proliferation and migration (Figure 8).
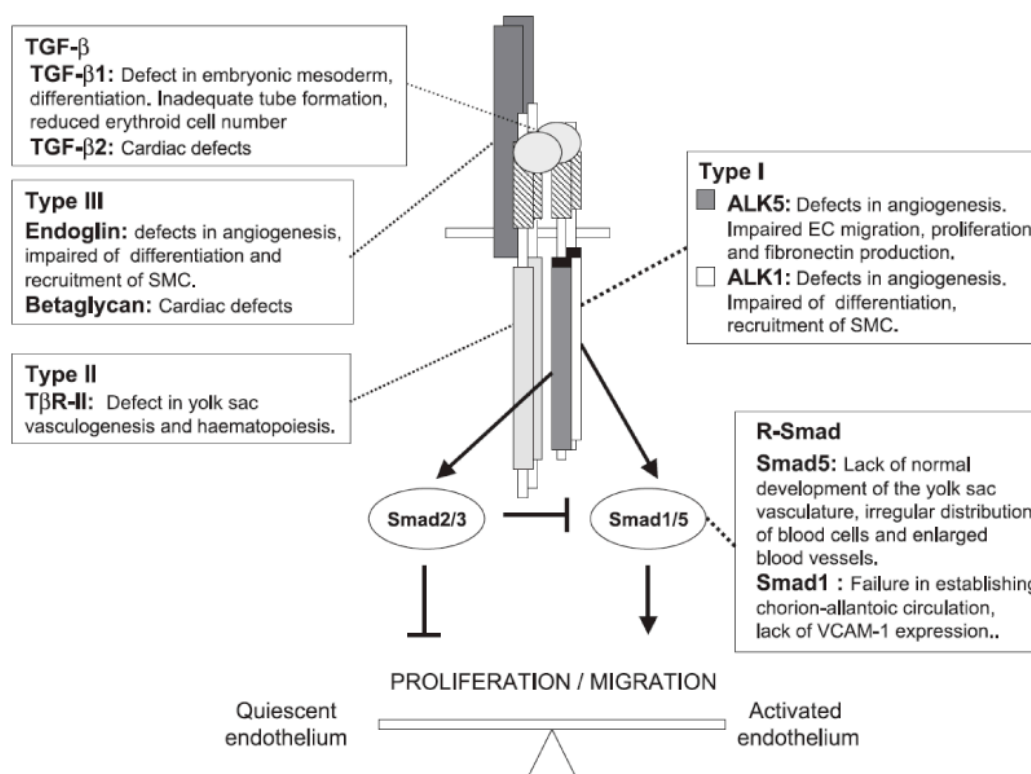
Figure 8. TGF-β signaling in angiogenesis

TGF-β ligand induces endothelial cell (EC) behavior via two distinct TGF-β type I receptors (TβR-I)-Smad pathways. Upon the formation of TGF-β-induced heteromeric complex, activin receptor-like kinase 1 (ALK1) and ALK5 are

phosphorylated and activated by TβR-II kinase. TGF-β signaling via ALK1 and subsequent Smad1/5 phosphorylation promotes EC proliferation and migration. Conversely, TGF-β signaling through ALK5 and subsequent Smad2/3 phosphorylation represses the proliferation and migration of ECs. In addition, ALK1-induced Smad2/3-dependent signaling can indirectly repress ALK5-induced Smad1/5-mediated transcriptional responses. SMC, smooth muscle cell; VCAM-1, vascular cell adhesion molecule-1. Adapted from Lebrin et al., 2005.

Human genetic studies in hereditary haemorrhagic teleangiectasia (HHT) characterized by vascular malformation, indicate that mutations in *ALK1* or *Endoglin* have been linked to this disorder (Johnson et al., 1996; McAllister et al., 1994). Moreover, ALK1-, ALK5-, Endoglin-, or TGF-βR2-deficient mice and *acvrl1* mutant zebrafish embryos exhibit similar defects in vascular formation (Figure 8) (Pardali et al., 2010). Functional implication of this signaling pathway in vascular development has also been supported by targeted inactivation of Smad proteins in mice (Pardali et al., 2010). In addition, two independent research groups recently demonstrated that ALK1 signaling by cooperating with Notch pathway inhibits sprouting angiogenesis (Larrivee et al., 2012; Moya et al., 2012).

3.3.5 PDGF signaling in angiogenesis

Platelet-derived growth factor (PDGF) family consists of four members PDGFA, PDGFB, PDGFC and PDGFD, with high sequence similarity to VEGF (Fredriksson et al., 2004). Signaling occurs by two transmembrane receptor tyrosine kinases PDGF receptor-α (PDGFR-α) and PDGFR-β, which function as homo and heterodimers.

During nascent blood vessel stabilization, angiogenic ECs express and release PDGFB, which functions as a chemoattractant to recruit pericytes that express PDGFR-β (Gaengel et al., 2009; Herbert and Stainier, 2011). Consequently, mice

deficient for PDGFB or PDGFR-β both exhibit reduced pericyte attachment of nascent vessels and blood vessel leakage (Hellstrom et al., 1999; Lindahl et al., 1997).

3.3.6 Nrp co-receptor in angiogenesis

Neuropilin (Nrp) family of transmembrane co-receptors consists of Nrp1 and Nrp2, well known for their ligand-receptor interaction with class 3 semaphorins (Sema3s) and VEGFs (Figure 9) (Adams and Eichmann, 2010; Neufeld et al., 2002). To date, seven secreted Sema3 members have been identified (from Sema3A to Sema3G), exhibiting distinct binding preference for Neuropilins. For example, Sema3A signals through Nrp1, while Sema3F binds to Nrp2 (Chen et al., 1997; He and Tessier-Lavigne, 1997; Maden et al., 2012). In addition to Sema3s, Neuropilins by binding to structurally distinct proteins such as VEGF family members form complexes with various VEGFRs and promote VEGFR-mediated angiogenic sprouting (Adams and Alitalo, 2007; Adams and Eichmann, 2010; Neufeld et al., 2002).

Consequently, Sema3A- or Nrp1-deficient mice manifest some vascular remodeling defects during development (Behar et al., 1996; Gerhardt et al., 2004; Kawasaki et al., 1999; Serini et al., 2003). Overexpression of Nrp1 in mice also leads to vascular defects including vascular expansion and excessive vessel growth (Kitsukawa et al., 1995).

3.3.7 Sema3-PlexinD1 signaling in angiogenesis

Semaphorins, characterized by an N-terminal Sema domain, represent a family of secreted or membrane-anchored proteins essential for axon guidance and vascular patterning (Adams and Eichmann, 2010; Sakurai et al., 2012). In

vertebrates, semaphorins are grouped into 5 classes including secreted type of Sema3 and membrane-associated types of Sema4-7 (Figure 9) (Sakurai et al., 2012). Plexins are single-pass transmembrane receptors, consisting of nine members PlexinA1-4, PlexinB1-3, PlexinC1, and PlexinD1 (Figure 9) (Sakurai et al., 2012). Membrane-anchored Semaphorins signal via binding directly to Plexins, whereas secreted Sema3s signal through binding to a holoreceptor complex consisting of a ligand binding subunit (Nrp1 or Nrp2) and a signal transducing subunit (one member of Plexins) (Figure 9) (Sakurai et al., 2012). One exception to this rule is Sema3E, which signals directly through EC-specific PlexinD1 receptor, independently of Neuropilins (Figure 9) (Adams and Eichmann, 2010; Oh and Gu, 2013; Sakurai et al., 2012).
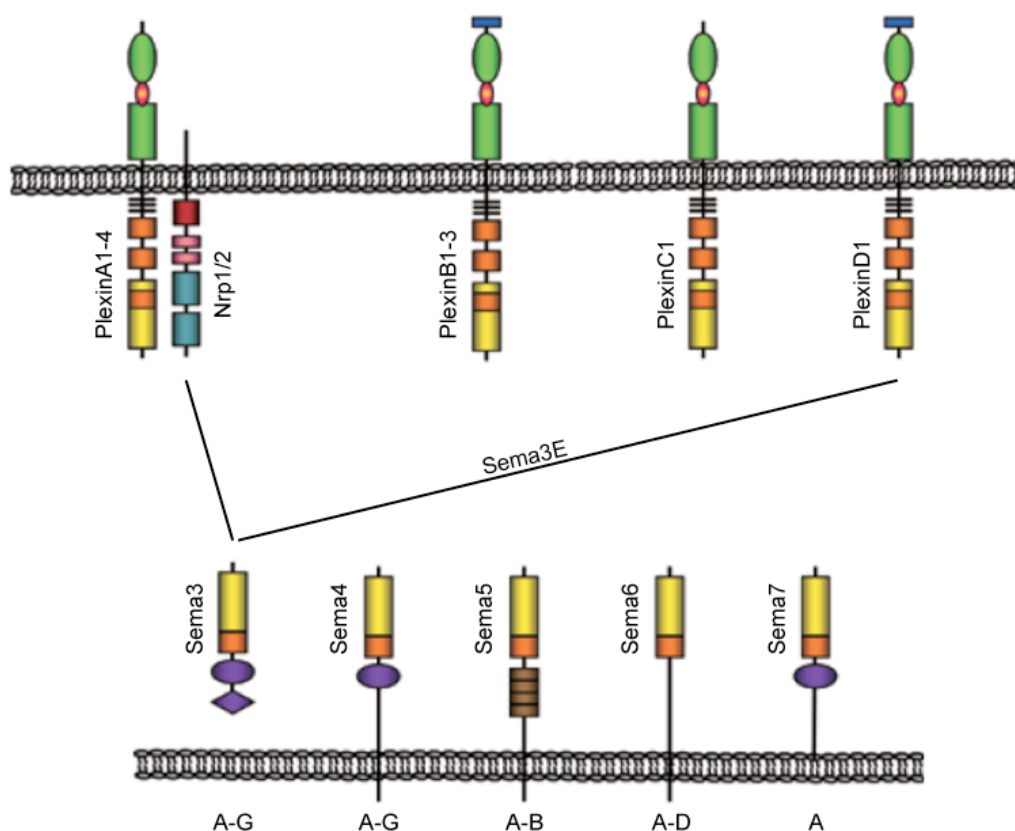
Figure 9. Semas, Plexins, and Nrps in angiogenesis

Vertebrates express Semaphorin classes 3-7 (Sema3-7), PlexinsA-D, and Neuropilins 1 and 2 (Nrp1/2). Members of the Sema3 class are secreted, while the

Sema4-7 members are membrane-anchored. Nrp1/2 requires their association with PlexinA1-4 or vascular endothelial growth factor receptors (VEGFRs, not shown) to facilitate signaling. Secreted Sema3s (such as Sema3E) through binding to their receptor PlexinD1 promote EC repulsion to inhibit angiogenesis. Modified from Sakurai et al., 2012.
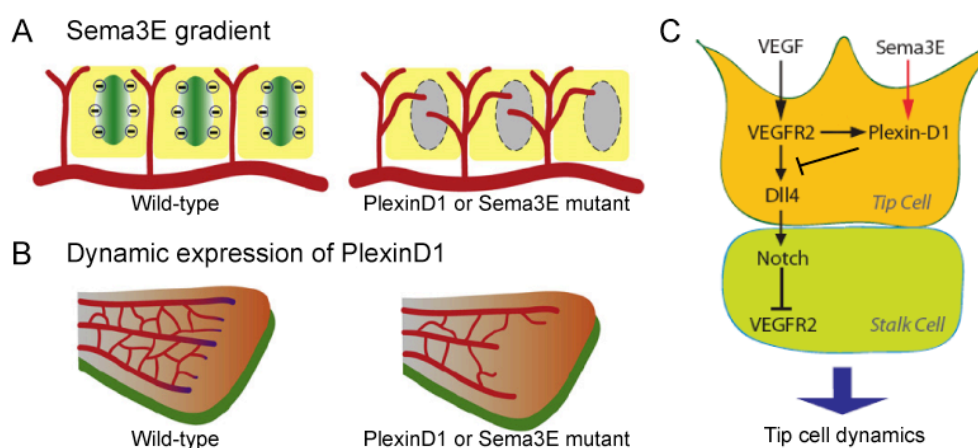
Figure 10. Sema3E-PlexinD1 signaling in angiogenesis

Spatial-temporal control of the expression of Sema3E ligand and PlexinD1 receptor results in two distinct mechanisms governing vascular patterning. (A) The repulsive gradient of Sema3E in mouse somites determines the proper patterning of PlexinD1-expressing intersomitic vessels (ISVs, in red). During ISV development, Sema3E gradient (in green) is formed in the caudal region of each somite (in yellow), whereas PlexinD1 is specifically expressed in adjacent ISVs on the rostral region of each somite. In wild-type mice, the repulsive guidance of Sema3E gradient restricts vessel branching in the intersomitic space, while mice deficient for PlexinD1 or Sema3E exhibit hyperbranching of ISVs in the entire somite. (B) Instead of the Sema3E gradient, dynamic control of PlexinD1 expression contributes to the proper pattern formation of mouse retinal vasculature (in red). In this process, PlexinD1 is dynamically expressed in endothelial cells (ECs, in purple) at the active sprout front in a VEGF-dependent manner, whereas Sema3E (in green) is uniformly expressed in retinal ganglion cells (RGCs) underneath the retinal vasculature. Mice lacking PlexinD1 or

Sema3E show uneven and decreased vessel sprouting in the retina. (C) Dynamic regulation of tip cells by Sema3E-PlexinD1 interaction modulating Dll4-Notch signaling via a VEGF-induced negative feedback mechanism. VEGF directly induces PlexinD1 expression selectively in ECs at the front of active sprouts. In turn, Sema3E–PlexinD1 signaling negatively modulates the VEGF-induced Dll4-Notch signaling, which controls the retinal vascular network topology via modulating the ratio between tip and stalk cells. Adapted from Oh and Gu, 2013.

Interestingly, spatial-temporal control of Sema3 ligands and PlexinD1 receptor generates two distinct mechanisms governing vascular patterning (Figure 10). For example, tight control of spatial-temporal pattern of repulsive guidance cue Sema3E gradient in mouse somites determines the intersomitic vascular topology through its direct interaction with the PlexinD1 receptor, as evidenced by two studies in *PlexinD1* knockout mice indicating that PlexinD1 deficiency disrupts intersomitic vascular pattern and promotes angiogenic sprouting, which was also observed in zebrafish *out-of-bounds* mutant (*obd,* encodes PlexinD1) (Figure 10A) (Gitler et al., 2004; Gu et al., 2005; Torres-Vazquez et al., 2004). In addition, VEGF-mediated control of spatial-temporal distribution of PlexinD1 in mouse retina determines retinal vascular pattern, as suggested in a recent study showing that PlexinD1 is dynamically restricted to the actively sprouting retinal vessels in a VEGF-dependent manner, and the Sema3E-PlexinD1 signaling promotes retinal angiogenesis via feedback inhibition of VEGF-induced Dll4-Notch signaling (Figure 10B and C) (Fukushima et al., 2011; Kim et al., 2011).

3.3.8 Slit-Robo signaling in angiogenesis

The large multidomain proteins Slits are secreted ECM protein, consisting of three structurally conserved members Slit1-3 (Adams and Eichmann, 2010; Dickson and Gilestro, 2006). Slit proteins are proteolytically cleaved to release an

N-terminal fragment that binds Roundabout (Robo) receptors to modulate axon guidance (Figure 11) (Ballard and Hinck, 2012).
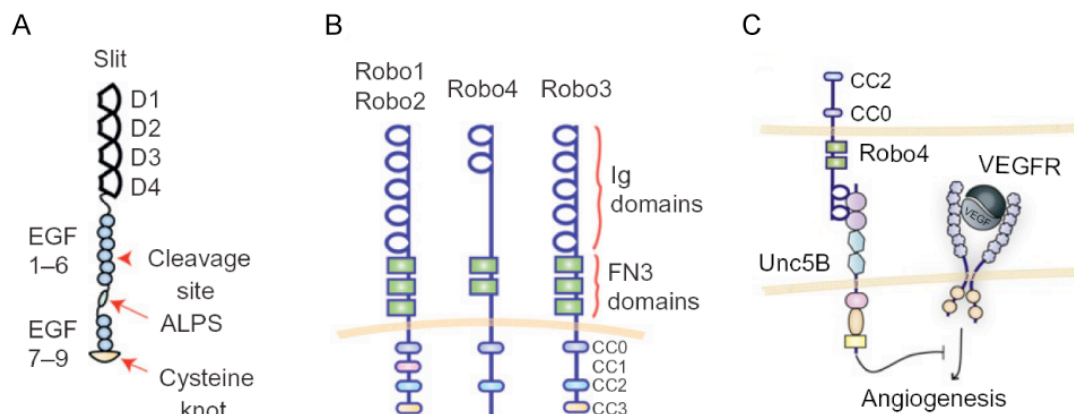
Figure 11. Slit-Robo signaling in angiogenesis

(A) Structural representation of Slits. Slits are proteolytically cleaved between two epidermal growth factor (EGF)-like domains. (B) Structural representation of Robos. Of the four single-pass transmembrane Robos (Robo1–4) in vertebrates, Robo1-3 contain five immunoglobulin (Ig) domains and three fibronectin type 3 (FN3) domains, while Robo4 contains only two Ig domains (three Ig domain-containing Robo4 in zebrafish) and two FN3 domains. All Robos contain between two and four conserved proline-rich domains (CC0–CC3) in their cytoplasmic tail. (C) Robo4 as the ligand binds to UNC5B receptor, and signals to block pro-angiogenic signaling downstream of VEGF-VEGFR interaction. Adapted from Ballard and Hinck, 2012.

Of the three known Slits, Slit2 and Slit3 are expressed by vascular mural cells and ECs (Ballard and Hinck, 2012). Of the four known single-pass transmembrane Robos (including Robo1-4) in vertebrates, Robo4 is structurally distinct from the other Robo family members and is expressed in ECs (Figure 11B) (Adams and Eichmann, 2010; Ballard and Hinck, 2012; Bedell et al., 2005).

Numbers of studies in mice and zebrafish indicate that Robo4 is required to maintain blood vessel integrity and blocks sprouting angiogenesis (Bedell et al., 2005; Koch et al., 2011). The mechanism for Robo4 signaling in angiogenesis is supported by a recent study indicating that Robo4 as the ligand binds to the uncoordinated-5B receptor (UNC5B, a chemorepellent receptor for Netrin1) in ECs, and this *in trans* interaction of UNC5B with Robo4 inhibits pro-angiogenic signaling downstream of VEGF-VEGFR interaction (Figure 11C) (Koch et al., 2011).

3.3.9 Netrin-UNC5B signaling in angiogenesis

Netrins represent a family of evolutionarily conserved secreted guidance proteins, including Netrin1-4 and Netrin-related molecules Netrin-G1 and Netrin-G2 (Adams and Eichmann, 2010; Ahmed and Bicknell, 2009). Of the Netrin receptors including the deleted in colorectal cancer (DCC) and the UNC5 families, only UNC5B is specifically expressed in some population of ECs such as arterial ECs and endothelial tip cells (Lu et al., 2004; Suchting et al., 2007). Further evidence indicates that UNC5B-deficient mice and zebrafish both exhibit excessive blood vessel branching with lavish filopodial extensions in tip cells, suggesting its negative modulation in tip cell guidance (Lu et al., 2004). Moreover, knockdown of UNC5B ligand Netrin1a in zebrafish leads to aberrant pathfinding of ISV, while treatment of ECs with Netrin1 promotes filopodial retraction of tip cells and inhibits angiogenesis (Klagsbrun and Eichmann, 2005; Lu et al., 2004). Collectively, Netrin1 binds to UNC5B and signals to negatively control sprouting angiogenesis.

Interestingly, a positive role for Netrins in angiogenesis is suggested by a recent study indicating that Netrin1 may also function as pro-angiogenic factors to promote angiogenesis by inhibiting EC apoptosis (Castets et al., 2009).

3.3.10 Other factors for angiogenesis

Using a combinatory strategy of pharmacological treatment and fluorescence-activated cell sorting (FACS) in zebrafish, Herbert et al. (2012) identified an essential role for Hlx1 (H2.0-like homeobox-1) in angiogenesis. Zebrafish hlx1 expression is restricted to sprouting ECs and cell-autonomously regulates angiogenesis via maintaining stalk cell potential (Herbert et al., 2012).

3.4 MicroRNA-mediated regulation of angiogenesis

3.4.1 MicroRNA biogenesis and function

Last 25 years witnessed the rapid development of vascular investigation, which have succeeded in identifying numbers of key regulator proteins that form a complicated regulatory network to control angiogenesis. However, recent studies are beginning to focus on post-transcriptional, translational and post-translational mechanisms that fine-tune the well-known angiogenic signaling pathways to adjust the cellular behaviors. Therefore, current studies are making more complicated and exquisite the aspects of molecular control of angiogenic signaling, with an emphasis on microRNA-mediated angiogenesis.

MicroRNAs represent a large and growing family of evolutionarily conserved single-stranded short non-coding RNAs, approximately 22 nt in length (Ambros, 2004; Bartel, 2004). They are encoded as autonomous transcripts, or are transcribed within the introns of protein-coding genes (Bartel, 2004; Ghildiyal and Zamore, 2009; He and Hannon, 2004). Mature microRNAs are generated via sequential processing of their primary transcripts by the enzymes Drosha and Dicer (Bernstein et al., 2001; Hutvagner et al., 2001; Lee et al., 2003). After their biogenesis, the resulting mature microRNAs are subsequently incorporated into the RNA-induced silencing complex (RISC) and used as a guide sequence that base-pairingly binds to certain sites within the 3' untranslated region (3'UTR) of target mRNAs, which leads to mRNA degradation and/or translational repression (Bazzini et al., 2012; Czech and Hannon, 2011; Djuranovic et al., 2012; Gregory et al., 2005; Guo et al., 2010). Thus, microRNAs usually provide a negative regulatory mechanism of gene expression to fulfill their biological tasks. For further reading on microRNA biogenesis and universal mechanisms that modulate their target gene expressions, refer to some classic reviews (Bushati and Cohen, 2007; Ghildiyal and Zamore, 2009; Inui et al., 2010; Selbach et al., 2008; Winter et

al., 2009). Functional significance of a specific microRNA itself relies on the contribution of its target genes in a given cellular context. Therefore, identifying functionally important microRNA targets becomes crucial to understand the corresponding microRNA functions.

3.4.2 Global evaluation of microRNAs-mediated angiogenesis

Dicer, involved in the maturation of microRNAs, has a ubiquitous expression pattern during development and in adults (Yang et al., 2005). A number of seminal studies uncovered the functional role of Dicer in vascular development, further implying the significance of microRNAs in angiogenesis (Giraldez et al., 2005; Kuehbacher et al., 2007; Suarez et al., 2007; Suarez et al., 2008; Yang et al., 2005).

Initially, global knockdown experiments using mutation or disruption of this rate-limiting enzyme Dicer were carried out in several *in vivo* studies (Giraldez et al., 2005; Yang et al., 2005). For example, knockdown of Dicer in mice caused early death (E12.5-14.5) with defective vascular formation, suggesting a possible role for Dicer in embryonic angiogenesis (Yang et al., 2005). In particular, Yang et al. (2005) generated the *dicer*$^{ex1/2}$ mice lacking the amino acid sequences corresponding to the first and second exons of the *dicer* gene and found that Dicer deficiency results in defects in embryonic angiogenesis, with altered expressions of VEGF, VEGFR1, VEGFR2, and Tie1. Probably, Dicer plays an essential role in the maturation of microRNAs that modulate sprouting angiogenesis by targeting angiogenic protein-coding transcripts. In addition, zebrafish embryos that lack maternal and zygotic Dicer, manifested severe defects in many developmental events such as brain morphogenesis and cardiovascular development (Giraldez et al., 2005).

To address the question of whether Dicer in ECs autonomously regulates angiogenesis or not, several laboratories turned to *in vitro* studies to analyze the global function of microRNAs in ECs (Kuehbacher et al., 2007; Suarez et al., 2007; Suarez et al., 2008). Knockdown of Dicer in human ECs resulted in a significant reduction in capillary sprouting and cell growth (Kuehbacher et al., 2007; Suarez et al., 2007; Suarez et al., 2008), with altered expression patterns of several key regulators of endothelial biology, such as Tie2, VEGFR2, endothelial nitric oxide synthase (eNOS), and interleukin-8 (IL-8) (Suarez et al., 2007). In addition, upregulated expression of the extracellular matrix glycoprotein TSP1, which was mentioned above as an angiogenic inhibitor, was observed in ECs deficient for Dicer (Kuehbacher et al., 2007; Suarez et al., 2008). Furthermore, using *in vivo* matrigel plug assay, Kuehbacher et al. found that subcutaneous injection of Dicer-deficient HUVECs into nude mice significantly reduced angiogenic sprout formation (Kuehbacher et al., 2007).

To further understand the EC-specific function of Dicer in *in vivo* angiogenesis, Suarez et al. (2008) generated two conditional EC-specific *Dicer* knockout mice including conditional *Tie2-Cre;Dicer$^{flox/flox}$* mice and Tamoxifen (TMX)-inducible *VECad-Cre-ER^{T2};Dicer$^{flox/flox}$* mice (Suarez et al., 2008). EC-specific inactivation of Dicer in these two conditional knockout mice resulted in a reduction in postnatal angiogenic response to a variety of pro-angniogenic stimuli, such as VEGF, tumors, limb ischemia, and would healing (Suarez et al., 2008).

3.4.3 Dissection of functional roles of specific microRNAs in angiogenesis

Using a primitive microarray platform for microRNAs, Poliseno et al. (2006) briefly reported the presence of microRNAs in human umbilical vein endothelial cells (HUVECs), which suggests the involvement of microRNAs in EC biology

(Poliseno et al., 2006). In particular, 15 highly expressed microRNAs identified in HUVECs were predicted to directly modulate the expression of the receptors for angiogenic factors such as Flt1, Flk1, Nrp1, Nrp2, C-kit, Tie2, and CXCR4. Furthermore, microRNA-221 (miR-221) and miR-222 were demonstrated in this study to regulate the angiogenic properties of stem cell factor (SCF) by targeting its receptor c-Kit (Figure 12). Additionally, other microRNA profiling studies identified a total of 200 endothelial microRNAs (Heusschen et al., 2010). More recently, the Lawson laboratory deep sequenced the small RNAs from zebrafish ECs and identified hundreds of endothelial microRNAs (Nicoli et al., 2012), which was strongly supported by our own unpublished microRNA profiling study. Their further study identified miR-221 as an essential regulator to promote sprouting angiogenesis (Nicoli et al., 2012). Specifically, endothelial miR-221 promotes endothelial tip cell migration and proliferation through inhibiting two targets cyclin dependent kinase inhibitor 1b (Cdkn1b) and phosphoinositide-3-kinase regulatory subunit 1 (PIK3R1) (Figure 12). Interestingly, this study also suggested that Notch signaling functions as a negative factor to regulate the expression of miR-221 (Figure 12) (Nicoli et al., 2012).

miR-126 is encoded within intron 7 of the *EGF-like domain 7* (*Egfl7*) gene and its expression appears to be highly enriched in ECs, with a similar endothelial expression pattern as Egfl7 (Fish et al., 2008; Harris et al., 2008; Wang et al., 2008). Using human ECs *in vitro*, miR-126 was suggested to promote EC migration, proliferation, and capillary-like tube stability (Fish et al., 2008). Further *in vivo* studies of miR-126 in zebrafish and mice indicate that targeted disruption of miR-126 caused a loss of blood vessel integrity and increased hemorrhages (Fish et al., 2008; Kuhnert et al., 2008; Wang et al., 2008). Mechanistically, miR-126 plays a positive role in maintaining vascular integrity by promoting MAPK and PI3K signaling, through targeting inhibitors for these signaling cascades, including Sprouty-related EVH-domain-containing protein 1 (Spred1) and PIK3R2 (Figure 12) (Fish et al., 2008; Kuhnert et al., 2008; Wang et al., 2008). In addition,

Harris et al. (2008) also found that miR-126 targets vascular cell adhesion molecule 1 (VCAM1), which is involved in the adhesion of leukocyte to the vessel wall (Figure 12) (Harris et al., 2008).

Figure 12. Modulation of angiogenic signaling by multiple microRNAs

Multiple microRNAs have been implicated in controlling the angiogenic response of endothelial cells (ECs) to multiple factors, such as vascular endothelial growth factors (VEGFs), hypoxia, and haemodynamics. Endothelial microRNAs that promote angiogenesis include miR-10, miR-27a/b, miR-126, miR-210, miR-221,

and miR-296. Known targets and modulators for each microRNA are illustrated. Two endothelial microRNAs that inhibit angiogenesis are miR-221 and miR-222. Non-endothelial microRNAs that also modulate angiogenesis include miR-1/206 (in somites) and miR-17-92 (in tumor cells). Cdkn1b, cyclin dependent kinase inhibitor 1b; CTGF, connective tissue growth factor; EphrinA3, eph-related receptor tyrosine kinase ligand 3; HGS, hepatocyte growth factor-regulated tyrosine kinase substrate; MAPK, mitogen-activated protein kinase; PI3K, phosphoinositide 3-kinase; PIK3R1, phosphoinositide-3-kinase regulatory subunit 1; SCF, stem cell factor; Spred1, spouty-related EVH-domain-containing protein; TSP1, thrombospondin-1; VCAM1, vascular cell adhesion molecule 1.

As for the upstream of miR-126 expression, Harris et al. (2010) found that Ets family members Ets-1 and Ets-2 drive the expression of miR-126; while Nicoli et al. (2010) demonstrated that zebrafish aortic arch vascular angiogenesis requires a blood flow-induced signaling pathway in which the mechano-sensitive zinc finger transcription factor Klf2a induces miR-126 expression to activate VEGFA-VEGFR2 signaling (Figure 12) (Harris et al., 2010; Nicoli et al., 2010).

The miR-17~92 cluster is a polycistronic microRNA gene encoding for six microRNAs, including miR-17, miR-18a, miR-19a, miR-20a, miR-19b-1, and miR-92a (Mendell, 2008). The miR-17~92 cluster was the first identified tumor-promoting microRNA, but the first report linking this cluster to angiogenic response came out in 2006 (Dews et al., 2006; Ota et al., 2004). In this study, Dews et al. (2006) observed that colon cancer cells expressing oncogenic transcription factor c-Myc activates the expression of the miR-17~92 cluster, which, in turn, suppresses the expression levels of the anti-angiogenic molecules TSP1 and connective tissue growth factor (CTGF) (Figure 12) (Dews et al., 2006). Further experiments demonstrated that angiogenic activity of c-Myc is partially due to activation of the miR-17~92 cluster, in which miR-19 and miR-18 promote angiogenesis and tumor growth via inhibiting TSP1 and CTGF, respectively.

Using human ECs *in vitro*, Suarez et al. (2008) revealed the EC-autonomous role for this microRNA cluster components in angiogenesis (Suarez et al., 2008). For example, transfection of VEGF-regulated miR-17~92 cluster members miR-17, miR-18a, and miR-20a greatly normalized the EC proliferation and organization in Dicer-deficient ECs, while knockdown of miR-17, miR-18a, and miR-20a reduced VEGF-induced vascular cord formation. Taken together, these data unraveled that VEGF-stimulated proliferation and morphogenesis are modulated partially by the miR-17-92 cluster.

Conversely, two studies from Dimmeler lab indicated anti-angiogenic properties of members of the miR-17-92 cluster (Bonauer et al., 2009; Doebele et al., 2010). Initially, an anti-angiogenic role for miR-92a in ECs was evidenced by Bonauer et al. (2009). Specifically, forced overexpression of miR-92a in ECs inhibits angiogenesis *in vitro* and *in vivo*, while antagomir-mediated knockdown of miR-92a in mice led to enhanced blood vessel growth and functional recovery of limb ischemia and myocardial infarction (Bonauer et al., 2009). Furthermore, the target mediating anti-angiogenic activity of miR-92a was demonstrated to be the pro-angiogenic protein integrin subunit alpha5 (ITGA5) (Bonauer et al., 2009). Subsequently, the anti-angiogenic activity of this miR-17-92 cluster was strengthened by the *in vitro* studies that overexpression of miR-17, miR-18a, miR-19a, and miR-20a dramatically inhibited 3-dimensional spheroid cell sprouting and inhibition of miR-17, miR-18a, and miR-20a promoted EC sprout formation (Doebele et al., 2010). However, only the combined antagomir-mediated inhibition of miR-17 and miR-20a *in vivo* significantly enhanced the number of perfused vessels in Matrigel plugs but did not influence tumor angiogenesis (Doebele et al., 2010). Further mechanistic data suggested that miR-17 targets several pro-angiogenic genes including cell cycle inhibitor p21, the S1P receptor EDG1, and the protein kinase Janus kinase 1 (Jak1) (Doebele et al., 2010).

miR-23~27~24 cluster consists of miR-23, miR-27, and miR-24, which are enriched in ECs (Kuehbacher et al., 2007; Zhou et al., 2011). Initially, an angiogenic action of miR-27b was supported by the observation that inhibition of miR-27b significantly reduces EC sprouting *in vitro* (Kuehbacher et al., 2007). Further studies of this microRNA cluster was made by Zhou et al. (2011), in which inhibition of miR-23 and miR-27 function represses angiogenesis *in vitro* and *in vivo*. The angiogenic actions of miR-23 and miR-27 are mediated possibly via repression of Sprouty2 and Sema6A proteins, which exert anti-angiogenic activity (Figure 12) (Zhou et al., 2011). More recently, the angiogenic role of miR-27a and miR-27b in ECs was further supported by two studies (Biyashev et al., 2012; Urbich et al., 2012). Overexpression of miR-27a and miR-27b significantly promoted EC sprouting *in vitro*, while their inhibition impaired EC sprout formation *in vitro* and embryonic vessel formation in zebrafish *in vivo* (Urbich et al., 2012). Mechanistically, miR-27a and miR-27b positively regulate sprouting angiogenesis by repression of the angiogenesis inhibitor Sema6A (Figure 12). In addition, Biyashev et al. (2012) showed that miR-27b turns on the angiogenic switch in zebrafish and mice by promoting endothelial tip cell fate and sprouting (Biyashev et al., 2012). Further mechanistic study confirmed that the positive role of miR-27b in angiogenesis is mediated, at least in part, via its essential targets Sprouty homologue 2 (Spry2) and Dll4 (Figure 12) (Biyashev et al., 2012).

A functional role of miR-10 in angiogenesis was reported in a recent study in zebrafish and human ECs (Hassel et al., 2012). miR-10 activates EC behavior during angiogenesis by positively titrating pro-angiogenic signaling. Specifically, knockdown of miR-10 led to premature truncation of zebrafish intersegmental vessel (ISV) growth, whereas forced overexpression of miR-10 promoted angiogenic behavior in zebrafish and cultured HUVECs (Hassel et al., 2012). Mechanistically, miR-10 functions, at least in part, through repression of membrane-associated Flt1 and its soluble isoform sFlt1, which antagonize the VEGFA-VEGFR2 signaling (Figure 12) (Hassel et al., 2012).

Upregulation of miR-210 in EC is an essential event in response to hypoxia (Figure 12) (Fasanaro et al., 2008). Overexpression of miR-210 promoted tubulogenesis and migration of human ECs in response to pro-angiogenic factor VEGF, whereas inhibiton of miR-210 in ECs blocked tube formation and migration in response to VEGF in both normoxia and hypoxia (Fasanaro et al., 2008). Furthermore, one relevant target mediating the angiogenic action of miR-210 was demonstrated to be the eph-related receptor tyrosine kinase ligand 3 (EphrinA3) in response to VEGF and hypoxia (Figure 12) (Fasanaro et al., 2008). As for the upstream of miR-210, hypoxia triggers hypoxia-inducible factor 1-alpha (HIF1α)-mediated expression of miR-210 in several types of cells including ECs (Fasanaro et al., 2008; Kulshreshtha et al., 2007a; Kulshreshtha et al., 2007b).

miR-296 has recently been identified as a pro-angiogenic microRNA in human brain microvascular ECs (Wurdinger et al., 2008). When co-cultured with angiogenesis stimulating glioma cells, miR-296 was observed to be significantly upregulated in the glioma-induced ECs (Wurdinger et al., 2008). Knockdown of miR-296 resulted in defects in tube branching, tube length, and EC migration in response to pro-angiogenic stimuli such as VEGF (Wurdinger et al., 2008). Further mechanistic analysis identified hepatocyte growth factor-regulated tyrosine kinase substrate (HGS), which degrades VEGFR2 and PDGFR-β, as a target of miR-296, suggesting that pro-angiogenic factors-mediated endothelial activation induces a positive feedback loop that increases the sensitivity of ECs to additional pro-angiogenic stimuli (Figure 12) (Wurdinger et al., 2008).

miR-1 and miR-206 are evolutionarily conserved microRNAs of highly similar sequence, and they share common expression patterns in the muscle from C. elegans to human (Boutz et al., 2007; King et al., 2011; Lagos-Quintana et al., 2001; Lagos-Quintana et al., 2002; Mishima et al., 2009; Sokol and Ambros, 2005; Wienholds et al., 2005). Recently, Stahlhut et al. (2012) supported an anti-angiogenic role for miR-1 and miR-206 during zebrafihs development

(Stahlhut et al., 2012). miR-1 and miR-206 directly regulate the levels of VEGFA in somites, controlling the strength of angiogenic signaling to neighboring ECs (Figure 12).

3.5 Zebrafish model

In recent years, the zebrafish (Danio rerio) has emerged as an excellent model system for studying vertebrate development in many research fields, including vascular development. Zebrafish model offers several advantages, such as the external and rapid development of the embryos, their optical transparency and high fecundity, the short generation time and, very importantly, the genetics, the sequencing of the genome and the high genomic conservation among vertebrates (Jekosch, 2004; Kimmel et al., 1995).

Vascular development in zebrafish proceeds via similar cellular and molecular mechanisms to those in human and other higher vertebrates (Gore et al., 2012; Isogai et al., 2001). Based on the features described above of the zebrafish model, it has become the ideal vertebrate model for studying vascular development *in vivo* (Gore et al., 2012; McKinney and Weinstein, 2008). Specifically, amenability of large-scale forward genetic analysis (ENU- and insertional-mutagenesis) makes zebrafish very helpful for genetic screens to identify vascular-specific mutations in genes regulating vascular development. The external development of the optically transparent zebrafish embryos, combined with the vascular-specific transgenic techniques and confocal imaging techniques, makes them easily accessible to vascular imaging. In addition, reverse genetics approaches in zebrafish allow to directly and rapidly evaluate the functional role of specific genes. One widely used technique for the knockdown of specific gene expression is the injection of modified antisense oligos named "morpholinos", which can block either the translation process ("ATG-morpholinos") or the correct splicing process ("Splice blocking-morpholinos") of individual genes for a few days (Nasevicius and Ekker, 2000). Here I intend to focus on vascular-specific transgenic tools.

3.5.1 Transgenic techniques in vascular research

In transgenic reporter lines, a fluorescent protein (i.e. green fluorescent protein (GFP) and mCherry), expressed under the control of a tissue-specific gene promoter, allows *in vivo* imaging of the organs or cell structures where the endogenous gene expression is normally driven by that promoter. Transgenic zebraifsh lines expressing GFP within vascular ECs have been particularly useful for studying vascular formation *in vivo*. Specifically, a combination of *in vivo* time-lapse imaging analysis and the use of EC-specific transgenic fish lines (such as *Tg(fli1:egfp)^{y1}*, in which GFP is used to label the entire ECs; *Tg(fli1:negfp)^{y7}*, in which GFP is targeted to be localized in the endothelial nuclei; *Tg(kdrl:hras-mcherry)^{s896}*, in which mCherry is used to label the endothelial membrane) facilitates to elucidate vascular patterning and cell dynamics such as cell-migration, cell-division, filopodial extension-retraction, and vascular lumen formation. In addition to being useful for imaging the development of the cardiovascular system, as well as the compilation of morphological atlases, transgenic reporter lines are amenable to forward genetic screening for vascular-specific phenotypes (Jin et al., 2007), and to the systems biology study in zebrafish embryonic ECs when combined with the FACS technique (Covassin et al., 2006; Nicoli et al., 2012).

Additionally, the application of transgenic technology to the zebrafish model results in the ability to spatially and/or temporally control the expression of exogenous signaling molecules. For example, the transgenics can have two constructs in order to be inducible via heat shock and Gal4-UAS system.

3.6 Aim of the study

DLL4-NOTCH signaling pathway is essential to regulate angiogenesis in health and diseases. To date, the paradoxical evidences in treatment of angiogenesis-related tumor with DLL4 disruption raise essential safety concerns and call for refined strategies necessary to harness the DLL4-NOTCH signaling pathway safely as a powerful tool to suppress tumor growth (Hoey et al., 2009; Li et al., 2007; Noguera-Troise et al., 2006; Ridgway et al., 2006; Thurston et al., 2007; Yan et al., 2010). Vascular development is sensitive to subtle alterations in DLL4 dosage (Gale et al., 2004; Trindade et al., 2012), underscoring the potential impact of relatively minor changes in DLL4 dosage on angiogenesis in health and diseases. Thus, in addition to its transcriptional control, DLL4 expression might also be subject to microRNA-guided fine-tuning for functional angiogenesis at the post-transcriptional level. A combinatory analysis of our previous endothelial microRNA profiles by deep sequencing and computational microRNA prediction for *dll4* suggests that *dll4* mRNA might be targeted by endothelial miR-30 family.

In this study, we would like to make the bioinformatics analysis first for better understanding the relationships of all miR-30 family members in vertebrates, and perform functional screen in zebrafish embryos by morpholino-mediated silencing of each miR-30 family member to evaluate their respective functional role in angiogenesis. Then, we will try to elucidate the mechanism of miR-30-mediated fine-tuning of Dll4 expression in zebrafish model. Finally, we hope that the miR-30-mediated regulation of Dll4 expression identified in zebrafish model can be translated to human ECs, providing therapeutic implications for pro- and anti-angiogenic treatment strategies in cardiovascular diseases and cancer.

4 Materials and methods

4.1 Materials

4.1.1 Animal models

Table 1. Zebrafish lines

Transgenic zebrafish line
Tg(fli1:egfp)^{y1}
Tg(fli1:negfp)^{y7}
Tg(kdrl:hras-mcherry)^{s896}
Tg(hsp70:Gal4)
Tg(uas:notch1a-ICD)

(Chi et al., 2008; Isogai et al., 2003; Krueger et al., 2011; Lawson and Weinstein, 2002; Siekmann and Lawson, 2007)

4.1.2 Oligonucleotides

Table 2. Morpholinos from Gene Tools

Morpholino	Sequence
control-MO (15 ng)	5'-CTCTTACCTCAGTTACAATTTATA-3'
dre-miR-30a-MO (15 ng)	5'-CTTCCAGTCGGGAATGTTTACAACT-3'
dre-miR-30a-MO2 (15 ng)	5'-CAACTTCCAGTCGGGAATGTTTACA-3'
dre-miR-30b-MO (15 ng)	5'-AGTGTAGGATGTTTACAGCGACTAC-3'
dre-miR-30c-MO (3.5 ng)	5'-CAGCTGAGAGTGTAGGATGTTTACA-3'
dre-miR-30d-MO (15 ng)	5'-GGGATGTTTACAGGCATGAACAACC-3'
dre-miR-30e-MO (15 ng)	5'-CTTCCAGTCAAGGATGTTTACAGTA-3'
dll4-MO (7 ng)	5'-GTTCGAGCTTACCGGCCACCCAAAG-3'

Table 3. Primers for conventional PCR

Primer	Sequence
pri-miR-30a-For	5'-TGTGTGGGTGGTTCTAGTGG-3'
pri-miR-30a-Rev	5'-GGGAACCCCTGGACTAACAG-3'
pri-miR-30b-For	5'-CAGTTCTGTCGCCTTGTATTACTTT-3'
pri-miR-30b-Rev	5'-AACAACAAACTGCACTCAAATTACA-3'
pri-miR-30c-For	5'-CATTGTTGTTGTTGTTTTGTTTTGT-3'
pri-miR-30c-Rev	5'-GATAGATAGATACGGATGGTTGGAA-3'
pri-miR-30d-For	5'-GGAGAGAGGACCTTTAACTTTCAAC-3'
pri-miR-30d-Rev	5'-GTTTACAGCGACTACACTGGAAGAT-3'
pri-miR-30e-For	5'-CATCGTAGATTTTATGCTGTGTTTG-3'
pri-miR-30e-Rev	5'-CTATCTTGGTCTGAGTGGGAGTAAA-3'
dll4-3'UTR-For (EcoR1)	5'-CCGGAATTCATGAGGAGAGGAGACGCAAA-3'
dll4-3'UTR-Rev (Xho1)	5'-CCGCTCGAGTGGGCACAAACATAGCACTC-3'
dll4-3'UTR(trunc)-For (EcoR1)	5'-CCGGAATTCCCACTGCTGCACTGAGAAAC-3'

For, forward; Rev, reverse; trunc, truncated.

Table 4. Primers and probes for TaqMan PCR

Primer	Sequence	Assay ID
dre-miR-30a	5'-UGUAAACAUUCCCGACUGGAAG-3'	007570_mat
dre-miR-30b	5'-UGUAAACAUCCUACACUCAGCU-3'	000602
dre-miR-30c	5'-UGUAAACAUCCUACACUCUCAG-3'	005548_mat
dre-miR-30d	5'-UGUAAACAUCCCCGACUGGAAG-3'	00420
dre-miR-30e-5p	5'-UGUAAACAUCCUUGACUGGAAG-3'	002223
dre-miR-21	5'-UAGCUUAUCAGACUGGUGUUGGC-3'	006837_mat
hsa-miR-30a-5p	5'-UGUAAACAUCCUCGACUGGAAG-3'	000417

For, forward; Rev, reverse.

4.1.3 Chemicals and kits

Chemicals were purchased from Roth, Invitrogen, or Sigma-Aldrich if not stated otherwise.

Table 5. Kits

Kit	Manufacturer
Zyppy^{TM} Plasmid Miniprep Kit	Epigenetics
QIAGEN$^®$ Plasmid Midi Kit	QIAGEN
Quick-gDNA^{TM} Miniprep Kit	Epigenetics
Zymoclean^{TM} Gel DNA Recovery Kit	Epigenetics
RNeasy Mini Kit	QIAGEN
pGEM$^®$-T Easy Vector System	Promega
TaqMan$^®$ Gene Expression Master Mix	Invitrogen
TaqMan$^®$ MicroRNA Reverse Transcription Kit	Invitrogen
RevertAid First Strand cDNA Synthesis Kit	Thermo SCIENTIFIC
DIG RNA Labeling Kit (SP6/T7)	Roche
mMESSAGE mMACHINE$^®$ SP6/T7 Kit	Invitrogen
Amaxa$^®$ HUVEC Nucleofector$^®$ Kit	Lonza
Lipofectamine$^®$ RNAiMAX Reagent	Invitrogen
Dual-Luciferase$^®$ Reporter Assay System	Promega
3D-Angiogenesis Assay (HUVEC)	PromoCell
Pierce$^®$ BCA Protein Assay Kit	Thermo SCIENTIFIC
ECL Advance Western Blotting Detection Kit	GE Healthcare

4.1.4 Enzymes

Table 6. Enzymes

Enzyme	Manufacturer
Proteinase K	Roche
Pronase	Roche
Taq DNA polymerase	Thermo SCIENTIFIC
Not1	NEB
EcoR1	NEB
Xho1	NEB
Sal1	NEB

4.1.5 Antibodies

Table 7. Antibodies for immunostaining (IS) and Western blotting (WB)

Antibody	Species	Dilution (IS)	Dilution (WB)	Manufacturer
Anti-mCherry	Rabbit	—	1:1000	Clontech
Anti-GFP	Goat	—	1:2000	Abcam
Anti-DLL4	Rabbit	—	1:1000	Cell Signaling
Anti-Digoxigenin-AP	Sheep	1:500	—	Roche
Anti-rabbit IgG-HRP	Goat	—	1:1000	Dako
Anti-goat IgG-HRP	Rabbit	—	1:2000	Sigma-Aldrich

4.2 Methods

4.2.1 Bioinformatics methods

4.2.1.1 Phylogenetic analysis

Five miR-30 family members in each species were obtained from miRBase (http://www.mirbase.org/) as of April, 2012. Multiple sequence alignments of miR-30 family members were generated using Clustal W (Larkin et al., 2007). The phylogenetic tree of primary miR-30 family was constructed using the neighbor-joining method with MEGA5 (Tamura et al., 2011).

4.2.1.2 Synteny analysis

The map locations of the orthologous genes in zebrafish, chick, mouse, and human were obtained from Zebrafish genome view (Zv 9, July 2010), Chicken genome view (Build 2.1, May 2006), Mouse genome view (Build 37.2, March 2011), and Human genome view (Build 37.2, November 2010), respectively.

4.2.2 Molecular biological methods

4.2.2.1 *In situ* hybridization for primary miR-30 family

4.2.2.1.1 Preparation of genomic DNA from zebrafish

30~40 zebrafish embryos (approximately 15 mg) were mechanically homogenized in 500 μl of genomic lysis buffer, and then the genomic DNA was isolated using the Quick-gDNA^{TM} Miniprep Kit according to the manufacturer's instructions. Genomic DNA was eluted in nuclease-free water and the final concentration was measured using the NanoDrop. The quality of isolated DNA was assessed by formaldehyde gel electrophoresis.

4.2.2.1.2 PCR and plasmid construction for riboprobes

The polymerase chain reaction (PCR) primers for the primary transcripts of intergenic *mir-30* family members were designed to span 400–550 nt of genomic DNA centered approximately on the mature sequences of miR-30 family as provided for the zebrafish genome at Ensembl (Zv9, July 2010). Primers and expected sizes of the PCR products are listed in Table 3 and Table 8. The PCR was performed in a Thermo cycler with Taq DNA polymerase and zebrafish genomic DNA (4.2.2.1.1), as displayed in Table 9.

Table 8. Primers for *in situ* probes and sizes of PCR products

PCR name	Forward primer	Reverse primer	Product size
pri-miR-30a	pri-miR-30a-For	pri-miR-30a-Rev	489 bp
pri-miR-30b	pri-miR-30b-For	pri-miR-30b-Rev	416 bp
pri-miR-30c	pri-miR-30c-For	pri-miR-30c-Rev	469 bp
pri-miR-30d	pri-miR-30d-For	pri-miR-30d-Rev	499 bp
pri-miR-30e	pri-miR-30e-For	pri-miR-30e-Rev	440 bp

Table 9. Step-down PCR of templates for *in situ* probes

PCR system		PCR cycle conditions			
		Step	Temperature	Time	Cyc.
Component	**Vol.**	Initial denaturation	95°C	3min	1
10x DreamTaq™ Buff.	5 μl	Denaturation	95°C	30s	2x6*
dNTP Mix, 2mM each	5 μl	Annealing	58,56,55,53,52,51°C	30s	
Forward primer	0.5 μM	Extension	72°C	50s	
Reverse primer	0.5 μM	Denaturation	95°C	30s	23
Taq DNA polymerase	1.25 u	Annealing	50°C	30s	
Genomic DNA	0.5 μg	Extension	72°C	50s	
Water, nuclease-free	to 50μl	Final extension	72°C	8min	1
Total volume	50 μl	Storage	4°C	∞	

2x6*, 2 cycles for each annealing temperature

PCR products for riboprobes were recovered using Zymoclean^TM Gel DNA Recovery Kit according to the manufacturer's instructions, and were subsequently cloned into pGEM®-T Easy vector to generate the pTeasy-pri-miR-30a/b/c/d/e vectors, which were sequenced for determining the orientation of an insert in a cloning and sequence alignment.

4.2.2.1.3 Preparation of Digoxigenin-labeled antisense RNA probes

The pTeasy-pri-miR-30a/b/c/d/e vectors (4.2.2.1.2) were linearized with Sal1 as displayed in Table 10, and used as a DNA template in Dig-labeled RNA probe synthesis reaction according to the manufacturer's instruments as shown in Table 11. Subsequently, the synthesized Dig-labeled RNA probe was digested with DNase1 for the removal of DNA template and purified with RNeasy Mini Kit according to the manufacturer's protocol. Quantity and quality of the synthesized RNA were analyzed by NanoDrop and formaldehyde gel electrophoresis, respectively.

Table 10. Linearization for *in situ* plasmids

Component	Amount
pTeasy-pri-miR-30a/b/c/d/e	2 μg
10x Buffer 3	5 μl
100x BSA	0.5 μl
Sal1	2.5 μl
Water, nuclease-free	to 50 μl
Total volume	50 μl

Table 11. Dig-labeled RNA probe synthesis

Component	Amount
Transcription Optimized 5x Buffer	4 μl
DTT, 100mM	2 μl
RNase inhibitor (20 u)	0.5 μl
Dig RNA Labeling Mix (10x)	2 μl
T7 polymerase (20 u)	1 μl
DNA template (linearized)	1 μg
Water, nuclease-free	to 20 μl
Total volume	20 μl

4.2.2.1.4 Whole-mount *in situ* hybridization

The whole-mount *in situ* hybridization with Dig-labeled RNA probes against primary microRNAs (4.2.2.1.3) was carried out as reported previously (He et al., 2011). Briefly, zebrafish embryos were fixed in 4% paraformaldehyde (PFA) overnight at 4°C, dehydrated in a sequential methanol gradient, and stored in 100% methanol at -20°C for several months. Embryos were rehydrated, permeabilized by Proteinase K treatment, and equilibrated in hybridization buffer for 2 hours at 65°C, which was followed by the hybridization with riboprobes for primary microRNAs at 65°C overnight. After hybridization, the embryos were washed in saline-sodium citrate (SSC) buffer, and equilibrated in blocking solution for 2~3 hours at 4°C, and then incubated with anti-digoxigenin-AP Fab at 4°C overnight. After antibody incubation, embryos were washed in phosphate-buffered saline (PBS) containing 0.1% Tween-20 and 2 mg/ml bovine serum albumin (BSA) for 2 hours, equilibrated in hybridization staining buffer, and then incubated in BCIP/NBT solution (Roche). The pri-miR-30a/b/c/d/e probes require staining for more than 5 hours. The staining reaction was stopped by washing embryos with PBS.

Hybridization buffer

50-65% Formamide, 5x SSC, 0.1% Tween-20, 50 µg/ml Heparin, 500 µg/ml tRNA, Citric acid to pH 6.0 (460 µl of 1M for 50 ml)

Blocking solution

PBS solution containing 0.1% Tween-20, 2 mg/ml BSA, and 5% Sheep serum

Hybridization staining buffer

100 mM Tris pH 9.5, 50 mM $MgCl_2$, 100 mM NaCl, 0.1% Tween-20

4.2.2.2 Gene and microRNA expression analysis by TaqMan PCR

Total RNA of zebrafish embryos of desired developmental stages was isolated with Trizol (Invitrogen) according to the manufacturer's instruments. Quantity and quality of extracted RNA were analyzed using NanoDrop and Agilent 2100 Bioanalyzer (Agilent Technologies) according to the manufacturer's instructions, followed by cDNA synthesis using Thermoscript First-Strand Synthesis System (Thermo SCIENTIFIC), as displayed in Table 12. Amplification was carried out in the ABI Prism 7000 thermocycler (Applied Biosystems), as shown in Table 13. Gene expression data was normalized against Elongation factor 1-alpha (Ef1-α).

Table 12. First strand cDNA synthesis

Component		Amount
Total RNA		3 μg
Random hexamer primer		1 μl
DEPC-treated water		to 11 μl
	Total volume	11 μl

<div align="center">

65°C, 5 min

Chill on ice

</div>

5x Reaction Buffer		4 μl
RiboLock^{TM} RNase Inhibitor (20 u/μl)		1 μl
10mM dNTP Mix		2 μl
M-MuLV Reverse Transcriptase (20 u/μl)		2 μl
	Total volume	20 μl

<div align="center">

25°C, 5 min

37°C, 60 min

Termination: 70°C, 5 min

</div>

Table 13. Universal TaqMan PCR

PCR reaction mix component	Vol. per 20-μl reaction		Cycling conditions		
	Single	Triplicates	Stage	Temp	Time
20x TaqMan® Gene Expr. Assays	1 μl	4 μl	Hold	50°C	2 min
2x TaqMan® Gene Expr. Master Mix	10 μl	40 μl	Hold	95°C	10 min
cDNA template (25 ng/μl)	4 μl	16 μl	40	95°C	15 s
RNase-free water	5 μl	20 μl	Cycles	60°C	60 s

The microRNA reverse transcription reaction was carried out using TaqMan®
MicroRNA Reverse Transcription Kit according to the manufacturer's instructions,
as displayed in Table 14. MicroRNA-specific amplification was performed using
the ABI Prism 7000 thermocycler, as shown in Table 15. For examining the

miR-30 expression in zebrafish embryos, dre-miR-21 was used for normalization. For examining miR-30a expression of human, U6 snRNA assay was used.

Table 14. TaqMan microRNA reverse transcription

Component	Master mix vol. per 15-µl reaction	RT conditions	
		Temp.	Time
100mM dNTPs (with dTTP)	0.15 µl	16°C	30 min
MultiScribe Reverse Transcriptase (50 u/µl)	1.00 µl	42°C	30 min
10x Reverse Transcription Buffer	1.50 µl	85°C	5 min
RNase Inhibitor (20 u/µl)	0.19 µl	4°C	∞
Nuclease-free water	4.16 µl		
RNA sample	5.00 µl		
Primer	3.00 µl		

Table 15. TaqMan PCR for microRNA

PCR reaction mix component	Vol. per 20-µl reaction		Cycling conditions		
	Single	Triplicate	Stage	Temp.	Time
20x TaqMan® Small RNA Assay	1.00 µl	3.60 µl	Hold	95°C	10 min
2x TaqMan® Expr. Master Mix	10.00 µl	36.00 µl	40	95°C	15 s
Product from RT reaction	1.33 µl	4.80 µl	Cycles	60°C	60 s
Nuclease-free water	7.67 µl	27.61 µl			

4.2.2.3 *In vitro* transcription using mMessage mMachine

Plasmids containing *egfp-dll4-3'UTR*, *egfp-dll4-3'UTR (truncated)*, or *mcherry* were linearized and sense-strand-capped mRNA was synthesized with the mMESSAGE mMACHINE Kit according to the manufacturer's instructions, as shown in Table 16. Subsequently, the synthesized capped mRNA was treated with DNase1 for the removal of linear template DNA and purified with RNeasy Mini Kit according to the manufacturer's instructions. Quantity and quality of the

synthesized mRNAs were analyzed with NanoDrop according to the manufacturer's instructions.

Table 16. *In vitro* transcription system

Component	Amount
10x Reaction Buffer	2 μl
2x NTP/CAP	10 μl
Linear template DNA	0.1~1 μg
Enzyme Mix	2 μl
Water, nuclease-free	to 20 μl
Total volume	20 μl

4.2.2.4 Whole-mount microRNA sensor assay

Whole-embryo microRNA sensor assay in zebrafish embryos was carried out as described (Nicoli et al., 2012; Nicoli et al., 2010). Briefly, the pCS2-egfp -dll4-3'UTR construct was generated by cloning nucleotides 2362 to 2975 of the zebrafish *dll4* mRNA (accession NM_001079835) into the pCS2-egfp vector, while pCS2-egfp-dll4-3'UTR (truncated) vector was generated by inserting only nucleotides 2495-2975 of the *dll4* mRNA into the pCS2-egfp vector. The truncated construct lacks the fraction of the *dll4*-3'UTR containing the miR-30 binding site. As an injection control, the pCS2-mcherry vector was used. The sense-strand -capped *egfp-dll4-3'UTR*, *egfp-dll4-3'UTR (truncated)*, and *mcherry* mRNAs were *in vitro* synthesized using the mMESSAGE mMACHINE Kit (4.2.2.3). Eventually, an injection combination of the synthesized mRNAs, together with control precursor or miR-30a precursor (Ambion), was injected into the cytoplasm of 1-2 cell-stage embryos (4.2.5) as displayed in Table 17, followed by further analyses at 24-26 hpf by imaging (4.2.6) and western blot with GFP and mCherry antibodies (4.2.2.5)

Table 17. Whole-mount microRNA sensor assay

Group 1 (per embryo)	Group 2 (per embryo)	Group 3 (per embryo)	Group 4 (per embryo)
egfp-dll4-3'UTR (75 pg)	*egfp-dll4-3'UTR* (75 pg)	*egfp-dll4-3'UTR(trunc)* (75 pg)	*egfp-dll4-3'UTR(trunc)* (75 pg)
mcherry (75 pg)	*mcherry* (75 pg)	*mcherry* (75 pg)	*mcherry* (75 pg)
control-pre (0.025 pmol)	miR-30a-pre (0.025 pmol)	control-pre (0.025 pmol)	miR-30a-pre (0.025 pmol)

4.2.2.5 Western blot

30~40 embryos injected with the *egfp-dll4-3' UTR* (or its truncated form), *mcherry control*, and miR-30a precursor (or control precursor, Ambion) (4.2.2.4) were dechorionated at 24 hpf and homogenized in lysis buffer containing proteinase inhibitor. Total proteins were isolated according to the standard protocol, followed by the measurement of protein concentration using the Pierce[®] BCA Protein Assay Kit and NanoDrop according to the manufacturer's instruments. Subsequently, SDS–PAGE and western blot analyses were performed according to standard procedures. The GFP and mCherry were sequentially detected using goat anti-GFP and rabbit anti-mChery antibodies (4.1.5), respectively, followed by the immunodetection using anti-goat or anti-rabbit IgG-HRP conjugate (4.1.5) and ECL Advanced Western Blotting Detection Kit. Isolation of total proteins from HUVEC was also carried out according to standard procedures. DLL4 level was detected using rabbit anti-DLL4 (4.1.5). Quantification of Western blot signal was performed using ImageJ software.

4.2.2.6 Northern blot

Total RNA was extracted from zebrafish embryos using Trizol (Invitrogen) according to the manufacturer's instruments. Northern blotting for miR-30a was performed as described previously (Lagos-Quintana et al., 2001). Briefly, 10 µg of zebrafish RNA was loaded onto an 12% acrylamide gel with 8 M urea, transferred to positively charged Nylon membrane (GE Healthcare), and hybridized with ^{32}P-end-labeled species-specific LNA probes (Exiqon) at 50°C for 16 hours. For loading control, the gel was stained with ethidium bromide and visualized under UV light.

4.2.2.7 Luciferase assay

Reporter assays in HUVECs were carried out with the Dual-Luciferase Reporter Assay System (Promega) in a Tecan Infinite 200 Pro plate reader. Shortly, 24 hours after co-transfection with the NOTCH luciferase reporters (4.2.3.2), the constitutive Renilla luciferase reporter pGL4.74hRluc/TK (Promega) and miR-30a LNA, cells were lysed and luciferase activity measured as indicated by the manufacturer. Reporter activity was adjusted for the internal Renilla luciferase controls and is expressed as relative to control.

4.2.3 Cellular and histological methods

4.2.3.1 Fluorescence-activated cell sorting and flow cytometry analysis

Tg(fli1:egfp)^{y1} embryos were kept in egg water to indicated developmental stage and dechorionated with 0.5 mg/ml pronase (Roche). Embryos were transferred into a 15-ml falcon tube with 5 ml PBS containing 0.25% trypsin and incubated for 60 min at 28°C during which they were triturated with a 1000-µl pipette tip every 15 min. After centrifuging for 5 min at 800 g at 4°C, cells were resuspended in PBS containing 0.25% trypsin and 15% fetal calf serum (FCS) to stop the

digestion and centrifuged for 5 min at 800 g at 4°C. Cells were rinsed with PBS containing 2% FCS for 2 times and resuspended in PBS at 10^7 cells/ml. FACS was performed on a FACS Aria2 (BD Biosciences), and approximately 1×10^6 positive cells were collected for deep sequencing or quantitative PCR.

4.2.3.2 Cell culture and transfection

Human umbilical vein endothelial cells (HUVECs) were purchased from PromoCell and cultured in EBM-2 media with SingleQuots supplements and Growth factors according to the protocol provide by manufacturer (Lonza).

The NOTCH-regulated luciferase reporter gene constructs TP1 and 4×CBF1 were a generous gift from M. Potente (Guarani et al., 2011). Transient transfections of HUVECs with these constructs were carried out by electroporation with Amaxa® HUVEC Nucleofector® Kit according to the manufacturer's protocol. Transfections of HUVECs with 50 nM miR-30a inhibitors miR-30a LNA (or control LNA, Exiqon), miR-30a antagomir (or control antagomir, Ambion), or with 50 nM miR-30a precursor (or control precursor, Ambion) were performed with Lipofectamine RNAiMAX (Invitrogen) according to the manufacturer's instruments.

4.2.3.3 Spheroid assay

Cell spheroids of defined cell number were generated as briefly described below. 24 hours after transfection, HUVECs were suspended in culture medium containing 0.20% (wt/vol) carboxymethylcellulose (Sigma-Aldrich) and seeded in non-adherent round-bottom 96-well plates (Greiner Bio-One). Under these conditions, all suspended cells contribute to the formation of a single spheroid per well of defined cell number (400 cells/spheroid). Spheroids were generated overnight, after which they were embedded into collagen gels. 500 µl of

spheroid-containing gel was transferred into prewarmed 24-well plates and allowed to polymerize (30 min), after which 50 μl of endothelial growth medium containing 10x SingleQuot supplements and growth factors (Lonza) was added on top of the gel. To stimulate sprouting, 20 ng recombinant human VEGF was added. After 24 hours, spheroids were stained with 50 ng/ml calcein AM (Invitrogen) for 3 hours, then fixed with 4% PFA for 3 hours, and finally DAPI stained for 16 hours. About 7 spheroids were analyzed per experimental group and experiments were repeated 3-5 times.

4.2.4 Animal procedures

4.2.4.1 Zebrafish maintenance

All procedures on live zebrafish were conducted in accordance with the local institutional laws, and the German law for the Protection of Animals. Zebrafish embryos and adult fish were raised and maintained under standard conditions at 28°C, with a constant 14-hour light/10-hour dark lighting cycle. Embryos were obtained by natural mating, and staged as described (Kimmel et al., 1995).

4.2.4.2 Conditional overexpression of NICD *in vivo*

Overactivation of Notch signaling was performed using *Tg(hsp70:Gal4) x(uas:notch1a-ICD)* double transgenic embryos which were heat shocked at 40°C for 20 minutes at the 16-18 somite stage and then kept at 28°C for further experiments (Krueger et al., 2011).

4.2.5 Microinjection

According to standard protocol, antisense morpholino oligomers (MO, Gene Tools) were diluted into Danieau solution. MOs, miR-30a precursor (Ambion), miR-30e duplex (IDT), or synthetic mRNAs were injected into 1-2-cell stage embryos using a Nanoliter 2000 Injector (World Precision Instruments).

Injection dose per embryo of each MO, synthetic mRNA and microRNA precursor was described in Table 2 and Table 17, except for the Notch1-ICD rescue experiments using the *Tg(hsp70:Gal4)x(uas:notch1a-ICD)* double transgenic line (4.2.4.2), in which we used 0.02pmol miR-30a precursor (at higher dosage, embryos died).

Danieau solution

58 mM NaCl, 0.7 mM KCl, 0.4 mM $MgSO_4$, 0.6 mM $Ca(NO_3)_2$, 5 mM HEPES, pH 7.6

4.2.6 Imaging

Zebrafish embryos were anesthetized with egg water/tricaine/PTU (0.016% tricaine (MS-222); 0.003% PTU, Sigma) solution, and embedded in 0.4-0.6% low-melt agarose (Invitrogen). Confocal imaging was performed with Zeiss-510-NLO (or Leica-SP5) microscopes and Zeiss-ZEN (or Leica-LAS-AF) softwares. For the images from microRNA sensor assay (4.2.2.4) and whole-mount *in situ* hybridization assay (4.2.2.1), we used a LEICA-MZ-16FA fluo-microscope and MetaVue software.

5 Results

5.1 miR-30 family is among the most abundant microRNAs in ECs.

The main new findings of Result 5.1

Our endothelial microRNA profiles by deep sequencing revealed microRNAs essential for zebrafish and human vascular development. Further analysis indicates that endothelial miR-30 family (consisting of 5 members miR-30a, miR-30b, miR-30c, miR-30d, and miR-30e) as a whole was among the most abundant endothelial microRNAs in zebrafish and human, with differential endogenous expression patterns of its members. Furthermore, computational microRNA target prediction suggests *dll4*, encoding a central protein during sprouting angiogenesis, as the highest scoring target for miR-30 family.

5.1.1 Endothelial profiles of miR-30 family by deep sequencing

To efficiently identify novel candidate microRNAs which are required for angiogenesis, endothelial microRNA expression profiles were obtained by deep sequencing microRNAs from two types of human ECs, HUVECs and human umbilical artery endothelial cells (HUAECs), and zebrafish embryonic ECs FAC-sorted from *Tg(fli1:egfp)*[y1] embryos at 24 hours post-fertilization (hpf), at which developmental stage there is robust vascular growth. Our microRNA profiles revealed endothelial microRNAs essential for zebrafish and human vascular development (data not shown). Further analysis of the endothelial microRNA profiles indicates differential endogenous expression of miR-30 family members (including miR-30a, miR-30b, miR-30c, miR-30d, and miR-30e), but miR-30 family as a whole was among the most abundant endothelial microRNAs, representing ~3.4% and ~1.7% of all known microRNAs sequences detected in human and zebrafish, respectively (Figure 13).
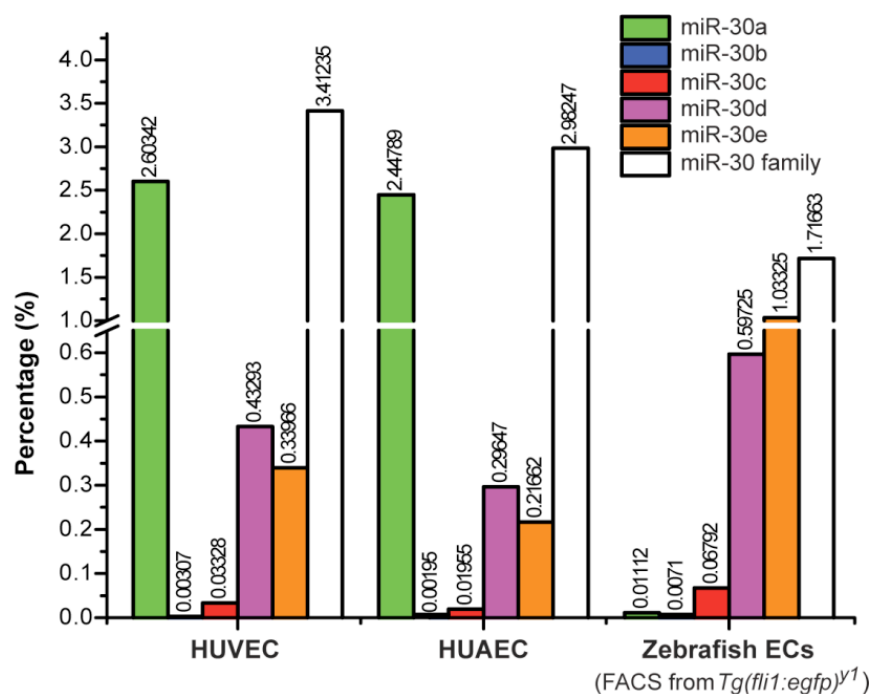
Figure 13. Endothelial profiles of miR-30 family by deep sequencing

miR-30 family members expression, indicated as percentage of known microRNAs identified by deep sequencing microRNA profiling in HUVECs, HUAECs and zebrafish ECs FAC-sorted from $Tg(fli1:egfp)^{y1}$ embryos. White bar shows cumulative percentages of all members of miR-30 family.

5.1.2 Target prediction of miR-30 family in ECs

Once incorporated into a RNA induced silencing complex (RISC) and used as a complementary guide sequence that binds to certain sites within the 3'UTR of its target mRNA, the mature microRNA suppresses target gene expression by leading to the degradation and/or translational repression of target transcripts. Computational microRNA target prediction programs list *dll4* mRNA, encoding a central player during angiogenesis, with the highest scores as a target for miR-30 family members (TargetScan version 6.2 (http://www.targetscan.org) and PicTar (pictar.mdc-berlin.de)) (Figure 14). In addition, we also turned to an endothelial autonomous microRNA sensor fish *Tg(fli1ep:egfp;mCherry-dll4-3'UTR)*, in which the bidirectional *fli1ep* promoter drives EGFP and mCherry-dll4-3'UTR expression in ECs during zebrafish embryogenesis. We observed that mCherry-dll4-3'UTR expression in *Tg(fli1ep:egfp;mCherry-dll4-3'UTR)* embryos was significantly downregulated when compared with the mCherry-ctrl-3'UTR expression in *Tg(fli1ep:egfp; mCherry-ctrl-3'UTR)* embryos (data not shown), suggesting that endothelial expression of Dll4 is probably fine-tuned by endothelial microRNAs in zebrafish embryos.

Figure 14. Computational target prediction of miR-30 family

Alignment of the mature miR-30 family from zebrafish and human miR-30a. Note the conserved sequences (particularly the seed sequences) across species.

5.2 Bioinformatic analyses of miR-30 family

The main new findings of Result 5.2

A combinatory analysis of our endothelial microRNA profiles and online microRNA database indicates that *mir-30* family consists of five members *mir-30a*, *mir-30b*, *mir-30c*, *mir-30d*, and *mir-30e* in zebrafish, chick, mouse, and human, with two *mir-30c* copies (*mir-30c-1* and *mir-30c-2*) in chick, mouse, and human. Construction of the phylogenetic tree of primary miR-30 family suggests that miR-30 family members clustered into five clades in vertebrates, with an exception for zebrafish miR-30a falling into the miR-30d clade. Furthermore, genomic environment analysis for *mir-30* family indicates that there are highly conserved syntenies of *mir-30* family members across species. Although *mir-30* family members have the same origin in vertebrates, zebrafish *mir-30a* might undergo some special evolutionary process.

5.2.1 Phylogenetic tree of primary miR-30 family in species

Online microRNA database indicates that zebrafish owns five miR-30 family members: miR-30a, miR-30b, miR-30c, miR-30d, and miR-30e-2 (namely, miR-30e), but there are two *mir-30c* copies (*mir-30c-1* and *mir-30c-2*) in chick, mouse, and human genome. To understand the relationships of the zebrafish miR-30 family members to each other and to those of other vertebrates, a phylogenetic tree was constructed using multiple alignments of homologous primary microRNAs belonging to zebrafish (Danio rerio/DR), chick (Gallus gallus/GG), mouse (Mus musculus/MM), and human (Homo sapiens/HS) (Figure 15). The miR-30 family members clustered into five clades, with the zebrafish primary miR-30b, miR-30c, miR-30d and miR-30e falling into different clades, except for zebrafish primary miR-30a, which falls into the primary miR-30d clade.
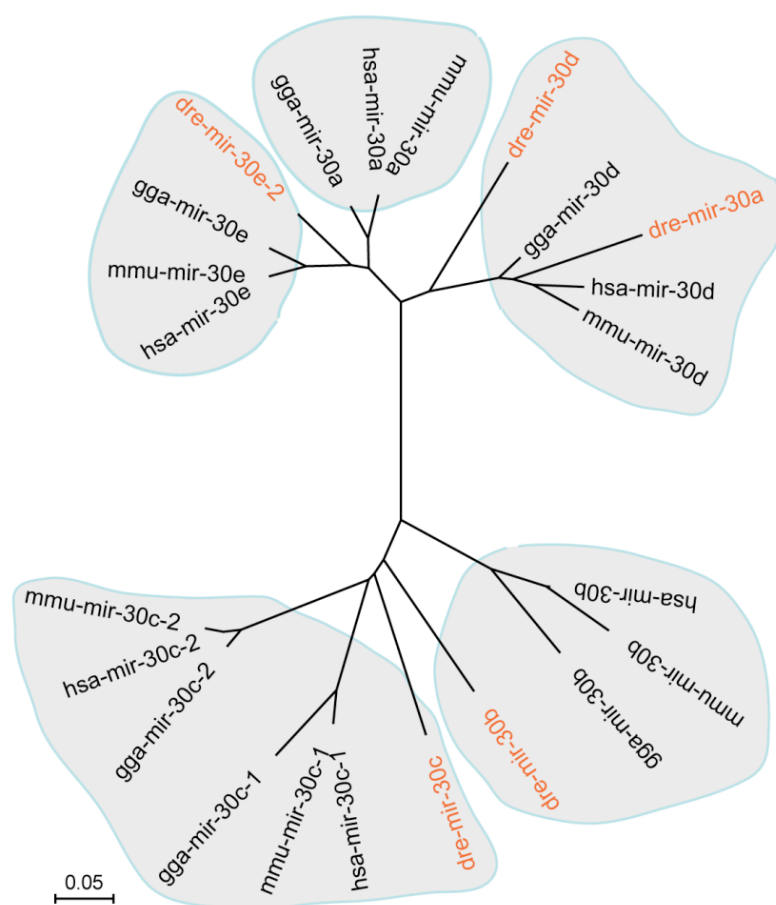
**Figure 15. Phylogenetic tree of primary miR-30 family in species**

A phylogenetic tree of selected zebrafish, chick, mouse and human primary miR-30 family was constructed using a neighbor-joining algorithm and displayed in radial format. The primary miR-30 family members clustered into five clades, with the zebrafish primary miR-30b, miR-30c, miR-30d and miR-30e falling into different clades, except for zebrafish primary miR-30a, which falls into the primary miR-30d clade. Zebrafish miR-30 family is highlighted in brown letters. Scale bar indicates substitutions per site. Accession: dre-mir-30a (MI0001940), dre-mir-30b (MI0001941), dre-mir-30c (MI0001944), dre-mir-30d (MI0001946), dre-mir-30e-2 (also named dre-mir-30e, MI0001950); gga-mir-30a (MI0001204), gga-mir-30b (MI0001199), gga-mir-30c-1 (MI0001257), gga-mir-30c-2 (MI0001205), gga-mir-30d (MI0001198), gga-mir-30e (MI0001256); mmu-mir-30a (MI0000144), mmu-mir-30b (MI0000145), mmu-mir-30c-1 (MI0000547), mmu-mir-30c-2 (MI0000548), mmu-mir-30d (MI0000549), mmu-mir-30e (MI0000259); hsa-mir-30a (MI0000088), hsa-mir-30b (MI0000441), hsa-mir-30c-1 (MI0000736), hsa-mir-30c-2 (MI0000254), hsa-mir-30d (MI0000255), hsa-mir-30e (MI0000749).

5.2.2 Genomic environment analysis for *mir-30* family in species

In addition to harboring similar coding sequences, evolutionarily conserved genes are often present in a similar genomic context. To investigate the degree of locus conservation, we performed a comparative synteny analysis of the *mir-30* family members in four genomes available using 5-8 genes that seem to be linked to *mir-30* family members, which revealed a conserved synteny around these loci (Figure 16). A set of *mir-30b* and *mir-30d* is located on Chromosome 16 at ~27.60 Mb (zebrafish, Zv9), on Chromosome 2 at ~148.30 Mb (chick, WASHUC2), on Chromosome 15 at ~68.20 Mb (mouse, NCBIM37), and on Chromosome 8 at ~135.80 Mb (human, GRCh37), respectively. A graphic view of the syntenic relationships in zebrafish, chick, mouse, and human is shown in Figure 16A. In particular, chick, mouse, and human maintain the same gene order for nine genes including *WISP1* (*WNT1 inducible signaling pathway protein 1*), *NDRG1* (*N-myc*

downstream regulated 1), *ST3GAL1* (*sialyltransferase 4A*), *ZFAT* (*zinc finger protein 406*), *mir-30b*, *mir-30d*, *KHDRBS3* (*KH domain containing, RNA binding, signal transduction associated 3*), *KCNK9* (*potassium channel subfamily K member 9, Kcnk9l in chick*), and *TRAPPC9* (*trafficking protein particle complex 9*). However, inversion is observed for three genes (including *zfat*, *ndrg1l*, and *wisp1b*) neighboring *mir-30b* and *mir-30d* in the zebrafish chromosome 16 region (Figure 16A).

The *mir-30c-1* and *mir-30e* cluster, as the intragenic microRNAs of the *NFYC* (*nuclear transcription factor Y, gamma*) gene, is present on Chromosome 23 at ~5.30 Mb (chick), on Chromosome 4 at ~120.40 Mb (mouse), and on Chromosome 1 at ~41.20 Mb (human), respectively. Particularly, a set of genes flanking *mir-30c-1* and *mir-30e* includes *CTPS* (*CTP synthase*), *CITED4* (*Cbp/p300-interacting transactivator, with Glu/Asp-rich carboxy-terminal domain, 4*), *COL9A2* (*collagen, type IX, alpha 2*), *SMAP2* (*small ArfGAP2*), *RIMS3* (*regulating synaptic membrane exocytosis 3*), *NFYC*, and *KCNQ4* (*potassium voltage-gated channel, KQT-like subfamily, member 4*), although the gene order was completely inverted in mouse Chromosome 4 region (Figure 16B). Surprisingly, the conserved syntenic relationships among *CTPS*, *CITED4*, *COL9A2*, *SMAP2*, *RIMS3*, *NFYC*, *KCNQ4* in chick, mouse, and human point to the zebrafish Chromosome 19 region, upstream of which *mir-30a* gene is located (on Chromosome 19 at ~4.50 Mb), rather than *mir-30c* (namely *mir-30c-1*) and *mir-30e* (namely *mir-30e-2*) cluster, which is located on Chromosome 13 at ~28.00 Mb (Figure 16B and C). In addition, zebrafish *TRAPPC9*, *KCNK9*, *wisp1a*, and *ndrg1* genes neighboring zebrafish *mir-30a* were observed in the neighborhood of *mir-30b* and *mir-30d* cluster from chick, mouse, and human (Figure 16A and B).
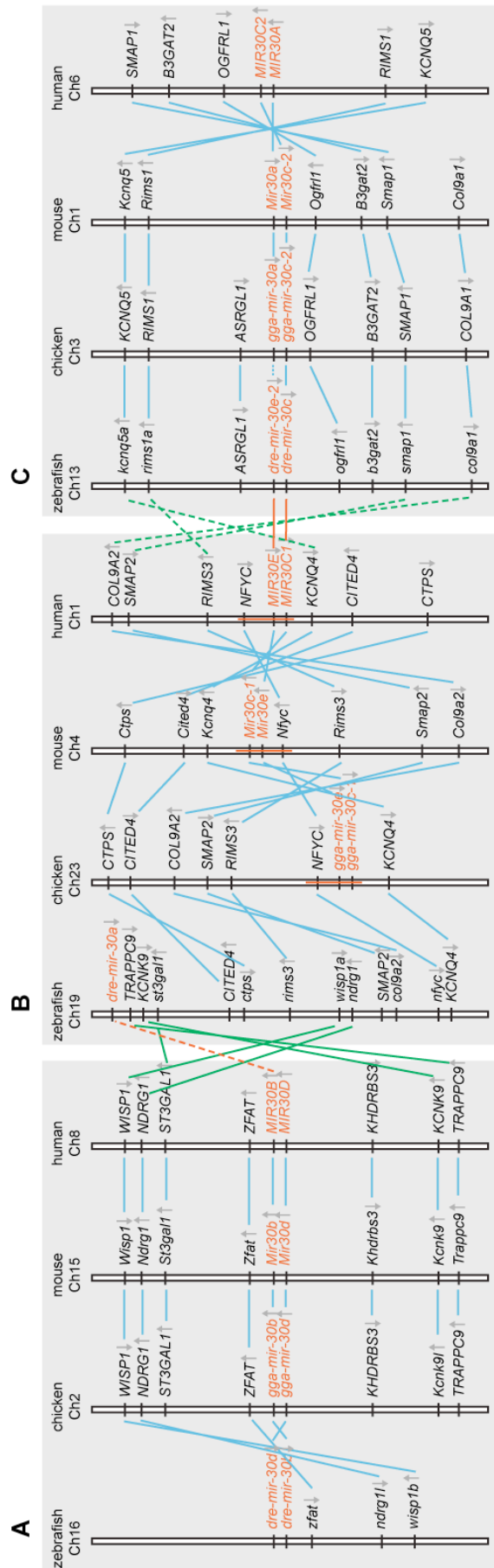
Figure 16. Conserved syntenies of *mir-30* family in species

(A-C) Chromosomal arrangement of conserved neighboring genes surrounding each *mir-30* family member gene locus in zebrafish, chicken, mouse, and human. *mir-30* family members are highlighted in brown letters. Solid lines between the compared chromosomes connect positions of orthologous gene pairs in the two species. Dashed lines indicate possible orthology relationships. Arrows indicate the direction of gene transcription. See details in the text.

Basically, chick and mouse keep the identical gene order for eight genes including *KCNQ5* (*potassium voltage-gated channel, KQT-like subfamily, member 5*), *RIMS1* (*regulating synaptic membrane exocytosis 1*), *mir-30a*, *mir-30c-2*, *OGFRL1* (*opioid growth factor receptor-like 1*), *B3GAT2* (*β-1,3-glucuronyl-transferase 2*), *SMAP1* (*small ArfGAP 1*), and *COL9A1* (*collagen, type IX, alpha 1*), whereas inversion is observed for almost all these genes flanking *MIR30C2* and *MIR30A* cluster in human chromosome 6 region (Figure 16C). Coincidentally, the conserved syntenic relationships in chick and zebrafish among a set of genes including *KCNQ5*, *RIMS1*, *ASRGL1* (*asparaginase like 1*), *OGFRL1*, *B3GAT2*, *SMAP1*, and *COL9A1*, which flank the chicken *mir-30a* and *mir-30c-2* cluster, point to zebrafish Chromosome 13 region, where zebrafish *mir-30e* and *mir-30c* cluster is flanked by these genes (Figure 16C). Interestingly, some genes belonging to the same family, including *KCNQ*, *RIMS*, *SMAP*, and *COL9A* family were observed in the region covering the *mir-30a* and *mir-30c-2* cluster, or the *mir-30e* and *mir-30c-1* cluster (Figure 16B and C).

5.3 miR-30a is required for angiogenesis during zebrafish embryogenesis

The main new findings of Result 5.3

miR-30 family has the same seed sequence and almost the identical predictable interaction with their target transcripts. We performed functional screen using morpholino-mediated knockdown technique to evaluate the angiogenic role for each miR-30 family member in zebrafish embryos *in vivo*, and found that only miR-30a-deficient embryos exhibit a high percentage of angiogenic defects, such as short ISVs.

5.3.1 Efficiency evaluation for morpholinos-mediated knockdown of each miR-30 family member expression

Reverse genetics approaches in zebrafish model allow to directly and efficiently evaluate the consequence of the loss of protein-coding genes or microRNAs. One widely used tool in zebrafish for the transient knockdown of specific microRNA expression is the injection of morpholino antisense oligos, which can block the maturation of microRNAs by binding to the Guide Drosha site, Guide Dicer site, or mature microRNA site (Figure 17A). We designed and injected MOs to embryos at one-cell stage, which were analyzed within the first 36 hpf (Figure 17B). According to the surviving rate, overall morphology and vascular phenotypes of each miR-30 family member morphant, we chose a proper injection dose for each MO targeting miR-30 family member for further analysis (Figures 17C and 18B). Moreover, microRNA-specific TaqMan assay demonstrated that each MO can efficiently block the maturation of its corresponding miR-30 family member (Figure 17C). Given the high early death rate of embryos injected with the same dose of miR-30c-MO as other miR-30-MOs (15 ng per embryo), we have to reduce miR-30c-MO injection dose to 3-4 ng per embryo for their surviving.

Figure 17. Efficiency evaluation for morpholino-mediated loss-of-function and gain-of-function, and miR-30a expression pattern

(A) Schematic strategy for morpholinos blocking the maturation of specific microRNAs. Modified from Gene Tools. (B) Schematic position of the direct

binding of each MO with its corresponding miR-30 family member. (C) Efficiency evaluation of MO-mediated knockdown of each miR-30 family member by TaqMan analysis. a, b, c, d, and e above the bars represent mature miR-30a, miR-30b, miR-30c, miR-30d, and miR-30e expression, respectively. (D) Northern blot for miR-30a in control and miR-30a morphants. (E) Mature miR-30a expression after injection of miR-30a-precursor. (F) Expression of the primary miR-30a transcript (pri-miR-30a) in a 24hpf zebrafish embryo as detected by *in situ* hybridization, in whole-mount (top panel, higher magnification of blue boxed area is presented in bottom left panel) and cross-section (anatomical position indicated by red line in top panel, in bottom right panel). The high magnification lateral view (bottom left) shows miR-30a expression in the dorsal aorta. Abbreviations: nt, neural tube; nc, notochord; da, dorsal aorta; cv, cardinal vein; pd, pronephric duct. MO sequence is indicated in green line, and mature microRNA sequence is highlighted in pink.

5.3.2 Functional screen using morpholinos to silence each miR-30 family member

To assess the function of each miR-30 family member, we injected a proper dose of MOs to block their maturation and observed vascular and overall morphology in *Tg(fli1:egfp)^{y1}* embryos. MO-mediated knockdown of miR-30a affected angiogenesis, whereas no significant effects on intersegmental vessel (ISV) development were noted with MOs for miR-30b, miR-30c, miR-30d, or miR-30e (Figure 18A and B). A second MO targeting miR-30a (miR-30a-MO2) was used and we found that miR-30a-MO2-mediated knockdown led to the similar high percentage of angiogenic defects phenotype (short ISVs) to that of miR-30a-MO-injected embryos (Figure 18C). Moreover, expression of miR-30a in zebrafish was validated by Northern blotting, Taqman analysis, and whole-mount *in situ* hybridization (Figure 17D and F). Based on our strong interest in identifying endothelial microRNAs involved in angiogenesis, we investigated the function of miR-30a in greater details.
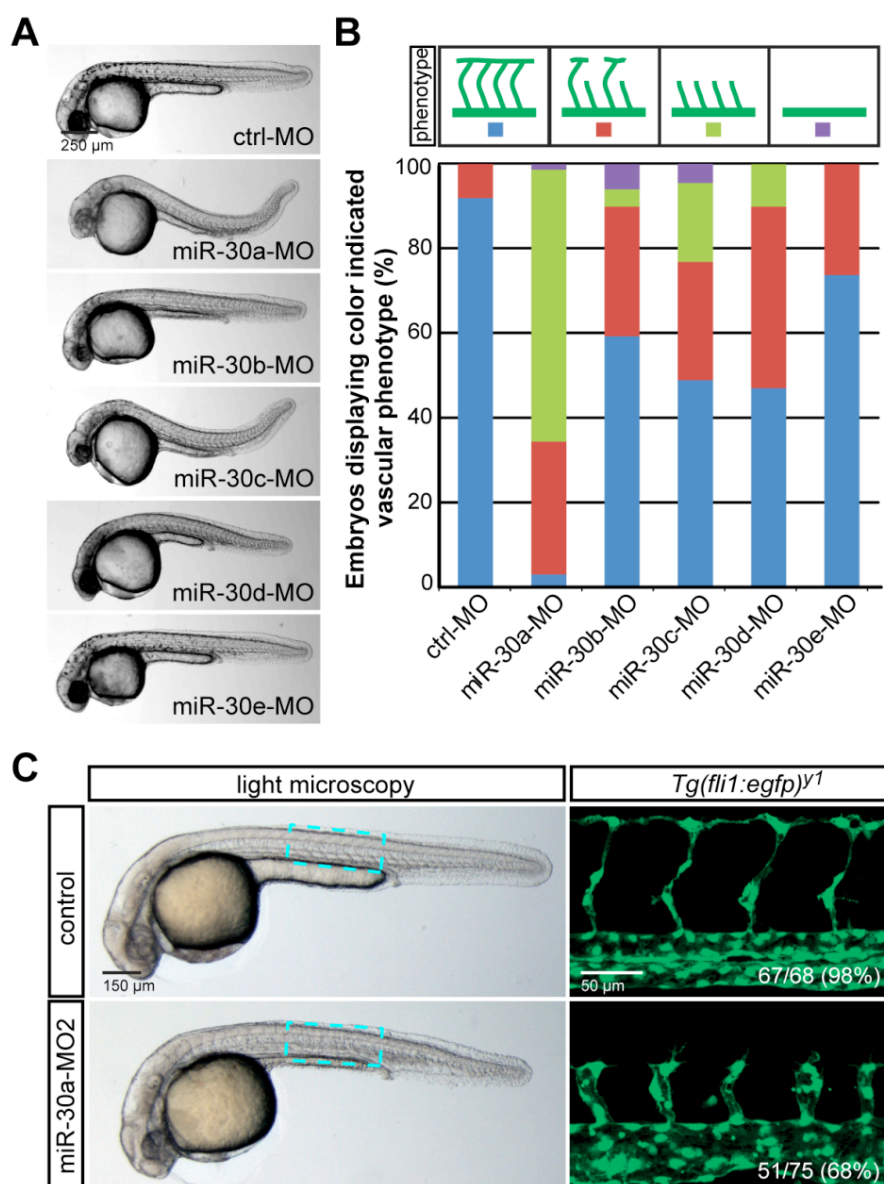
Figure 18. Functional screen via morpholinos to silence each miR-30 family member during zebrafish embryogenesis

(A) Representative light microscopic images of *Tg(fli1:egfp)^{y1}* zebrafish embryos injected with control-MO, or injected with miR-30a, b, c, d, or e morpholino as indicated. (B) Occurence of ISV phenotypes in *Tg(fli1:egfp)^{y1}* zebrafish embryos injected with control-MO, or injected with miR-30a, b, c, d, or e morpholino as indicated. The vascular phenotypes are color indicated and schematically represented in the top panel part. Note that reduced ISV sprouting is most prominent in the miR-30a morphants. Measurements from n=40-60

embryos/group. (C) *Tg(fli1:egfp)^{y1}* embryos injected with miR-30a-MO2 show reduced ISV sprouting. Left panels, light microscopic images, confocal images of the boxed areas are shown at high magnification in the right panels. Numbers at bottom right indicate the fraction of embryos showing the phenotype presented in the image.

5.4 miR-30a promotes zebrafish sprouting angiogenesis by targeting *dll4* and inhibiting Notch signaling

The main new findings of Result 5.4

Previous evidence indicated that silencing of miR-30a resulted in short ISVs in zebrafish embryos. However, the miR-30a-mediated mechanism underlying the angiogenic behavior of ISVs is unknown. Through systemic inspection of the angiogenic phenotypes in miR-30a loss-of-function and gain-of-function embryos using different vascular-specific transgenic zebrafish lines including *Tg(fli1:egfp)^{y1}* and *Tg(fli1:negfp)^{y7}* x *Tg(kdrl:hras-mchery)^{s896}*, we found that miR-30a knockdown resulted in reduced ISV length, with fewer ECs and less tip cell filopodial extensions, whereas forced overexpression of miR-30a displayed ISV hyperbranching, with more ECs and tip cell filopodial extensions. Time-lapse analysis suggested that the angiogenic phenotype of more ECs in the ISVs of miR-30a gain-of-function embryos is due to enhanced endothelial proliferation and migration from dorsal aorta to ISVs. Furthermore, microRNA sensor assay confirmed the direct interaction of miR-30a with *dll4*-3'UTR. Finally, two alternative rescue studies indicated that normalization of Dll4-Notch signaling could, at least in part, restore the angiogenic defects in miR-30a loss-of-function and gain-of-function embryos. Taken together, these findings demonstrated that miR-30a enhances sprouting angiogenesis in zebrafish embryos by targeting *dll4* and inhibiting Notch signaling.

5.4.1 miR-30a acts as a positive modulator of sprouting angiogenesis in zebrafish embryos.

We systematically performed miR-30a loss-of-function and gain-of-function experiments in zebrafish *Tg(fli1:egfp)^{y1}* embryos and examined ISV branching morphogenesis (Figure 19). MO-mediated knockdown of miR-30a reduced ISV sprouting when compared to age-matched controls (Figures 18C and 19A-D). In miR-30a morphants, sprouts usually failed to cross the horizontal myoseptum and as a consequence, formation of the dorsal longitudinal anastomotic vessel (DLAV) was severely disturbed (Figure 19C' and D). Closer observation indicated that tip cell filopodial extensions of ISVs appeared smaller and fewer in miR-30a morphants than in control embryos (Figure 19A'' and C'').
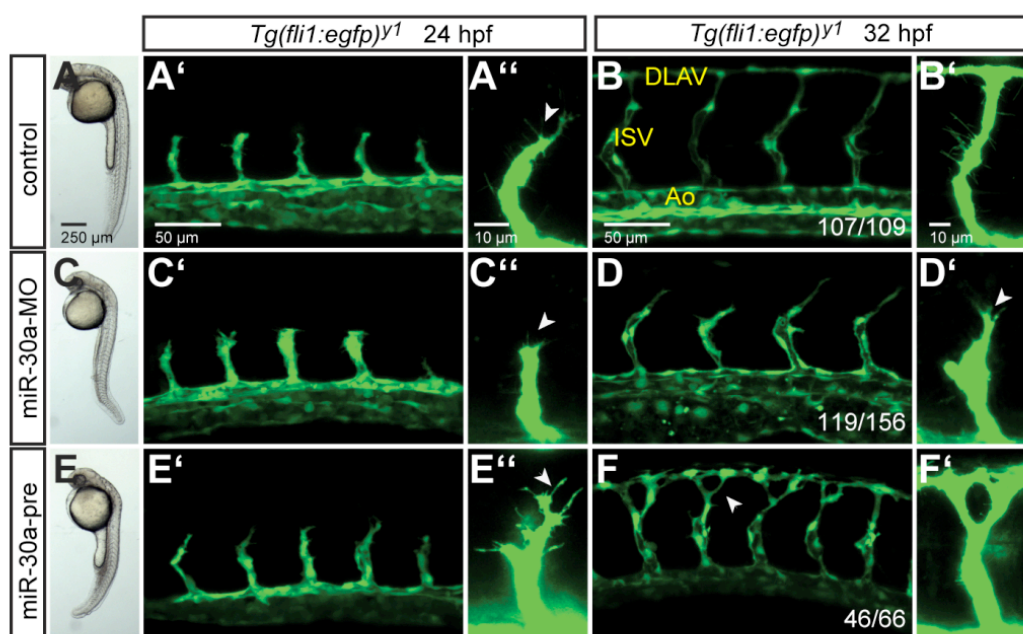
Figure 19. miR-30a regulates ISV branching in zebrafish embryos

(A, C, E) Light microscopy images of embryos at 32 hpf injected with miR-30a-MO or miR-30a-precursor as indicated. (A', C', E') Confocal stack images of trunk vessels at 24 hpf; and (B, D, F) at 32 hpf in *Tg(fli1:egfp)^{y1}* embryos. miR-30a

morphants show reduced ISV sprouting (D) and reduced filopodia extensions (C'',

D', arrowhead). miR-30a overexpression induced ISV hyperbranching at 32 hpf

(F, F') and augmented tip cell filopodia (E'', arrowhead). DLAV, dorsal longitudinal

anastomotic vessel; Ao, aorta; ISV, intersegmental vessel.

Injection of miR-30a precursor (miR-30a-pre) increased miR-30a expression as

evidenced by real time PCR; on average mature miR-30a levels were increased

by 15-fold at 36 hpf (Figure 17E). miR-30a overexpression induced ISV

hyperbranching, predominantly in the most dorsal aspect (Figure 19F and F').

Detailed examination showed that endothelial tip cell filopodial extensions of ISV

sprouts appeared more abundant in miR-30a gain-of-function embryos than in

control embryos (Figure 19A'' and E''). Both the timing and the anatomical position

of the hyperbranched ISVs are reminiscent of the vascular phenotypes reported in

zebrafish Dll4 loss-of-function embryos (Leslie et al., 2007).

5.4.2 Overexpression of miR-30a increases EC number in zebrafish ISVs

To observe the angiogenic defects in EC number in embryos overexpressing

miR-30a, we turned to $Tg(fli1:negfp)^{y7}$x $Tg(kdrl:hras-mchery)^{s896}$ double

transgenic zebrafish line, which allows us to better visualize the endothelial nuclei

in green and blood vessels in red (Figure 20). We noted that overexpression of

miR-30a enhances the EC number in ISVs, which is reminiscent of the angiogenic

phenotypes in Dll4-Notch signaling-deficient embryos (Leslie et al., 2007;

Siekmann and Lawson, 2007).
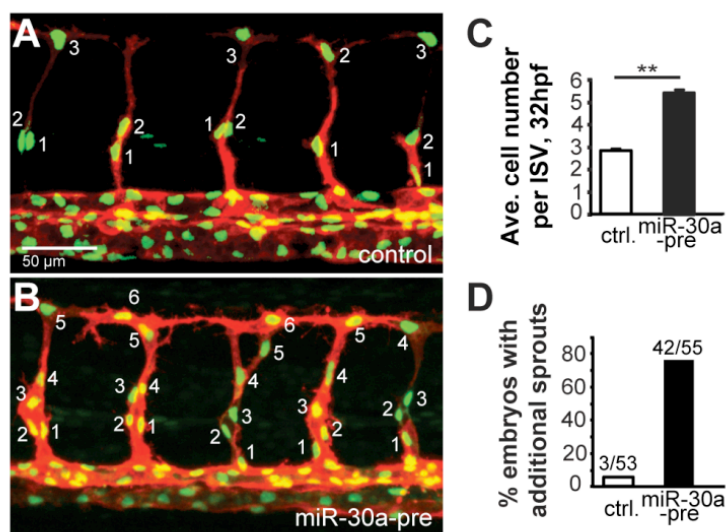
Figure 20. Enhanced EC number in ISVs of miR-30a gain-of-function embryos

(A, B) Imaging of endothelial nuclei in control and embryos overexpressing miR-30a using *Tg(fli1:negfp)^{y7}xTg(kdrl:hras-mCherry)^{s896}* double transgenic embryos at 32 hpf.   Numbers denote EC nuclei, vessels in red. (C) Quantification of EC numbers per ISV. (D) Quantification of hypersprouting. Data are presented as mean ± standard error; measurements from 4 adjacent ISVs/embryo, n=20 embryos, **, P<0.01; Student's t-test.

5.4.3 miR-30a promotes endothelial proliferation and migration in zebrafish ISVs

Previous studies indicated that Dll4-Notch signaling-deficient embryos display more ECs in the ISVs via promoting endothelial proliferation and/or migration (Siekmann and Lawson, 2007). To investigate if the angiogenic phenotype of more ECs in the ISVs of miR-30a gain-of-function embryos is due to much more endothelial migration, enhanced proliferative activity of ECs, or both, we performed the time-lapse confocal microscopy on embryos overexpressing miR-30a using *Tg(fli1:negfp)^{y7}*x *Tg(kdrl:hras-mchery)^{s896}* transgenic line (Figure 21). Our observation indicates enhanced endothelial migration from dorsal aorta to ISVs and increased endothelial proliferation in miR-30a-pre-injected embryos

from 22 hpf to 30 hpf, further demonstrating its consistency with loss of Dll4-Notch signaling in this model (Siekmann and Lawson, 2007).
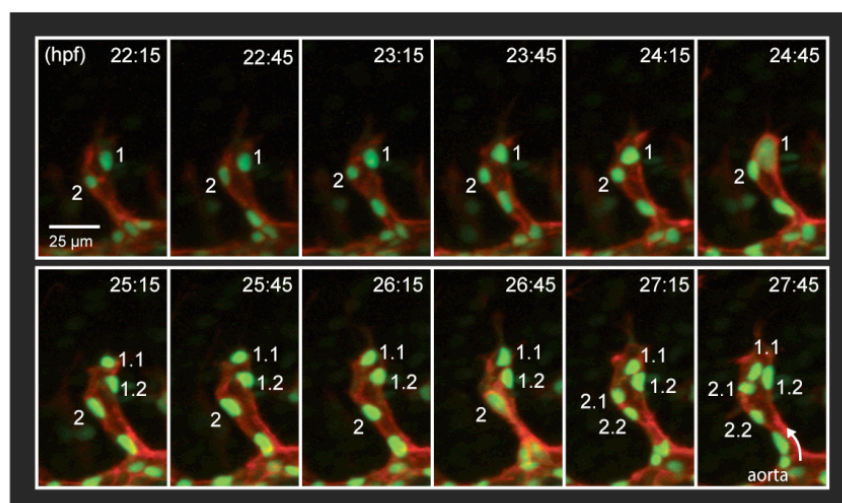
Figure 21. Time-lapse analysis indicates that miR-30a enhances endothelial proliferation and migration in zebrafish ISVs

Time-lapse images of *Tg(fli1:negfp)^{y7}xTg(kdrl:hras-mCherry)^{s896}* double transgenic embryos injected with miR-30a-pre. Time (hpf) is indicated in top right corner; nuclei are numbered and decimals indicate daughter cells arising from cell division.

5.4.4 miR-30a activates subintestinal angiogenesis in zebrafish embryos

Here we would like to know if changes of miR-30a expression could influence the growth of subintestinal vasculature given that too much subintestinal angiogenesis was also observed in Dll4 deficient zebrafish embryos (Leslie et al., 2007). Using *Tg(fli1:egfp)^{y1}* embryos, we observed that miR-30a morphants showed reduced subintestinal vessel (SIV) branching, whereas miR-30a gain-of-function resulted in SIV hyperbranching (Figure 22). These observations are consistent with the implication of Dll4 as a negative regulator of zebrafish SIV development (Leslie et al., 2007).
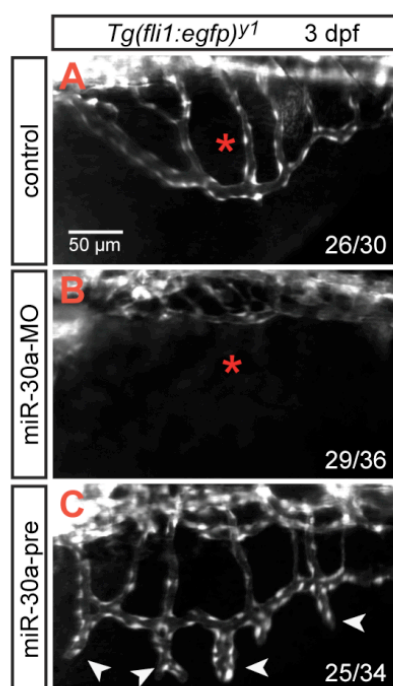
Figure 22. miR-30a promotes subintestinal vessel (SIV) branching in zebrafish

miR-30a morphants at 3 dpf (B, asterisk) show reduced SIV branching versus control (A, asterisk); miR-30a overexpression augmented SIV branching (C, arrowheads). Bottom right corner: fraction of embryos with phenotype similar to image.

5.4.5 miR-30a directly targets *dll4*-3'UTR and inhibits its expression

The miR-30a loss-of-function and gain-of-function experiments suggested that miR-30a acts as a positive modulator to control angiogenic sprouting. Previous reports indicated that Dll4-Notch signaling functions as a negative regulator of sprouting angiogenesis in this setting (Leslie et al., 2007; Siekmann and Lawson, 2007), and *in silico* analysis predicted the direct binding of miR-30a with *dll4*-3'UTR (Figures 14 and 23A). Given the similarities between the vascular phenotypes of miR-30a loss-of-function and gain-of-function embryos and Dll4-Notch signaling gain-of-function and loss-of-function, respectively, and the

predicted interaction of miR-30a with *dll4*-3'UTR, we reasoned that *dll4* transcript might be a functional target of miR-30a during zebrafish ISV angiogenesis.

Theoretically, miR-30a can bind to miR-30 binding site within the 3'UTR of the target *dll4* mRNA, eventually leading to the degradation and translational inhibition of the *dll4* mRNA (Figure 23A). Therefore, we performed the microRNA sensor assay to demonstrate the functional interaction of miR-30a with *dll4*-3'UTR. In this assay, we constructed three plasmids: in the first one, the intact *dll4*-3'UTR containing miR-30 binding site was inserted after GFP; in the second one, the truncated *dll4*-3'UTR lacking miR-30 binding site was inserted after GFP; in the last one, there was no *dll4*-3'UTR inserted after mCherry (Figure 23A). We injected a GFP-dll4-3'UTR- or a GFP-dll4-3'UTR (truncated) RNA (lacking a miR-30 binding site) into zebrafish embryos at 1-2-cell stage, together with a mCherry injection control RNA and miR-30a precursor or control (Figure 23). In the GFP-dll4-3'UTR RNA-injected embryos, overexpression of miR-30a reduced GFP expression as evidenced by *in vivo* imaging analysis (Figure 23B), and by Western blot analysis using GFP and mCherry antibodies (Figure 23C). Deleting the miR-30 binding site in the *dll4*-3'UTR annihilated this response (Figure 23B and C). Taken together, the microRNA sensor assay suggests that miR-30a directly targets *dll4* and inhibits, at least in part, its expression.
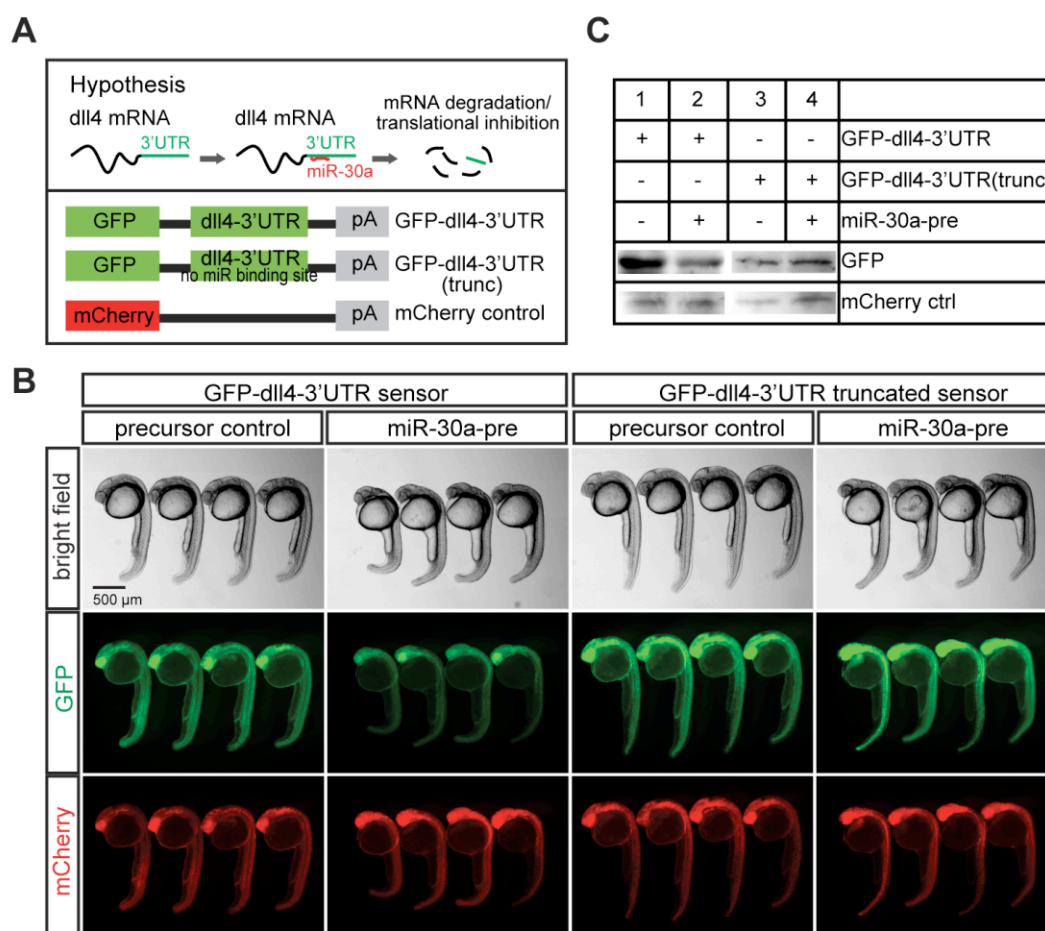
Figure 23. miR-30a targets *dll4*-3'UTR and inhibits its expression

(A) Schematic representation of the hypothesis that degradation and/or translational inhibition of *dll4* mRNA be induced by the interaction of *dll4*-3'UTR with miR-30a (upper panel). Schematic representation of GFP sensor constructs containing the zebrafish *dll4*-3'UTR or truncated *dll4*-3'UTR without miR-30 binding site; and the mCherry injection control lacking *dll4*-3'UTR (lower panel). (B) GFP sensors were co-injected with mCherry control as indicated. miR-30a-precursor injection reduced GFP levels in GFP-dll4-3'UTR sensor (second column) while mCherry levels were unchanged. In the truncated sensor, no reduction in GFP was noted. (C) Western blot analysis of GFP and mCherry expression in whole 24hpf embryos. miR-30a reduced GFP in wild-type (lanes 1, 2) but not in truncated *dll4*-3'UTR (lanes 3, 4).

5.4.6 miR-30e promotes sprouting angiogenesis by targeting *dll4*

The miR-30 family members share the same seed, predicting that they all probably be capable of targeting *dll4* mRNA. To demonstrate that this is the case, we selected miR-30e (the most abundant member in zebrafish) (Figure 13). Overexpression of miR-30e induced ISV hyperbranching both in *Tg(fli1:egfp)^{y1}* embryos and in *Tg(fli1:negfp)^{y7}xTg(kdrl:hras-mCherry)^{s896}* double transgenic zebrafish embryos (Figure 24A-E). Similar to miR-30a gain-of-function, miR-30e gain-of-function embryos also showed more ECs per ISV than the control embryos did (Figures 20, 24A, and 24B). Furthermore, in sensor assays overexpression of miR-30e in GFP-dll4-3'UTR RNA-injected embryos reduced GFP expression (Figure 24F), and elimination of the miR-30 binding site in the *dll4*-3'UTR reporter annihilated this response (Figure 24F). Taken together, miR-30e and miR-30a share the same seed, and miR-30e can also target *dll4* and exogenously stimulates angiogenic cell behavior in zebrafish embryos.
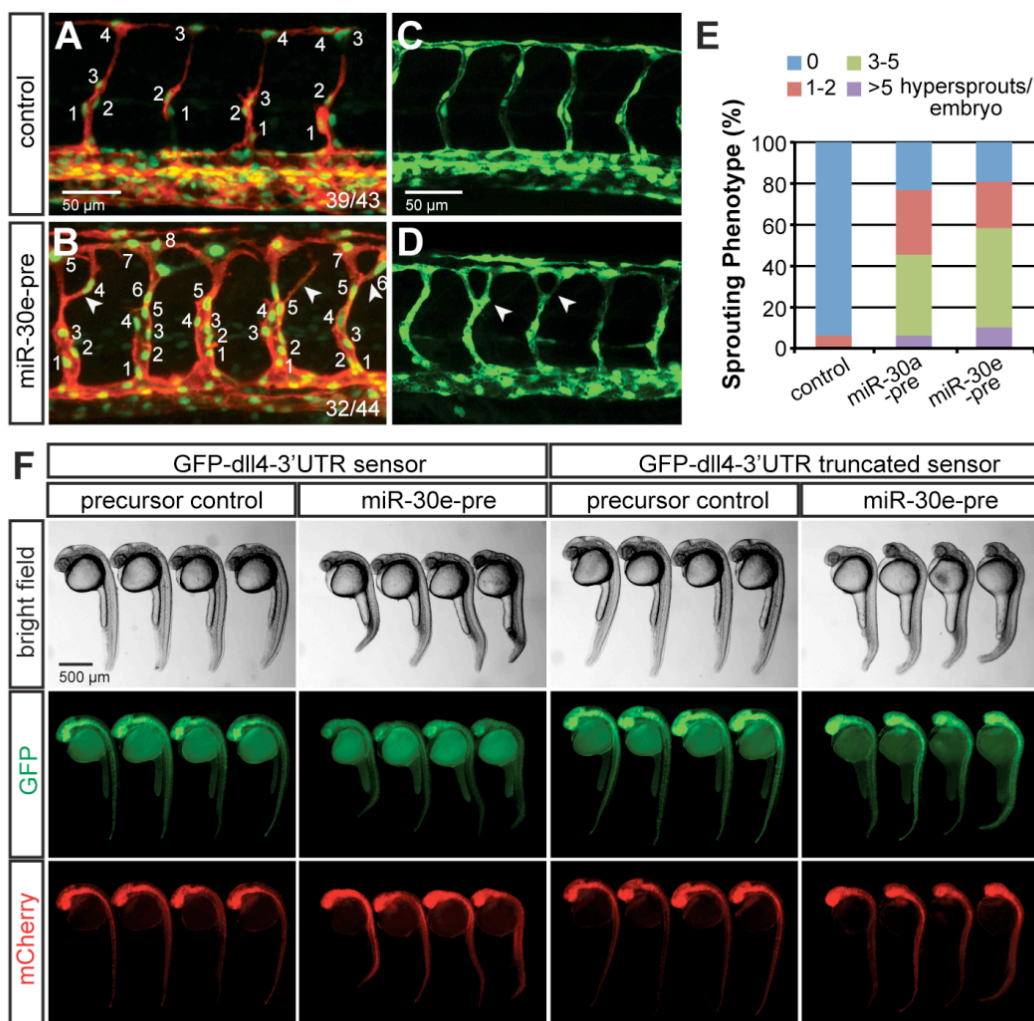
Figure 24. miR-30e overexpression affects ISV properties involving *dll4* similar to miR-30a

(A, B) Confocal images of *Tg(fli1:negfp)^{y7}xTg(kdrl:hras-mcherry)^{s896}* double transgenic embryos at 32 hpf, after injection of control or miR-30e-pre. EC nuclei in green; vessels in red, arrowheads indicate hyperbranching. Ratio in lower right corner: fraction of embryos showing phenotype similar to the image. Note hyperbranching in miR-30e-pre-injected embryos. Numbers denote cell nuclei of representative ISVs. On average, control ISVs showed 3 nuclei, whereas embryos overexpressing miR-30e showed 5.8 nuclei/ISV. (C, D) Confocal images of *Tg(fli1:egfp)^{y1}* embryos injected with control or miR-30e-pre. Quantification in (E). Arrowheads indicate hyperbranching. (E) Quantification of hypersprouting events in control, and after overexpression of miR-30a or miR-30e. Note that both microRNAs caused hypersprouting; n=80 embryos/group. (F) *dll4*-3'UTR sensor

assays. GFP sensors were co-injected with mCherry control as indicated. miR-30e-pre injection reduced GFP levels in GFP-dll4-3'UTR sensor (second column) while mCherry levels were unchanged. In the absence of a miR-30 binding site, GFP expression was not greatly affected by miR-30e overexpression (fourth column).

5.4.7 Normalization of Dll4-Notch signaling restores the angiogenic phenotypes in miR-30a loss-of-function and gain-of-function embryos.

We then reasoned that if imbalances in angiogenesis in miR-30a loss-of-function and gain-of-function embryos are due to Dll4 misregulation, normalizing the levels of Dll4-Notch signaling would rescue these angiogenic phenotypes observed in miR-30a loss-of-function and gain-of-function embryos. Here two alternative approaches were used to demonstrate this.

Knockdown of miR-30a would upregulate the expression of Dll4 in this model (Figure 30). We tested if MO-mediated knockdown of Dll4 expression could restore the angiogenic phenotype in miR-30a loss-of-function embryos displaying short ISVs with fewer ECs. In this rescue experiment, miR-30a morphants exhibited reduced sprout length and EC number of ISVs when compared to control (Figure 25A-D, G and H), whereas knockdown of Dll4 expression partially normalized the ISV length and EC numbers in miR-30a-deficient embryos (Figure 25E-H). Moreover, in addition to EC number of ISVs, knockdown of Dll4 expression can even rescue, at least in part, the formation of DLAV in miR-30a morphant embryos at 48 hpf (Figure 25B, D, and F).
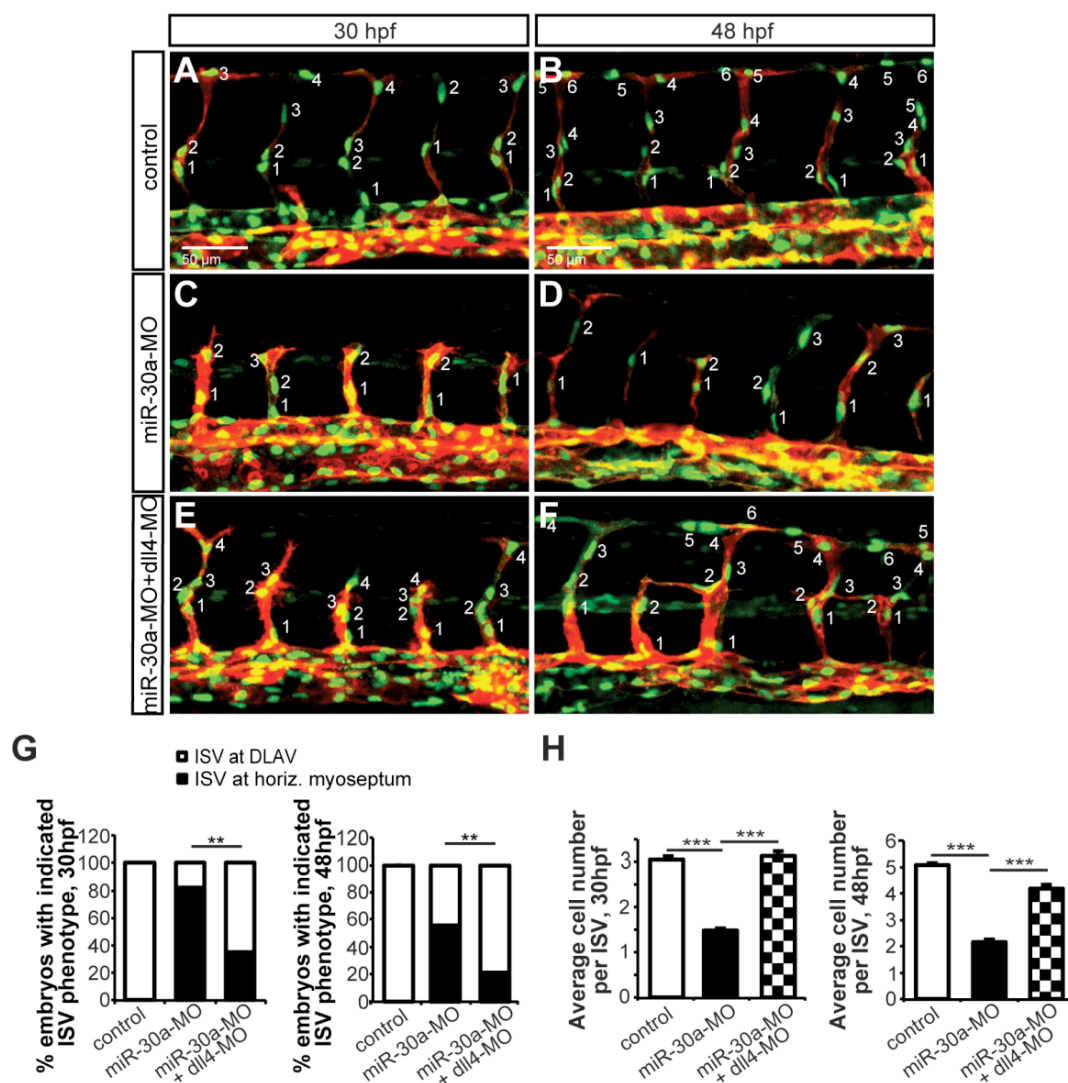
Figure 25. dll4-MO restores ISV properties in miR-30a morphants

(A, B) Imaging of endothelial nuclei at 30 hpf and 48 hpf in control, (C, D) miR-30a morphants, and (E, F) miR-30a morphants co-injected with dll4-MO using *Tg(fli1:negfp)^{y7}xTg(kdrl:hras-mCherry)^{s896}* double transgenic embryos. Vessels in red, endothelial nuclei in green. miR-30a morphants showed reduced ISV length and endothelial nuclei number, which were partially normalized after co-injection of dll4-MO. (G) Quantification of sprout length. (H) Quantification of ISV nuclei number. Measurements from four adjacent ISVs/embryo, n=25 embryos, from three independent experiments. **, P<0.01; ***, P<0.001, Student's t-test. (Statistical analysis of the experimental data was made in cooperation with Dr. Dong Liu.)

Dll4 in tip cell binds to and activates Notch receptor in adjacent ECs, releasing Notch-intracellular domain (NICD) to the nuclei, and subsequently activating or inactivating its target gene expression. In this model (Figure 30), overexpresion of miR-30a would downregulate the expression of Dll4, which would suppress the Notch activity in adjacent ECs. In other words, the NICD level would be reduced in miR-30a gain-of-function embryos. Therefore, we tried to investigate if conditionally overexpressing NICD could rescue the angiogenic phenotype in miR-30a gain-of-function embryos displaying more ECs in ISVs. We performed this resuce experiment using the double transgenic zebrafish line *Tg(hsp70:Gal4) x(uas:notch1a-ICD)*. Briefly, through heat shocked at 40°C, the *hsp70* promoter drives the global overexpression of NICD in zebrafish embryos via the Gal4-uas system (Figure 26A). We found that without heat shocking, miR-30a-pre-injected embryos manifested more ECs in the ISVs than in the control ISVs at 32 hpf, as described above, whereas after heat shock treatment, conditional overpression of NICD partially normalized the EC number in the ISVs of miR-30a gain-of-function embryos (Figure 26).
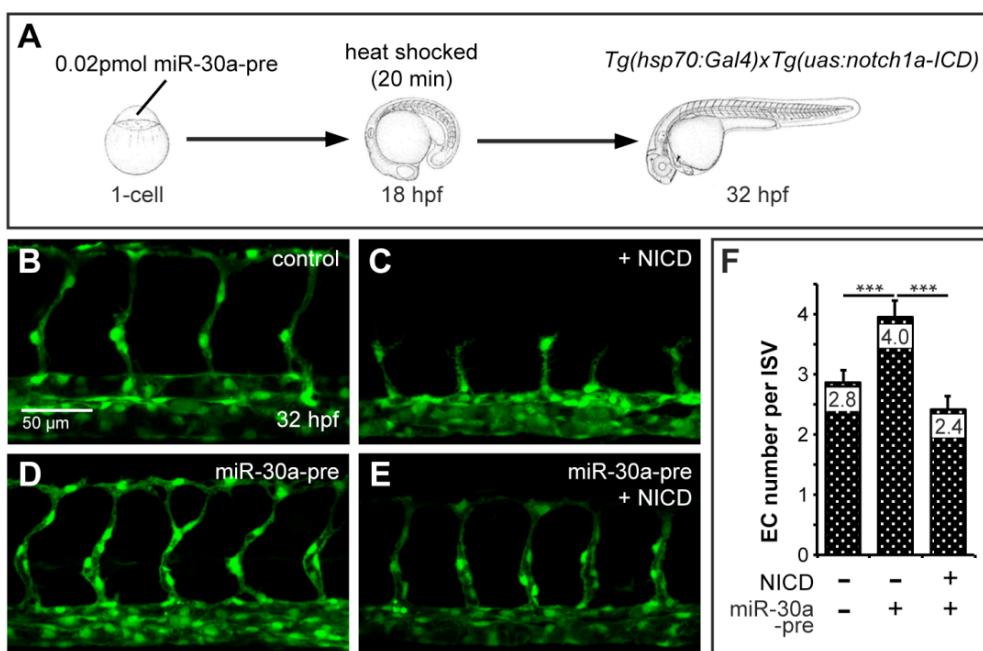
Figure 26. Conditional overactivation of Notch signaling rescues ISV properties in miR-30a gain-of-function embryos

(A) Schematic representation of this assay strategy for conditional overexpression of NICD in zebrafish embryos overexpressing miR-30a. (B) Confocal images of ISVs in control, (C) conditional overexpression of NICD, (D) miR-30a overexpression, and (E) combination of miR-30a overexpression and conditional overexpression of NICD using *Tg(hsp70:Gal4)xTg(uas:notch1a-ICD)* embryos. (F) Quantification of EC numbers per ISV. Data are presented as mean ± standard error; measurements from 4 adjacent ISVs/embryo, n=20 embryos; ***, P<0.001; Student's t-test.

5.5 miR-30a targets DLL4-NOTCH signaling to enhance angiogenic cell behavior in human ECs

The main new findings of Result 5.5

Previously in zebrafish model, we identified miR-30a as an essential regulatory node to promote sprouting angiogenesis by targeting *dll4* and inhibiting Notch signaling. Here we confirmed the application of miR-30a-mediated modulation of DLL4-NOTCH signaling to human ECs. Our miR-30a loss-of-function and gain-of-function studies in HUVECs-composed spheroid assay demonstrated that knockdown of miR-30a blocked angiogenic cell behavior whereas overexpression of miR-30a enhanced angiogenic cell behavior. In human ECs, loss of miR-30a increased DLL4 protein levels, activated NOTCH signaling as indicated in NOTCH target gene promoter luciferase assays, and augmented the expression of NOTCH downstream effectors *Hey2* and *EFNB2*.

5.5.1 miR-30a enhances sprout formation and EC migration *in vitro*

The miR-30 family is conserved between human and zebrafish, and so are the binding sites for miR-30a in *dll4*-3'UTR (Figure 14). Based on this high degree of sequence conservation, we postulated that similar to zebrafish, miR-30a might enhance angiogenesis in human ECs. To assess the angiogenic property of miR-30a in human ECs, we used miR-30a loss-of-function and gain-of-function studies in HUVECs-composed spheroid assay (namely three-dimensional angiogenesis assay), which involves the sprouting of HUVECs *in vitro* in response to pro-angiogenic factors (i.e. VEGF). Consistent with our zebrafish data, we found that locked nucleic acid (LNA)-mediated silencing of miR-30a blocked angiogenic cell behavior whereas overexpression of miR-30a by transfecting HUVECs with miR-30a-precursor enhanced angiogenic cell behavior, which were evidenced by reduced and increased number of migrating ECs, respectively (Figure 27).
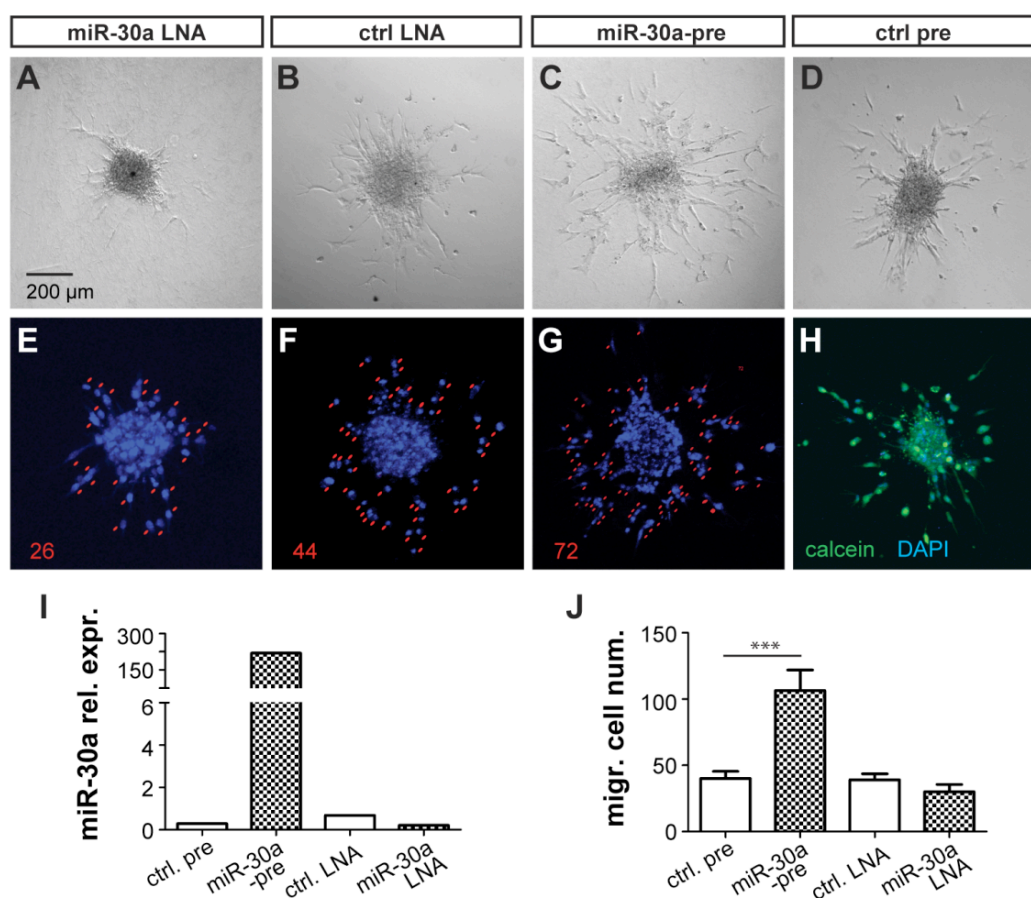
Figure 27. miR-30a promotes angiogenic cell behavior in human ECs

(A-D) Phase contrast images of HUVEC spheroids after transfection with miR-30a-LNA, control-LNA, miR-30a-pre or control-pre. (E-H) Confocal micrographs of spheroids transfected as (A-D) stained with calcein (green) and DAPI (blue) for quantification of nuclei number. Cell migrating away from the spheroid incorporated into the sprout were counted. Red dots indicate DAPI stained nuclei that were counted in representative images. (I) Taqman analysis of miR-30a expression after transfection with miR-30a-LNA and miR-30a-pre compared to controls. (J) Number of ECs in angiogenic front. ***, P<0.001; Student's t-test. (This work was made in cooperation with Dr. Mariana Lagos -Quintana.)

5.5.2 miR-30a targets *DLL4* and inhibits NOTCH signaling in HUVECs

In this model (Figure 30), which has been identified by our previous findings in zebrafish embryos, loss of miR-30a could upregulate the expression of Dll4, leading to overactivation of the Notch activity and the resulting overexpression of Notch target genes. Our western blot result confirmed that knockdown of miR-30a augmented DLL4 protein expression about two-fold when compared to the controls (Figure 28A). We then performed the NOTCH target gene promoter luciferase assay to test the NOTCH activity in miR-30a-deficient HUVECs (Figure 28B-D). In this assay, induction of luciferase expression was under the control of NOTCH target gene *terminal protein 1* (*TP1*) promoter or 4 tandem *CBF1* binding elements (*4xCBF1*) (Figure 28B). Knockdown of miR-30a upregulates the luciferase expression, suggesting that miR-30a deficiency increases NOTCH receptor activity (Figure 28C and D). Specific mutations in the *CBF1* binding elements annihilated this response, indicating that the effect of miR-30a is NOTCH specific in human ECs (Figure 28D). Furthermore, activation of NOTCH signaling upon loss of miR-30a was demonstrated by significant upregulation of the NOTCH downstream targets *hairy/enhancer-of-split related with YRPW motif protein 2* (*Hey2*) and *ephrin B2* (*EFNB2*) (Figure 28E and F). These data are consistent with a model in which loss of miR-30a in human ECs induces DLL4 expression, resulting in activation of NOTCH receptor signaling and restriction of angiogenic cell behavior.
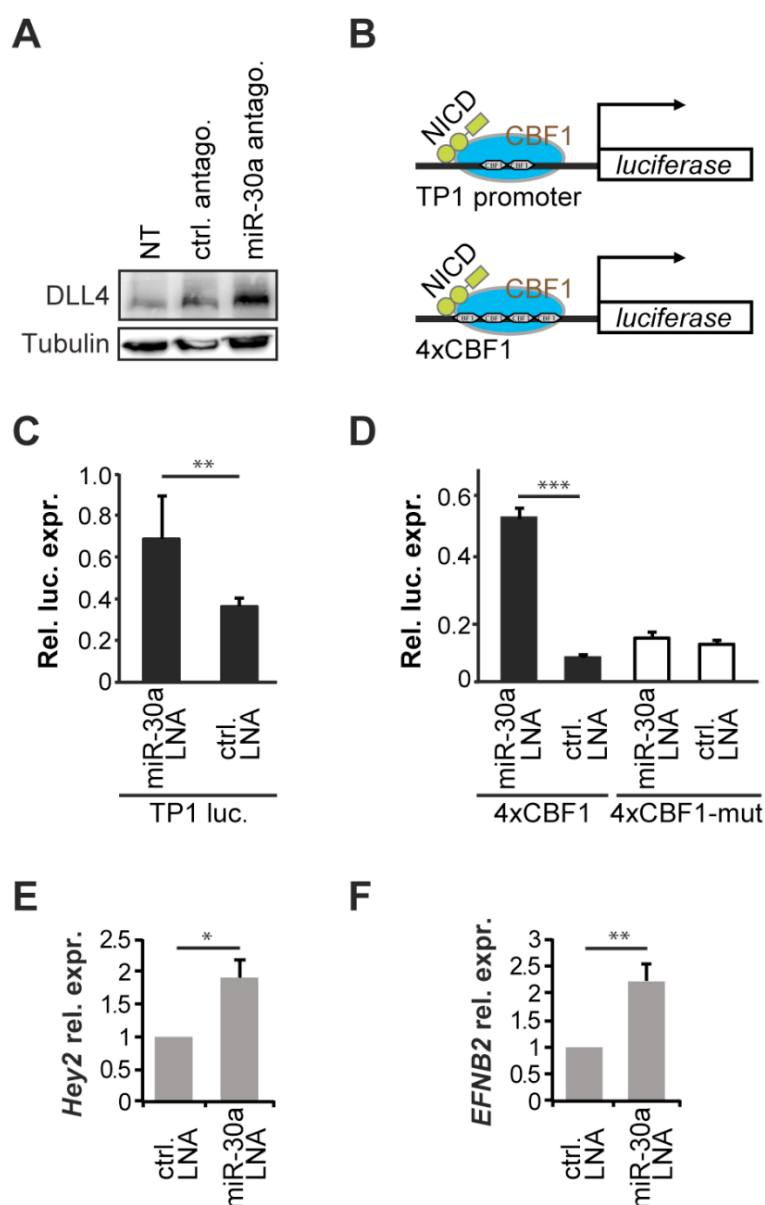
Figure 28. Loss of miR-30a upregulates DLL4 and activates NOTCH signaling in human ECs

(A) Western blot analysis of DLL4 after treatment with miR-30a-LNA or control-LNA; NT, not treated. Note upregulated DLL4 in miR-30a-LNA-treated group. (B) Schematic models for the NOTCH signaling-dependent luciferase assays in panel C and D. (C) *TP1* promoter construct driving luciferase and (D) *CBF1* promoter construct driving luciferase; to verify NOTCH specificity *CBF1* elements were mutated in *CBF1*-mut. NOTCH signaling is upregulated in the presence of miR-30a-LNA. (E, F) Relative mRNA expression of NOTCH

downstream targets *Hey2* and *EFNB2*. Both are upregulated in cells treated with miR-30a-LNA. *, P<0.05; **, P<0.01; ***, P<0.001; Student's t-test. (This work was made in cooperation with Dr. Mariana Lagos-Quintana.)

6 Discussion

The Notch ligand Dll4 acts as a negative regulator of tip cell differentiation and vessel sprouting, and its vascular function is conserved between zebrafish and human (Phng and Gerhardt, 2009). Using a systems biology approach, we examined the potential post-transcriptional regulators of Dll4 in ECs of these species. Deep sequencing analysis of human and zebrafish ECs combined with microRNA target prediction algorithms suggested that the miR-30 family might target *dll4* across species. To determine the physiological roles of the miR-30 family members in sprouting angiogenesis, we first performed loss-of-function experiments for each family member and found that miR-30a morphants showed a strong reduction in ISV sprouting, consistent with the angiogenic phenotype of Dll4-Notch gain-of-function (Krueger et al., 2011; Siekmann and Lawson, 2007). While knockdown of the other miR-30 family members resulted in variable effects on ISV development and in general the observed phenotypes are relatively mild, suggesting that endogenous miR-30a might be physiologically the most relevant family member during normal ISV development.

Loss of miR-30a increases Dll4 level and reduces ISV sprouting. The influence of miR-30a on vessel sprouting could be traced to an effect on tip cell differentiation. Loss of miR-30a impairs tip cell formation, whereas miR-30a overexpression induces hyperactive endothelial tip cells, displaying numerous tip cell filopodial extensions and endothelial proliferation in developing ISVs all resembling the vascular phenotypes previously reported in Dll4-Notch loss-of-function and gain-of-function zebrafish embryos (Leslie et al., 2007; Siekmann and Lawson, 2007). To confirm the direct interaction of miR-30a with Dll4-Notch signaling at the genetic level, we demonstrated in an *in vivo* microRNA sensor assay that miR-30a targets the *dll4*-3'UTR, and that this effect depends on the miR-30 binding site in the *dll4*-3'UTR. Furthermore, we showed that morpholino-mediated knockdown of Dll4 expression rescues the ISV sprouting defects in miR-30a morphants,

consistent with elevated Dll4 being responsible for the vascular phenotype in miR-30a loss-of-function embryos. Conversely, overexpression of miR-30a results in ISV hypersprouting, a phenotype reminiscent of previous reports on loss of Dll4-Notch signaling in zebrafish embryos (Leslie et al., 2007). In line with loss of Notch signaling, we found that conditional overactivation of Notch activity in miR-30a gain-of-function embryos rescues, at least in part, the ISV hypersprouting and EC number. This supports the concept that miR-30a reduces Dll4-Notch signaling thus allowing ECs to acquire sprouting properties (Siekmann and Lawson, 2007). Conservation of the miR-30a-mediated modulation of Dll4 expression was confirmed using loss-of-function and gain-of-function approaches in human ECs. Loss of miR-30a augments DLL4 protein expression, activates NOTCH receptors, and NOTCH downstream signaling events, restricting angiogenic cell behavior in developing sprouts. Taken together, these data suggest that endothelial miR-30a may act as an evolutionarily conserved regulator of Dll4 relevant for sprouting angiogenesis in zebrafish and human ESs.

6.1 Molecular evolution of *mir-30* family

In the present thesis, we described the phylogenetic tree of primary miR-30 family and genomic environment flanking the *mir-30* family member genes. Accordingly, a model is proposed here to explain the evolutionary relationships of all these *mir-30* family members in species (Figure 29).

Our synteny information indicates that *mir-30a* and *mir-30c-2* are clustered in chicken, mouse and human, whereas *mir-30e* and *mir-30c-1* are clustered in these three species (Figure 16). In addition, some of the *mir-30e* and *mir-30c-1* cluster neighboring genes in chicken, mouse and human are also partially syntenic to *mir-30e* and *mir-30c* cluster on zebrafish Chromosome 13 and *mir-30a* and *mir-30c-2* cluster on chicken Chromosome 3, mouse Chromosome 1 and

human Chromosome 6, suggesting that *mir-30a* and *mir-30e* might be of the same origin in chicken, mouse and human. Actually, this suggestion is supported by our phylogenetic analysis showing that *mir-30* family can be divided into the *mir-30a/d/e* and *mir-30b/c* subgroups (Figure 15).

Based on our synteny analysis, *mir-30b* and *mir-30d* are clustered in zebrafish, chicken, mouse and human. Interestingly, some of the *mir-30b* and *mir-30d* cluster neighboring genes such as *WISP1*, *NDRG1*, *ST3GAL1*, *KCNK9*, and *TRAPPC9* in chicken, mouse and human are syntenic to *mir-30a* on zebrafish Chromosome 19. Together with the suggestion mentioned above that *mir-30a* and *mir-30e* were evolved from the same ancestor and the phylogenetic data that zebrafish *mir-30a* was included into the *mir-30d* cluster, we suggest here that *mir-30a*, *mir-30e* and *mir-30d* are from the same ancestor *mir-30a/d/e*, which is completely consistent with our phylogenetic analysis.

Taken together, our proposed model for molecular evolution of *mir-30* family was established and might be a plausible explanation for how this family formed during vertebrate evolution (Figure 29). First, the ancestral *mir-30* (namely *mir-30a/b/c/d/e*) underwent tandem duplication and evolution to form a cluster consisting of ancestral *mir-30a/d/e* and ancestral *mir-30b/c*. It further evolved after the first round of genome/segmental amplification into two sets of ancestral *mir-30* clusters: one was composed of ancestral *mir-30a/e* and ancestral *mir-30c*; the other consisted of ancestral *mir-30a/d* and ancestral *mir-30b*. The former *mir-30* cluster then underwent the second round of segmental amplification and evolved into two sets of current *mir-30* family member clusters: the *mir-30a* and *mir-30c-2* cluster, which is located in chick, mouse, and human; and the *mir-30e* and *mir-30c-1* cluster, which is present in zebrafish, chick, mouse, and human. The latter *mir-30* cluster experienced a complicated evolutionary process. Specifically, in chicken, mouse and human, the *mir-30a/d* and *mir-30b* cluster directly evolved into the *mir-30d* and *mir-30b* cluster without undergoing the second round of

segmental amplification. However, in zebrafish, the *mir-30a/d* and *mir-30b* cluster underwent the second round of segmental amplification and afterwards evolved into two sets of *mir-30* family member clusters: the current *mir-30d* and *mir-30b* cluster, and the *mir-30a* and *mir-30b* cluster, the latter of which eventually evolved into the current *mir-30a* after *mir-30b* deletion.
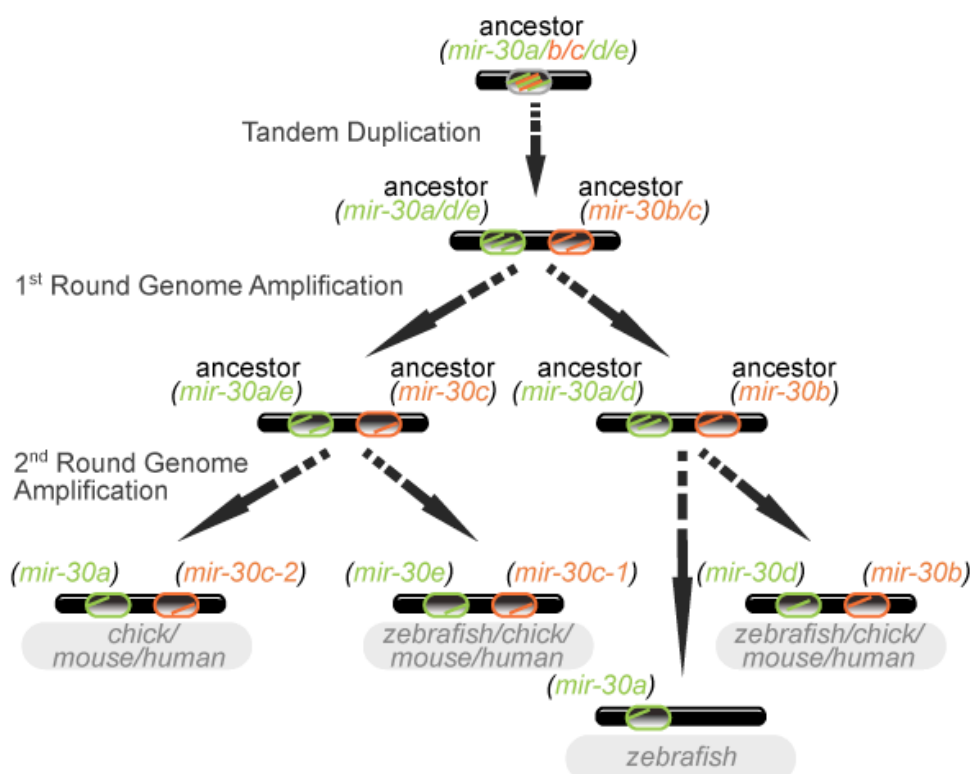
Figure 29. A proposed model for molecular evolution of *mir-30* family

See text for details.

6.2 Endogenous miR-30a, rather than other miR-30 family members, is essential for angiogenic sprouting in zebrafish

Our functional screen using morpholinos to silence each member of the miR-30 family revealed that only miR-30a morphants showed a high proportion of phenotype efficiently affecting sprouting angiogenesis, with short ISVs at 32 hpf

(Figure 18A and B). It seems incredible that so lowly expressed miR-30a, rather than miR-30d and miR-30e with abundant expression in zebrafish total ECs at 24 hpf, efficiently regulates vessel branching during ISV development. Actually, our microRNA expression profiles by deep sequencing zebrafish endothelial microRNAs just reflect the overall expression levels of every miR-30 family member in total ECs consisting of different populations of embryonic ECs. We believe that only in a subset of embryonic ECs from dorsal aorta and ISVs co-expressing Dll4, miR-30 family members could activate sprouting angiogenesis through physically binding to *dll4*-3'UTR and suppressing its expression. Moreover, our preliminary whole-mount *in situ* hybridization using five primary miR-30 antisense probes (data not shown) indicated that only primary miR-30a was readily detectable in zebrafish trunk axial vessels including dorsal aorta in which some populations of ECs would migrate to the intersomitic space to form the ISVs (Figure 17F). Thus, mature miR-30a may still exist in ECs of arterial ISVs where it promotes angiogenic spouting by targeting *dll4* and repressing its expression.

6.3 Incoherent interaction of miR-30a with *dll4*

A number of reports claimed the binary on/off effects of microRNAs on their target mRNA expression in vertebrates, but such dramatic effects are challenged by the recent systems biology studies where the maximal contribution of microRNAs in determining their cognate mRNA levels is about 50% at a genome-wide scale (Selbach et al., 2008). Through *in vivo* and *in vitro* sensor assays combined with Western blot, we indeed observed approximately 50% change in reporter sensor expression levels in microRNA gain-of-function approaches. Specifically, our *in vivo* GFP-dll4-3'UTR sensor assay provided the evidence for *dll4* mRNA representing a direct miR-30a target, displaying what seems only weak sensitivity to miR-30a (Figure 23).

In cases where the target is preferentially expressed with the microRNA, the targeting interaction is considered "incoherent" because microRNA-directed target repression opposes the overall action of transcription factors and other regulatory processes that affect mRNA levels (Shkumatava et al., 2009). Thus, our expression and functional data indicate that Dll4 suppression by miR-30a is "incoherent". Our understanding is that miR-30a-mediated repression of Dll4 is mild as it is frequently observed for microRNA-dependent gene regulation (Baek et al., 2008; Selbach et al., 2008), and nevertheless necessary to optimally adjust the Dll4 protein levels throughout vascular development and between different EC types.

Given its importance, it may not be surprising that Dll4 can be regulated or fine-tuned in ECs by multiple microRNAs, including the miR-30 and miR-27 family members (Biyashev et al., 2012; Bridge et al., 2012). Beyond the scope of our data, in the systems biology field it is debated how and to what extent multiple microRNAs can collaborate to repress targets, and multiple factors including target availability, occupancy and presence of other microRNA binding molecules potentially affect the efficacy. However, a complete microRNA-mediated endothelial repression of Dll4 expression to inconsequential levels thus favoring excessive sprouting could impair functional vascular network development, and in general vascular beds resulting from Dll4 loss-of-function show undesirable perfusion and remodeling deficits in zebrafish and mouse (Leslie et al., 2007; Lobov et al., 2011). Therefore, a scenario allowing tuning interactions in which miR-30a and miR-27b act as a rheostat to dampen Dll4 protein output to an optimal level, one that is still functional in the cell in a context-dependent manner, may enable customized outputs in tip/stalk cells or arteries/veins and appears physiologically more plausible than the binary on/off model. Some subtle differences exist in the vascular phenotypes obtained with miR-27b and miR-30a loss-of-function and gain-of-function, which may relate to slightly different cellular expression patterns and effects on other targets beyond *dll4*.

6.4 The miR-30a gradient shaping Dll4 expression in zebrafish ISVs

To our knowledge, completion of the normal formation of ISVs requires a combination of key signaling pathways such as VEGF and Dll4-Notch signaling. In the present thesis, we demonstrated that miR-30a acts as a positive modulator to control ISV formation by targeting *dll4* and inhibiting Notch signaling in zebrafish model. Spatiotemporal information on microRNA and its candidate target mRNA expression is essential for us to understand the functional significance of a potential microRNA-mRNA interaction. Although our *in vitro* evidence indicates that the identified miR-30a-mediated repression of Dll4-Notch signaling in zebrafish can also be applied to human ECs, we don't have the direct evidence for the presence of mature miR-30a in zebrafish ISVs. The only relevant evidence we have is from the whole-mount *in situ* hybridization using antisense probe against primary miR-30a indicating the trunk axial vessel (including dorsal aorta and posterior cardinal vein) transcription of *mir-30a* gene. Thereby, we put forward a proposed model to explain the possible presence of mature miR-30a in ISVs (Figure 30).

Before illustrating this model, I would like to summarize first the microRNA-specific whole-mount *in situ* hybridization technique. To date, the LNA-based probes complementary to mature microRNA sequences are the most commonly used oligos for *in situ* hybridization-assisted microRNA detection in zebrafish embryos (Kloosterman et al., 2006; Wienholds et al., 2005). However, their use in detecting microRNA expression during early developmental stages can be impeded by the appearance of non-specific background signals, probably due to the diffusion of small microRNAs into the surrounding tissue after formaldehyde fixation (Lagendijk et al., 2012). Based on the fact that microRNA

genes are initially transcribed into long primary microRNAs, we therefore turned to the conventional digoxigenin-labeled antisense riboprobes that bind to primary microRNAs in zebrafish embryos, as described by He et al. (2011).
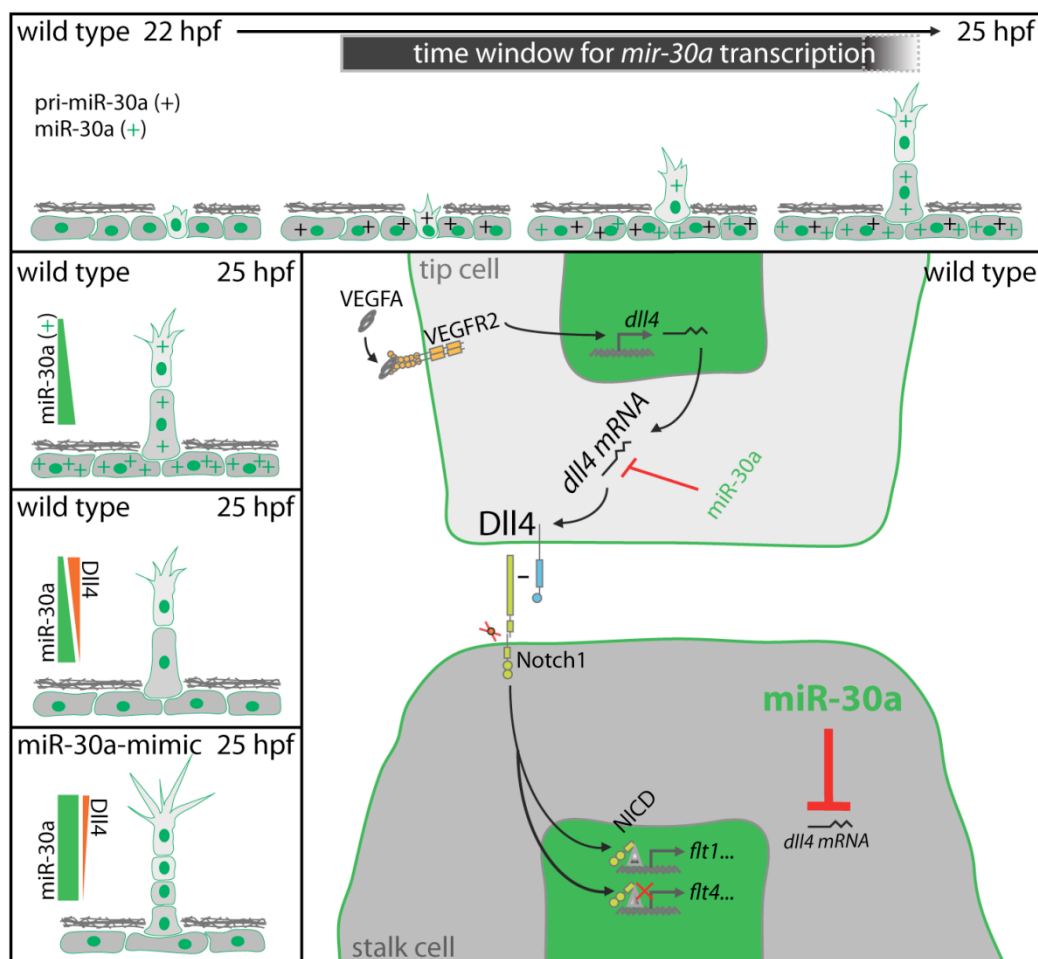
Figure 30. A proposed model for the formation of miR-30a gradient in zebrafish ISVs

See details in the text.

In zebrafish embryos, the first angiogenic sprouts that ultimately form the ISVs, branch from the dorsal aorta, and hence are considered to be of arterial origin. The expression pattern of primary miR-30a at 24 hpf indicates that *mir-30a* gene was transcribed in the trunk axial vessel including dorsal aorta, but not in the ISVs,

suggesting a possible scenario in which the transcription of *mir-30a* gene might be controlled by the endogenous promoter, and is restricted to trunk axial vessels in a limited time window (Figures 17F and 30A).

The angiogenic imbalances of ISVs in miR-30a loss-of-function and gain-of-function by modulating the Dll4-dependent regulatory network suggest that Dll4 expression in wild type might be efficiently contained by miR-30a to define a temporal and spatial expression pattern that underlies the proper formation of ISVs. Combined with our *in vitro* evidence using human ECs, we further confirmed miR-30a-mediated regulation of Dll4 expression in an EC autonomous manner. Here we establish a model to explain for the formation of mature miR-30a gradient and the interaction status of miR-30a with its cognate target transcripts *dll4* mRNA (Figure 30).

In this model, as certain ECs migrate out from the dorsal aorta to form the ISV sprouts, the efficient gradient of mature miR-30a might be created within the new sprouts. Assumably, this control is released throughout the ISV growth by the gradual increase of miR-30a and the synchronous decrease of Dll4 that trigger the ISV formation. Specifically, low miR-30a expression level in tip cells might lead to increased Dll4 expression reaching certain threshold levels to trigger sprouting formation, whereas in the basal regions of new ISV sprouts, cumulative miR-30a expression is sufficient to reduce Dll4 expression to a lower level. Thus, miR-30a may act as a buffer system capable of controlling Dll4 expression levels within specific tissues to prevent overaccumulation of Dll4 protein and subsequent bud formation. These findings indicate the functional importance of miR-30a in the regulation of Dll4 expression, but we still await direct evidence that links angiogenic action to miR-30a-mediated formation of Dll4 gradient in this process.

6.5 Therapeutic implication

Angiogenesis-related tumor overgrowth is mainly attributable to the formation of more functional blood vessels. Based on the known mechanisms underlying angiogenesis, several approaches have been utilized to target tumor angiogenesis to provide a brake for tumor growth. To date, VEGF-VEGFR signaling has become the primary target for anti-angiogenic drugs. Clinical use of VEGF inhibitors was initially reported to result in modest improvements in progression-free survival. However, recent preclinical evidence also raised concerns that VEGF blockade might promote tumor invasiveness and metastasis by aggravating tumor hypoxia and generating a pro-inflammatory niche (Ebos and Kerbel, 2011). Thus, refractoriness to VEGF blockade in a certain proportion of cancer patients has spurred investigation into deeper mechanisms underlying tumor resistance to VEGF inhibition, and calls for more suitable anti-angiogenic drugs against tumor growth.

DLL4-NOTCH signaling pathway is also essential to regulate angiogenesis in health and diseases. Overactivation of NOTCH signaling within tumor by increased DLL4 level enhanced the blood vessel size and improved tumor vascular function, eventually promoting tumor growth (Li et al., 2007). Conversely, targeted inhibition of DLL4-NOTCH signaling induced unfunctional angiogenesis, which is characterized by the enhanced formation of hypoperfused blood vessels, eventually resulting in increased tumor hypoxia and tumor growth inhibition (Hoey et al., 2009; Li et al., 2007; Noguera-Troise et al., 2006; Ridgway et al., 2006; Thurston et al., 2007). These data indicate that inhibition of DLL4 has emerged as an attractive approach for cancer therapy. However, Yan et al. recently also observed that chronic DLL4 inhibition causes pathological activation of ECs and induces vascular tumors (Yan et al., 2010). This paradoxical evidence raises essential safety concerns and calls for refined strategies necessary to harness the DLL4-NOTCH signaling pathway safely as a powerful tool to inhibit tumor growth.

Vascular development is sensitive to subtle changes in DLL4 dosage (Gale et al., 2004; Trindade et al., 2012), underscoring the potential impact of relatively minor alterations in DLL4 dosage on angiogenesis in health and disease. Thus, in addition to its transcriptional control, DLL4 expression might also be subject to microRNA-mediated fine-tuning for functional angiogenesis at the post-transcriptional level. In the present thesis, we provide the *in vivo* and *in vitro* evidence that during evolution the miR-30 family (i.e. miR-30a) has been co-opted by the vascular system to fine-tune DLL4 expression and help determining the fraction of ECs that can acquire a tip cell phenotype and initiate sprouting. Such findings have obvious therapeutic implications for pro- and anti-angiogenic treatment strategies in cardiovascular diseases and cancer.

7 Bibliography

Adams, R. H. and Alitalo, K. (2007). Molecular regulation of angiogenesis and lymphangiogenesis. *Nat Rev Mol Cell Biol* 8, 464-78.

Adams, R. H. and Eichmann, A. (2010). Axon guidance molecules in vascular patterning. *Cold Spring Harb Perspect Biol* 2, a001875.

Ahmad, S., Hewett, P. W., Wang, P., Al-Ani, B., Cudmore, M., Fujisawa, T., Haigh, J. J., le Noble, F., Wang, L., Mukhopadhyay, D. et al. (2006). Direct evidence for endothelial vascular endothelial growth factor receptor-1 function in nitric oxide-mediated angiogenesis. *Circ Res* 99, 715-22.

Ahmed, Z. and Bicknell, R. (2009). Angiogenic signalling pathways. *Methods Mol Biol* 467, 3-24.

Almagro, S., Durmort, C., Chervin-Petinot, A., Heyraud, S., Dubois, M., Lambert, O., Maillefaud, C., Hewat, E., Schaal, J. P., Huber, P. et al. (2010). The motor protein myosin-X transports VE-cadherin along filopodia to allow the formation of early endothelial cell-cell contacts. *Mol Cell Biol* 30, 1703-17.

Ambros, V. (2004). The functions of animal microRNAs. *Nature* 431, 350-5.

Augustin, H. G., Koh, G. Y., Thurston, G. and Alitalo, K. (2009). Control of vascular morphogenesis and homeostasis through the angiopoietin-Tie system. *Nat Rev Mol Cell Biol* 10, 165-77.

Autiero, M., Waltenberger, J., Communi, D., Kranz, A., Moons, L., Lambrechts, D., Kroll, J., Plaisance, S., De Mol, M., Bono, F. et al. (2003). Role of PlGF in the intra- and intermolecular cross talk between the VEGF receptors Flt1 and Flk1. *Nat Med* 9, 936-43.

Baek, D., Villen, J., Shin, C., Camargo, F. D., Gygi, S. P. and Bartel, D. P. (2008). The impact of microRNAs on protein output. *Nature* 455, 64-71.

Ballard, M. S. and Hinck, L. (2012). A roundabout way to cancer. *Adv Cancer Res* 114, 187-235.

Bartel, D. P. (2004). MicroRNAs: genomics, biogenesis, mechanism, and function. *Cell* 116, 281-97.

Bazzini, A. A., Lee, M. T. and Giraldez, A. J. (2012). Ribosome profiling shows that miR-430 reduces translation before causing mRNA decay in zebrafish. *Science* 336, 233-7.

Bedell, V. M., Yeo, S. Y., Park, K. W., Chung, J., Seth, P., Shivalingappa, V., Zhao, J., Obara, T., Sukhatme, V. P., Drummond, I. A. et al. (2005). roundabout4 is essential for angiogenesis in vivo. *Proc Natl Acad Sci U S A* 102, 6373-8.

Behar, O., Golden, J. A., Mashimo, H., Schoen, F. J. and Fishman, M. C. (1996). Semaphorin III is needed for normal patterning and growth of nerves, bones and heart. *Nature* 383, 525-8.

Benedito, R., Roca, C., Sorensen, I., Adams, S., Gossler, A., Fruttiger, M. and Adams, R. H. (2009). The notch ligands Dll4 and Jagged1 have opposing effects on angiogenesis. *Cell* 137, 1124-35.

Benedito, R., Rocha, S. F., Woeste, M., Zamykal, M., Radtke, F., Casanovas, O., Duarte, A., Pytowski, B. and Adams, R. H. (2012). Notch-dependent VEGFR3 upregulation allows angiogenesis without VEGF-VEGFR2 signalling. *Nature* 484, 110-4.

Bernstein, E., Caudy, A. A., Hammond, S. M. and Hannon, G. J. (2001). Role for a bidentate ribonuclease in the initiation step of RNA interference. *Nature* 409, 363-6.

Biyashev, D., Veliceasa, D., Topczewski, J., Topczewska, J. M., Mizgirev, I., Vinokour, E., Reddi, A. L., Licht, J. D., Revskoy, S. Y. and Volpert, O. V. (2012). miR-27b controls venous specification and tip cell fate. *Blood* 119, 2679-87.

Blasi, F. and Carmeliet, P. (2002). uPAR: a versatile signalling orchestrator. *Nat Rev Mol Cell Biol* 3, 932-43.

Blum, Y., Belting, H. G., Ellertsdottir, E., Herwig, L., Luders, F. and Affolter, M. (2008). Complex cell rearrangements during intersegmental vessel sprouting and vessel fusion in the zebrafish embryo. *Dev Biol* 316, 312-22.

Bonauer, A., Carmona, G., Iwasaki, M., Mione, M., Koyanagi, M., Fischer, A., Burchfield, J., Fox, H., Doebele, C., Ohtani, K. et al. (2009). MicroRNA-92a controls angiogenesis and functional recovery of ischemic tissues in mice. *Science* 324, 1710-3.

Boutz, P. L., Chawla, G., Stoilov, P. and Black, D. L. (2007). MicroRNAs regulate the expression of the alternative splicing factor nPTB during muscle development. *Genes Dev* 21, 71-84.

Bridge, G., Monteiro, R., Henderson, S., Emuss, V., Lagos, D., Georgopoulou, D., Patient, R. and Boshoff, C. (2012). The microRNA-30 family targets DLL4 to modulate endothelial cell behavior during angiogenesis. *Blood* 120, 5063-72.

Bushati, N. and Cohen, S. M. (2007). microRNA functions. *Annu Rev Cell Dev Biol* 23, 175-205.

Carmeliet, P., Ferreira, V., Breier, G., Pollefeyt, S., Kieckens, L., Gertsenstein, M., Fahrig, M., Vandenhoeck, A., Harpal, K., Eberhardt, C. et al. (1996). Abnormal blood vessel development and lethality in embryos lacking a single VEGF allele. *Nature* 380, 435-9.

Carmeliet, P. and Jain, R. K. (2011). Molecular mechanisms and clinical applications of angiogenesis. *Nature* 473, 298-307.

Castets, M., Coissieux, M. M., Delloye-Bourgeois, C., Bernard, L., Delcros, J. G., Bernet, A., Laudet, V. and Mehlen, P. (2009). Inhibition of endothelial cell apoptosis by netrin-1 during angiogenesis. *Dev Cell* 16, 614-20.

Chen, H., Chedotal, A., He, Z., Goodman, C. S. and Tessier-Lavigne, M. (1997). Neuropilin-2, a novel member of the neuropilin family, is a high affinity receptor for the semaphorins Sema E and Sema IV but not Sema III. *Neuron* 19, 547-59.

Chen, Q., Jiang, L., Li, C., Hu, D., Bu, J. W., Cai, D. and Du, J. L. (2012). Haemodynamics-driven developmental pruning of brain vasculature in zebrafish. *PLoS Biol* 10, e1001374.

Chi, N. C., Shaw, R. M., De Val, S., Kang, G., Jan, L. Y., Black, B. L. and Stainier, D. Y. (2008). Foxn4 directly regulates tbx2b expression and atrioventricular canal formation. *Genes Dev* 22, 734-9.

Claxton, S. and Fruttiger, M. (2005). Oxygen modifies artery differentiation and network morphogenesis in the retinal vasculature. *Dev Dyn* 233, 822-8.

Coultas, L., Chawengsaksophak, K. and Rossant, J. (2005). Endothelial cells and VEGF in vascular development. *Nature* 438, 937-45.

Covassin, L., Amigo, J. D., Suzuki, K., Teplyuk, V., Straubhaar, J. and Lawson, N. D. (2006). Global analysis of hematopoietic and vascular endothelial gene expression by tissue specific microarray profiling in zebrafish. *Dev Biol* 299, 551-62.

Cudmore, M. J., Hewett, P. W., Ahmad, S., Wang, K. Q., Cai, M., Al-Ani, B., Fujisawa, T., Ma, B., Sissaoui, S., Ramma, W. et al. (2012). The role of heterodimerization between VEGFR-1 and VEGFR-2 in the regulation of endothelial cell homeostasis. *Nat Commun* 3, 972.

Czech, B. and Hannon, G. J. (2011). Small RNA sorting: matchmaking for Argonautes. *Nat Rev Genet* 12, 19-31.

Davis, G. E. and Senger, D. R. (2005). Endothelial extracellular matrix: biosynthesis, remodeling, and functions during vascular morphogenesis and neovessel stabilization. *Circ Res* 97, 1093-107.

De Smet, F., Segura, I., De Bock, K., Hohensinner, P. J. and Carmeliet, P. (2009). Mechanisms of vessel branching: filopodia on endothelial tip cells lead the way. *Arterioscler Thromb Vasc Biol* 29, 639-49.

Dews, M., Homayouni, A., Yu, D., Murphy, D., Sevignani, C., Wentzel, E., Furth, E. E., Lee, W. M., Enders, G. H., Mendell, J. T. et al. (2006). Augmentation of tumor angiogenesis by a Myc-activated microRNA cluster. *Nat Genet* 38, 1060-5.

Dickson, B. J. and Gilestro, G. F. (2006). Regulation of commissural axon pathfinding by slit and its Robo receptors. *Annu Rev Cell Dev Biol* 22, 651-75.

Djuranovic, S., Nahvi, A. and Green, R. (2012). miRNA-mediated gene silencing by translational repression followed by mRNA deadenylation and decay. *Science* 336, 237-40.

Doebele, C., Bonauer, A., Fischer, A., Scholz, A., Reiss, Y., Urbich, C., Hofmann, W. K., Zeiher, A. M. and Dimmeler, S. (2010). Members of the microRNA-17-92 cluster exhibit a cell-intrinsic antiangiogenic function in endothelial cells. *Blood* 115, 4944-50.

Eble, J. A. and Niland, S. (2009). The extracellular matrix of blood vessels. *Curr Pharm Des* 15, 1385-400.

Ebos, J. M. and Kerbel, R. S. (2011). Antiangiogenic therapy: impact on invasion, disease progression, and metastasis. *Nat Rev Clin Oncol* 8, 210-21.

Eilken, H. M. and Adams, R. H. (2010). Dynamics of endothelial cell behavior in sprouting angiogenesis. *Curr Opin Cell Biol* 22, 617-25.

Fantin, A., Vieira, J. M., Gestri, G., Denti, L., Schwarz, Q., Prykhozhij, S., Peri, F., Wilson, S. W. and Ruhrberg, C. (2010). Tissue macrophages act as cellular chaperones for vascular anastomosis downstream of VEGF-mediated endothelial tip cell induction. *Blood* 116, 829-40.

Fasanaro, P., D'Alessandra, Y., Di Stefano, V., Melchionna, R., Romani, S., Pompilio, G., Capogrossi, M. C. and Martelli, F. (2008). MicroRNA-210 modulates endothelial cell response to hypoxia and inhibits the receptor tyrosine kinase ligand Ephrin-A3. *J Biol Chem* 283, 15878-83.

Ferrara, N., Carver-Moore, K., Chen, H., Dowd, M., Lu, L., O'Shea, K. S., Powell-Braxton, L., Hillan, K. J. and Moore, M. W. (1996). Heterozygous embryonic lethality induced by targeted inactivation of the VEGF gene. *Nature* 380, 439-42.

Fischer, C., Mazzone, M., Jonckx, B. and Carmeliet, P. (2008). FLT1 and its ligands VEGFB and PlGF: drug targets for anti-angiogenic therapy? *Nat Rev Cancer* 8, 942-56.

Fish, J. E., Santoro, M. M., Morton, S. U., Yu, S., Yeh, R. F., Wythe, J. D., Ivey, K. N., Bruneau, B. G., Stainier, D. Y. and Srivastava, D. (2008). miR-126 regulates angiogenic signaling and vascular integrity. *Dev Cell* 15, 272-84.

Fong, G. H., Rossant, J., Gertsenstein, M. and Breitman, M. L. (1995). Role of the Flt-1 receptor tyrosine kinase in regulating the assembly of vascular endothelium. *Nature* 376, 66-70.

Fong, G. H., Zhang, L., Bryce, D. M. and Peng, J. (1999). Increased hemangioblast commitment, not vascular disorganization, is the primary defect in flt-1 knock-out mice. *Development* 126, 3015-25.

Fredriksson, L., Li, H. and Eriksson, U. (2004). The PDGF family: four gene products form five dimeric isoforms. *Cytokine Growth Factor Rev* 15, 197-204.

Fukushima, Y., Okada, M., Kataoka, H., Hirashima, M., Yoshida, Y., Mann, F., Gomi, F., Nishida, K., Nishikawa, S. and Uemura, A. (2011).

Sema3E-PlexinD1 signaling selectively suppresses disoriented angiogenesis in ischemic retinopathy in mice. *J Clin Invest* 121, 1974-85.

Gaengel, K., Genove, G., Armulik, A. and Betsholtz, C. (2009). Endothelial-mural cell signaling in vascular development and angiogenesis. *Arterioscler Thromb Vasc Biol* 29, 630-8.

Gale, N. W., Dominguez, M. G., Noguera, I., Pan, L., Hughes, V., Valenzuela, D. M., Murphy, A. J., Adams, N. C., Lin, H. C., Holash, J. et al. (2004). Haploinsufficiency of delta-like 4 ligand results in embryonic lethality due to major defects in arterial and vascular development. *Proc Natl Acad Sci U S A* 101, 15949-54.

Gerhardt, H., Golding, M., Fruttiger, M., Ruhrberg, C., Lundkvist, A., Abramsson, A., Jeltsch, M., Mitchell, C., Alitalo, K., Shima, D. et al. (2003). VEGF guides angiogenic sprouting utilizing endothelial tip cell filopodia. *J Cell Biol* 161, 1163-77.

Gerhardt, H., Ruhrberg, C., Abramsson, A., Fujisawa, H., Shima, D. and Betsholtz, C. (2004). Neuropilin-1 is required for endothelial tip cell guidance in the developing central nervous system. *Dev Dyn* 231, 503-9.

Geudens, I. and Gerhardt, H. (2011). Coordinating cell behaviour during blood vessel formation. *Development* 138, 4569-83.

Ghildiyal, M. and Zamore, P. D. (2009). Small silencing RNAs: an expanding universe. *Nat Rev Genet* 10, 94-108.

Giraldez, A. J., Cinalli, R. M., Glasner, M. E., Enright, A. J., Thomson, J. M., Baskerville, S., Hammond, S. M., Bartel, D. P. and Schier, A. F. (2005). MicroRNAs regulate brain morphogenesis in zebrafish. *Science* 308, 833-8.

Gitler, A. D., Lu, M. M. and Epstein, J. A. (2004). PlexinD1 and semaphorin signaling are required in endothelial cells for cardiovascular development. *Dev Cell* 7, 107-16.

Gore, A. V., Monzo, K., Cha, Y. R., Pan, W. and Weinstein, B. M. (2012). Vascular development in the zebrafish. *Cold Spring Harb Perspect Med* 2, a006684.

Gregory, R. I., Chendrimada, T. P., Cooch, N. and Shiekhattar, R. (2005). Human RISC couples microRNA biogenesis and posttranscriptional gene silencing. *Cell* 123, 631-40.

Gu, C., Yoshida, Y., Livet, J., Reimert, D. V., Mann, F., Merte, J., Henderson, C. E., Jessell, T. M., Kolodkin, A. L. and Ginty, D. D. (2005). Semaphorin 3E and plexin-D1 control vascular pattern independently of neuropilins. *Science* 307, 265-8.

Guarani, V., Deflorian, G., Franco, C. A., Kruger, M., Phng, L. K., Bentley, K., Toussaint, L., Dequiedt, F., Mostoslavsky, R., Schmidt, M. H. et al. (2011). Acetylation-dependent regulation of endothelial Notch signalling by the SIRT1 deacetylase. *Nature* 473, 234-8.

Guo, H., Ingolia, N. T., Weissman, J. S. and Bartel, D. P. (2010). Mammalian microRNAs predominantly act to decrease target mRNA levels. *Nature* 466, 835-40.

Harris, T. A., Yamakuchi, M., Ferlito, M., Mendell, J. T. and Lowenstein, C. J. (2008). MicroRNA-126 regulates endothelial expression of vascular cell adhesion molecule 1. *Proc Natl Acad Sci U S A* 105, 1516-21.

Harris, T. A., Yamakuchi, M., Kondo, M., Oettgen, P. and Lowenstein, C. J. (2010). Ets-1 and Ets-2 regulate the expression of microRNA-126 in endothelial cells. *Arterioscler Thromb Vasc Biol* 30, 1990-7.

Hassel, D., Cheng, P., White, M. P., Ivey, K. N., Kroll, J., Augustin, H. G., Katus, H. A., Stainier, D. Y. and Srivastava, D. (2012). MicroRNA-10 regulates the angiogenic behavior of zebrafish and human endothelial cells by promoting vascular endothelial growth factor signaling. *Circ Res* 111, 1421-33.

He, L. and Hannon, G. J. (2004). MicroRNAs: small RNAs with a big role in gene regulation. *Nat Rev Genet* 5, 522-31.

He, X., Yan, Y. L., DeLaurier, A. and Postlethwait, J. H. (2011). Observation of miRNA gene expression in zebrafish embryos by in situ hybridization to microRNA primary transcripts. *Zebrafish* 8, 1-8.

He, Z. and Tessier-Lavigne, M. (1997). Neuropilin is a receptor for the axonal chemorepellent Semaphorin III. *Cell* 90, 739-51.

Hedlund, E. M., Yang, X., Zhang, Y., Yang, Y., Shibuya, M., Zhong, W., Sun, B., Liu, Y., Hosaka, K. and Cao, Y. (2013). Tumor cell-derived placental growth factor sensitizes antiangiogenic and antitumor effects of anti-VEGF drugs. *Proc Natl Acad Sci U S A* 110, 654-9.

Hellstrom, M., Kalen, M., Lindahl, P., Abramsson, A. and Betsholtz, C. (1999). Role of PDGF-B and PDGFR-beta in recruitment of vascular smooth muscle cells and pericytes during embryonic blood vessel formation in the mouse. *Development* 126, 3047-55.

Hellstrom, M., Phng, L. K., Hofmann, J. J., Wallgard, E., Coultas, L., Lindblom, P., Alva, J., Nilsson, A. K., Karlsson, L., Gaiano, N. et al. (2007). Dll4 signalling through Notch1 regulates formation of tip cells during angiogenesis. *Nature* 445, 776-80.

Herbert, S. P., Cheung, J. Y. and Stainier, D. Y. (2012). Determination of endothelial stalk versus tip cell potential during angiogenesis by H2.0-like homeobox-1. *Curr Biol* 22, 1789-94.

Herbert, S. P. and Stainier, D. Y. (2011). Molecular control of endothelial cell behaviour during blood vessel morphogenesis. *Nat Rev Mol Cell Biol* 12, 551-64.

Heusschen, R., van Gink, M., Griffioen, A. W. and Thijssen, V. L. (2010). MicroRNAs in the tumor endothelium: novel controls on the angioregulatory switchboard. *Biochim Biophys Acta* 1805, 87-96.

Hiratsuka, S., Nakao, K., Nakamura, K., Katsuki, M., Maru, Y. and Shibuya, M. (2005). Membrane fixation of vascular endothelial growth factor receptor 1 ligand-binding domain is important for vasculogenesis and angiogenesis in mice. *Mol Cell Biol* 25, 346-54.

Hoey, T., Yen, W. C., Axelrod, F., Basi, J., Donigian, L., Dylla, S., Fitch-Bruhns, M., Lazetic, S., Park, I. K., Sato, A. et al. (2009). DLL4 blockade inhibits tumor growth and reduces tumor-initiating cell frequency. *Cell Stem Cell* 5, 168-77.

Hogan, B. M., Herpers, R., Witte, M., Helotera, H., Alitalo, K., Duckers, H. J. and Schulte-Merker, S. (2009). Vegfc/Flt4 signalling is suppressed by Dll4 in developing zebrafish intersegmental arteries. *Development* 136, 4001-9.

Huang, H., Bhat, A., Woodnutt, G. and Lappe, R. (2010). Targeting the ANGPT-TIE2 pathway in malignancy. *Nat Rev Cancer* 10, 575-85.

Huang, K., Andersson, C., Roomans, G. M., Ito, N. and Claesson-Welsh, L. (2001). Signaling properties of VEGF receptor-1 and -2 homo- and heterodimers. *Int J Biochem Cell Biol* 33, 315-24.

Hutvagner, G., McLachlan, J., Pasquinelli, A. E., Balint, E., Tuschl, T. and Zamore, P. D. (2001). A cellular function for the RNA-interference enzyme Dicer in the maturation of the let-7 small temporal RNA. *Science* 293, 834-8.

Inui, M., Martello, G. and Piccolo, S. (2010). MicroRNA control of signal transduction. *Nat Rev Mol Cell Biol* 11, 252-63.

Isogai, S., Horiguchi, M. and Weinstein, B. M. (2001). The vascular anatomy of the developing zebrafish: an atlas of embryonic and early larval development. *Dev Biol* 230, 278-301.

Isogai, S., Lawson, N. D., Torrealday, S., Horiguchi, M. and Weinstein, B. M. (2003). Angiogenic network formation in the developing vertebrate trunk. *Development* 130, 5281-90.

Jakobsson, L., Franco, C. A., Bentley, K., Collins, R. T., Ponsioen, B., Aspalter, I. M., Rosewell, I., Busse, M., Thurston, G., Medvinsky, A. et al. (2010). Endothelial cells dynamically compete for the tip cell position during angiogenic sprouting. *Nat Cell Biol* 12, 943-53.

Jekosch, K. (2004). The zebrafish genome project: sequence analysis and annotation. *Methods Cell Biol* 77, 225-39.

Jin, S. W., Herzog, W., Santoro, M. M., Mitchell, T. S., Frantsve, J., Jungblut, B., Beis, D., Scott, I. C., D'Amico, L. A., Ober, E. A. et al. (2007). A transgene-assisted genetic screen identifies essential regulators of vascular development in vertebrate embryos. *Dev Biol* 307, 29-42.

Johnson, D. W., Berg, J. N., Baldwin, M. A., Gallione, C. J., Marondel, I., Yoon, S. J., Stenzel, T. T., Speer, M., Pericak-Vance, M. A., Diamond, A. et al. (1996). Mutations in the activin receptor-like kinase 1 gene in hereditary haemorrhagic telangiectasia type 2. *Nat Genet* 13, 189-95.

Kanno, S., Oda, N., Abe, M., Terai, Y., Ito, M., Shitara, K., Tabayashi, K., Shibuya, M. and Sato, Y. (2000). Roles of two VEGF receptors, Flt-1 and KDR, in the signal transduction of VEGF effects in human vascular endothelial cells. *Oncogene* 19, 2138-46.

Kawasaki, T., Kitsukawa, T., Bekku, Y., Matsuda, Y., Sanbo, M., Yagi, T. and Fujisawa, H. (1999). A requirement for neuropilin-1 in embryonic vessel formation. *Development* 126, 4895-902.

Kim, J., Oh, W. J., Gaiano, N., Yoshida, Y. and Gu, C. (2011). Semaphorin 3E-Plexin-D1 signaling regulates VEGF function in developmental angiogenesis via a feedback mechanism. *Genes Dev* 25, 1399-411.

Kimmel, C. B., Ballard, W. W., Kimmel, S. R., Ullmann, B. and Schilling, T. F. (1995). Stages of embryonic development of the zebrafish. *Dev Dyn* 203, 253-310.

King, I. N., Qian, L., Liang, J., Huang, Y., Shieh, J. T., Kwon, C. and Srivastava, D. (2011). A genome-wide screen reveals a role for microRNA-1 in modulating cardiac cell polarity. *Dev Cell* 20, 497-510.

Kitsukawa, T., Shimono, A., Kawakami, A., Kondoh, H. and Fujisawa, H. (1995). Overexpression of a membrane protein, neuropilin, in chimeric mice causes anomalies in the cardiovascular system, nervous system and limbs. *Development* 121, 4309-18.

Klagsbrun, M. and Eichmann, A. (2005). A role for axon guidance receptors and ligands in blood vessel development and tumor angiogenesis. *Cytokine Growth Factor Rev* 16, 535-48.

Kloosterman, W. P., Wienholds, E., de Bruijn, E., Kauppinen, S. and Plasterk, R. H. (2006). In situ detection of miRNAs in animal embryos using LNA-modified oligonucleotide probes. *Nat Methods* 3, 27-9.

Koch, A. W., Mathivet, T., Larrivee, B., Tong, R. K., Kowalski, J., Pibouin-Fragner, L., Bouvree, K., Stawicki, S., Nicholes, K., Rathore, N. et al. (2011). Robo4 maintains vessel integrity and inhibits angiogenesis by interacting with UNC5B. *Dev Cell* 20, 33-46.

Krueger, J., Liu, D., Scholz, K., Zimmer, A., Shi, Y., Klein, C., Siekmann, A., Schulte-Merker, S., Cudmore, M., Ahmed, A. et al. (2011). Flt1 acts as a negative regulator of tip cell formation and branching morphogenesis in the zebrafish embryo. *Development* 138, 2111-20.

Kuehbacher, A., Urbich, C., Zeiher, A. M. and Dimmeler, S. (2007). Role of Dicer and Drosha for endothelial microRNA expression and angiogenesis. *Circ Res* 101, 59-68.

Kuhnert, F., Mancuso, M. R., Hampton, J., Stankunas, K., Asano, T., Chen, C. Z. and Kuo, C. J. (2008). Attribution of vascular phenotypes of the murine Egfl7 locus to the microRNA miR-126. *Development* 135, 3989-93.

Kulshreshtha, R., Ferracin, M., Negrini, M., Calin, G. A., Davuluri, R. V. and Ivan, M. (2007). Regulation of microRNA expression: the hypoxic component. *Cell Cycle* 6, 1426-31.

Kulshreshtha, R., Ferracin, M., Wojcik, S. E., Garzon, R., Alder, H., Agosto-Perez, F. J., Davuluri, R., Liu, C. G., Croce, C. M., Negrini, M. et al. (2007). A microRNA signature of hypoxia. *Mol Cell Biol* 27, 1859-67.

Lagendijk, A. K., Moulton, J. D. and Bakkers, J. (2012). Revealing details: whole mount microRNA in situ hybridization protocol for zebrafish embryos and adult tissues. *Biol Open* 1, 566-9.

Lagos-Quintana, M., Rauhut, R., Lendeckel, W. and Tuschl, T. (2001). Identification of novel genes coding for small expressed RNAs. *Science* 294, 853-8.

Lagos-Quintana, M., Rauhut, R., Yalcin, A., Meyer, J., Lendeckel, W. and Tuschl, T. (2002). Identification of tissue-specific microRNAs from mouse. *Curr Biol* 12, 735-9.

Lahteenvuo, J. E., Lahteenvuo, M. T., Kivela, A., Rosenlew, C., Falkevall, A., Klar, J., Heikura, T., Rissanen, T. T., Vahakangas, E., Korpisalo, P. et al. (2009). Vascular endothelial growth factor-B induces myocardium-specific angiogenesis and arteriogenesis via vascular endothelial growth factor receptor-1- and neuropilin receptor-1-dependent mechanisms. *Circulation* 119, 845-56.

Larkin, M. A., Blackshields, G., Brown, N. P., Chenna, R., McGettigan, P. A., McWilliam, H., Valentin, F., Wallace, I. M., Wilm, A., Lopez, R. et al. (2007). Clustal W and Clustal X version 2.0. *Bioinformatics* 23, 2947-8.

Larrivee, B., Prahst, C., Gordon, E., del Toro, R., Mathivet, T., Duarte, A., Simons, M. and Eichmann, A. (2012). ALK1 signaling inhibits angiogenesis by cooperating with the Notch pathway. *Dev Cell* 22, 489-500.

Lawson, N. D. and Weinstein, B. M. (2002). In vivo imaging of embryonic vascular development using transgenic zebrafish. *Dev Biol* 248, 307-18.

Lebrin, F., Deckers, M., Bertolino, P. and Ten Dijke, P. (2005). TGF-beta receptor function in the endothelium. *Cardiovasc Res* 65, 599-608.

Lee, Y., Ahn, C., Han, J., Choi, H., Kim, J., Yim, J., Lee, J., Provost, P., Radmark, O., Kim, S. et al. (2003). The nuclear RNase III Drosha initiates microRNA processing. *Nature* 425, 415-9.

Leslie, J. D., Ariza-McNaughton, L., Bermange, A. L., McAdow, R., Johnson, S. L. and Lewis, J. (2007). Endothelial signalling by the Notch ligand Delta-like 4 restricts angiogenesis. *Development* 134, 839-44.

Li, J. L., Sainson, R. C., Shi, W., Leek, R., Harrington, L. S., Preusser, M., Biswas, S., Turley, H., Heikamp, E., Hainfellner, J. A. et al. (2007). Delta-like 4 Notch ligand regulates tumor angiogenesis, improves tumor vascular function, and promotes tumor growth in vivo. *Cancer Res* 67, 11244-53.

Lindahl, P., Johansson, B. R., Leveen, P. and Betsholtz, C. (1997). Pericyte loss and microaneurysm formation in PDGF-B-deficient mice. *Science* 277, 242-5.

Lobov, I. B., Cheung, E., Wudali, R., Cao, J., Halasz, G., Wei, Y., Economides, A., Lin, H. C., Papadopoulos, N., Yancopoulos, G. D. et al. (2011). The Dll4/Notch pathway controls postangiogenic blood vessel remodeling and regression by modulating vasoconstriction and blood flow. *Blood* 117, 6728-37.

Lobov, I. B., Renard, R. A., Papadopoulos, N., Gale, N. W., Thurston, G., Yancopoulos, G. D. and Wiegand, S. J. (2007). Delta-like ligand 4 (Dll4) is induced by VEGF as a negative regulator of angiogenic sprouting. *Proc Natl Acad Sci U S A* 104, 3219-24.

Lohela, M., Bry, M., Tammela, T. and Alitalo, K. (2009). VEGFs and receptors involved in angiogenesis versus lymphangiogenesis. *Curr Opin Cell Biol* 21, 154-65.

Lu, X., Le Noble, F., Yuan, L., Jiang, Q., De Lafarge, B., Sugiyama, D., Breant, C., Claes, F., De Smet, F., Thomas, J. L. et al. (2004). The netrin receptor UNC5B mediates guidance events controlling morphogenesis of the vascular system. *Nature* 432, 179-86.

Maden, C. H., Gomes, J., Schwarz, Q., Davidson, K., Tinker, A. and Ruhrberg, C. (2012). NRP1 and NRP2 cooperate to regulate gangliogenesis, axon guidance and target innervation in the sympathetic nervous system. *Dev Biol* 369, 277-85.

Maisonpierre, P. C., Suri, C., Jones, P. F., Bartunkova, S., Wiegand, S. J., Radziejewski, C., Compton, D., McClain, J., Aldrich, T. H., Papadopoulos, N. et al. (1997). Angiopoietin-2, a natural antagonist for Tie2 that disrupts in vivo angiogenesis. *Science* 277, 55-60.

Mazzone, M., Dettori, D., Leite de Oliveira, R., Loges, S., Schmidt, T., Jonckx, B., Tian, Y. M., Lanahan, A. A., Pollard, P., Ruiz de Almodovar, C. et al. (2009). Heterozygous deficiency of PHD2 restores tumor oxygenation and inhibits metastasis via endothelial normalization. *Cell* 136, 839-51.

McAllister, K. A., Grogg, K. M., Johnson, D. W., Gallione, C. J., Baldwin, M. A., Jackson, C. E., Helmbold, E. A., Markel, D. S., McKinnon, W. C., Murrell, J. et al. (1994). Endoglin, a TGF-beta binding protein of endothelial cells, is the gene for hereditary haemorrhagic telangiectasia type 1. *Nat Genet* 8, 345-51.

McKinney, M. C. and Weinstein, B. M. (2008). Chapter 4. Using the zebrafish to study vessel formation. *Methods Enzymol* 444, 65-97.

Mendell, J. T. (2008). miRiad roles for the miR-17-92 cluster in development and disease. *Cell* 133, 217-22.

Mishima, Y., Abreu-Goodger, C., Staton, A. A., Stahlhut, C., Shou, C., Cheng, C., Gerstein, M., Enright, A. J. and Giraldez, A. J. (2009). Zebrafish miR-1 and miR-133 shape muscle gene expression and regulate sarcomeric actin organization. *Genes Dev* 23, 619-32.

Moya, I. M., Umans, L., Maas, E., Pereira, P. N., Beets, K., Francis, A., Sents, W., Robertson, E. J., Mummery, C. L., Huylebroeck, D. et al. (2012). Stalk cell phenotype depends on integration of Notch and Smad1/5 signaling cascades. *Dev Cell* 22, 501-14.

Napp, L. C., Augustynik, M., Paesler, F., Krishnasamy, K., Woiterski, J., Limbourg, A., Bauersachs, J., Drexler, H., Le Noble, F. and Limbourg, F. P. (2012). Extrinsic Notch ligand Delta-like 1 regulates tip cell selection and vascular branching morphogenesis. *Circ Res* 110, 530-5.

Nasevicius, A. and Ekker, S. C. (2000). Effective targeted gene 'knockdown' in zebrafish. *Nat Genet* 26, 216-20.

Neagoe, P. E., Lemieux, C. and Sirois, M. G. (2005). Vascular endothelial growth factor (VEGF)-A165-induced prostacyclin synthesis requires the activation of VEGF receptor-1 and -2 heterodimer. *J Biol Chem* 280, 9904-12.

Neufeld, G., Cohen, T., Shraga, N., Lange, T., Kessler, O. and Herzog, Y. (2002). The neuropilins: multifunctional semaphorin and VEGF receptors that modulate axon guidance and angiogenesis. *Trends Cardiovasc Med* 12, 13-9.

Nicoli, S., Knyphausen, C. P., Zhu, L. J., Lakshmanan, A. and Lawson, N. D. (2012). miR-221 is required for endothelial tip cell behaviors during vascular development. *Dev Cell* 22, 418-29.

Nicoli, S., Standley, C., Walker, P., Hurlstone, A., Fogarty, K. E. and Lawson, N. D. (2010). MicroRNA-mediated integration of haemodynamics and Vegf signalling during angiogenesis. *Nature* 464, 1196-200.

Nilsson, I., Bahram, F., Li, X., Gualandi, L., Koch, S., Jarvius, M., Soderberg, O., Anisimov, A., Kholova, I., Pytowski, B. et al. (2010). VEGF receptor 2/-3 heterodimers detected in situ by proximity ligation on angiogenic sprouts. *EMBO J* 29, 1377-88.

Noguera-Troise, I., Daly, C., Papadopoulos, N. J., Coetzee, S., Boland, P., Gale, N. W., Lin, H. C., Yancopoulos, G. D. and Thurston, G. (2006). Blockade of Dll4 inhibits tumour growth by promoting non-productive angiogenesis. *Nature* 444, 1032-7.

Oh, W. J. and Gu, C. (2013). The role and mechanism-of-action of Sema3E and Plexin-D1 in vascular and neural development. *Semin Cell Dev Biol* 24, 156-62.

Ota, A., Tagawa, H., Karnan, S., Tsuzuki, S., Karpas, A., Kira, S., Yoshida, Y. and Seto, M. (2004). Identification and characterization of a novel gene, C13orf25, as a target for 13q31-q32 amplification in malignant lymphoma. *Cancer Res* 64, 3087-95.

Pardali, E., Goumans, M. J. and ten Dijke, P. (2010). Signaling by members of the TGF-beta family in vascular morphogenesis and disease. *Trends Cell Biol* 20, 556-67.

Phng, L. K. and Gerhardt, H. (2009). Angiogenesis: a team effort coordinated by notch. *Dev Cell* 16, 196-208.

Phng, L. K., Potente, M., Leslie, J. D., Babbage, J., Nyqvist, D., Lobov, I., Ondr, J. K., Rao, S., Lang, R. A., Thurston, G. et al. (2009). Nrarp coordinates endothelial Notch and Wnt signaling to control vessel density in angiogenesis. *Dev Cell* 16, 70-82.

Poliseno, L., Tuccoli, A., Mariani, L., Evangelista, M., Citti, L., Woods, K., Mercatanti, A., Hammond, S. and Rainaldi, G. (2006). MicroRNAs modulate the angiogenic properties of HUVECs. *Blood* 108, 3068-71.

Poole, T. J. and Coffin, J. D. (1989). Vasculogenesis and angiogenesis: two distinct morphogenetic mechanisms establish embryonic vascular pattern. *J Exp Zool* 251, 224-31.

Potente, M., Gerhardt, H. and Carmeliet, P. (2011). Basic and therapeutic aspects of angiogenesis. *Cell* 146, 873-87.

Pugh, C. W. and Ratcliffe, P. J. (2003). Regulation of angiogenesis by hypoxia: role of the HIF system. *Nat Med* 9, 677-84.

Ridgway, J., Zhang, G., Wu, Y., Stawicki, S., Liang, W. C., Chanthery, Y., Kowalski, J., Watts, R. J., Callahan, C., Kasman, I. et al. (2006). Inhibition of Dll4 signalling inhibits tumour growth by deregulating angiogenesis. *Nature* 444, 1083-7.

Roca, C. and Adams, R. H. (2007). Regulation of vascular morphogenesis by Notch signaling. *Genes Dev* 21, 2511-24.

Sakurai, A., Doci, C. L. and Gutkind, J. S. (2012). Semaphorin signaling in angiogenesis, lymphangiogenesis and cancer. *Cell Res* 22, 23-32.

Sato, T. N., Tozawa, Y., Deutsch, U., Wolburg-Buchholz, K., Fujiwara, Y., Gendron-Maguire, M., Gridley, T., Wolburg, H., Risau, W. and Qin, Y. (1995). Distinct roles of the receptor tyrosine kinases Tie-1 and Tie-2 in blood vessel formation. *Nature* 376, 70-4.

Selbach, M., Schwanhausser, B., Thierfelder, N., Fang, Z., Khanin, R. and Rajewsky, N. (2008). Widespread changes in protein synthesis induced by microRNAs. *Nature* 455, 58-63.

Serini, G., Valdembri, D., Zanivan, S., Morterra, G., Burkhardt, C., Caccavari, F., Zammataro, L., Primo, L., Tamagnone, L., Logan, M. et al. (2003). Class 3 semaphorins control vascular morphogenesis by inhibiting integrin function. *Nature* 424, 391-7.

Shalaby, F., Rossant, J., Yamaguchi, T. P., Gertsenstein, M., Wu, X. F., Breitman, M. L. and Schuh, A. C. (1995). Failure of blood-island formation and vasculogenesis in Flk-1-deficient mice. *Nature* 376, 62-6.

Shkumatava, A., Stark, A., Sive, H. and Bartel, D. P. (2009). Coherent but overlapping expression of microRNAs and their targets during vertebrate development. *Genes Dev* 23, 466-81.

Siekmann, A. F. and Lawson, N. D. (2007). Notch signalling limits angiogenic cell behaviour in developing zebrafish arteries. *Nature* 445, 781-4.

Sokol, N. S. and Ambros, V. (2005). Mesodermally expressed Drosophila microRNA-1 is regulated by Twist and is required in muscles during larval growth. *Genes Dev* 19, 2343-54.

Stahlhut, C., Suarez, Y., Lu, J., Mishima, Y. and Giraldez, A. J. (2012). miR-1 and miR-206 regulate angiogenesis by modulating VegfA expression in zebrafish. *Development* 139, 4356-64.

Suarez, Y., Fernandez-Hernando, C., Pober, J. S. and Sessa, W. C. (2007). Dicer dependent microRNAs regulate gene expression and functions in human endothelial cells. *Circ Res* 100, 1164-73.

Suarez, Y., Fernandez-Hernando, C., Yu, J., Gerber, S. A., Harrison, K. D., Pober, J. S., Iruela-Arispe, M. L., Merkenschlager, M. and Sessa, W. C. (2008). Dicer-dependent endothelial microRNAs are necessary for postnatal angiogenesis. *Proc Natl Acad Sci U S A* 105, 14082-7.

Suchting, S., Freitas, C., le Noble, F., Benedito, R., Breant, C., Duarte, A. and Eichmann, A. (2007). The Notch ligand Delta-like 4 negatively regulates endothelial tip cell formation and vessel branching. *Proc Natl Acad Sci U S A* 104, 3225-30.

Tammela, T., Zarkada, G., Nurmi, H., Jakobsson, L., Heinolainen, K., Tvorogov, D., Zheng, W., Franco, C. A., Murtomaki, A., Aranda, E. et al. (2011). VEGFR-3 controls tip to stalk conversion at vessel fusion sites by reinforcing Notch signalling. *Nat Cell Biol* 13, 1202-13.

Tammela, T., Zarkada, G., Wallgard, E., Murtomaki, A., Suchting, S., Wirzenius, M., Waltari, M., Hellstrom, M., Schomber, T., Peltonen, R. et al. (2008). Blocking VEGFR-3 suppresses angiogenic sprouting and vascular network formation. *Nature* 454, 656-60.

Tamura, K., Peterson, D., Peterson, N., Stecher, G., Nei, M. and Kumar, S. (2011). MEGA5: molecular evolutionary genetics analysis using maximum likelihood, evolutionary distance, and maximum parsimony methods. *Mol Biol Evol* 28, 2731-9.

Thurston, G., Noguera-Troise, I. and Yancopoulos, G. D. (2007). The Delta paradox: DLL4 blockade leads to more tumour vessels but less tumour growth. *Nat Rev Cancer* 7, 327-31.

Torres-Vazquez, J., Gitler, A. D., Fraser, S. D., Berk, J. D., Van, N. P., Fishman, M. C., Childs, S., Epstein, J. A. and Weinstein, B. M. (2004). Semaphorin-plexin signaling guides patterning of the developing vasculature. *Dev Cell* 7, 117-23.

Trindade, A., Djokovic, D., Gigante, J., Badenes, M., Pedrosa, A. R., Fernandes, A. C., Lopes-da-Costa, L., Krasnoperov, V., Liu, R., Gill, P. S. et al. (2012). Low-dosage inhibition of Dll4 signaling promotes wound healing by inducing functional neo-angiogenesis. *PLoS One* 7, e29863.

Trindade, A., Kumar, S. R., Scehnet, J. S., Lopes-da-Costa, L., Becker, J., Jiang, W., Liu, R., Gill, P. S. and Duarte, A. (2008). Overexpression of delta-like 4 induces arterialization and attenuates vessel formation in developing mouse embryos. *Blood* 112, 1720-9.

Tvorogov, D., Anisimov, A., Zheng, W., Leppanen, V. M., Tammela, T., Laurinavicius, S., Holnthoner, W., Helotera, H., Holopainen, T., Jeltsch, M. et al. (2010). Effective suppression of vascular network formation by combination of antibodies blocking VEGFR ligand binding and receptor dimerization. *Cancer Cell* 18, 630-40.

Urbich, C., Kaluza, D., Fromel, T., Knau, A., Bennewitz, K., Boon, R. A., Bonauer, A., Doebele, C., Boeckel, J. N., Hergenreider, E. et al. (2012). MicroRNA-27a/b controls endothelial cell repulsion and angiogenesis by targeting semaphorin 6A. *Blood* 119, 1607-16.

Wang, S., Aurora, A. B., Johnson, B. A., Qi, X., McAnally, J., Hill, J. A., Richardson, J. A., Bassel-Duby, R. and Olson, E. N. (2008). The endothelial-specific microRNA miR-126 governs vascular integrity and angiogenesis. *Dev Cell* 15, 261-71.

Wienholds, E., Kloosterman, W. P., Miska, E., Alvarez-Saavedra, E., Berezikov, E., de Bruijn, E., Horvitz, H. R., Kauppinen, S. and Plasterk, R. H. (2005).

MicroRNA expression in zebrafish embryonic development. *Science* 309, 310-1.

Winter, J., Jung, S., Keller, S., Gregory, R. I. and Diederichs, S. (2009). Many roads to maturity: microRNA biogenesis pathways and their regulation. *Nat Cell Biol* 11, 228-34.

Wurdinger, T., Tannous, B. A., Saydam, O., Skog, J., Grau, S., Soutschek, J., Weissleder, R., Breakefield, X. O. and Krichevsky, A. M. (2008). miR-296 regulates growth factor receptor overexpression in angiogenic endothelial cells. *Cancer Cell* 14, 382-93.

Yan, M., Callahan, C. A., Beyer, J. C., Allamneni, K. P., Zhang, G., Ridgway, J. B., Niessen, K. and Plowman, G. D. (2010). Chronic DLL4 blockade induces vascular neoplasms. *Nature* 463, E6-7.

Yang, W. J., Yang, D. D., Na, S., Sandusky, G. E., Zhang, Q. and Zhao, G. (2005). Dicer is required for embryonic angiogenesis during mouse development. *J Biol Chem* 280, 9330-5.

Zhang, J., Fukuhara, S., Sako, K., Takenouchi, T., Kitani, H., Kume, T., Koh, G. Y. and Mochizuki, N. (2011). Angiopoietin-1/Tie2 signal augments basal Notch signal controlling vascular quiescence by inducing delta-like 4 expression through AKT-mediated activation of beta-catenin. *J Biol Chem* 286, 8055-66.

Zhou, Q., Gallagher, R., Ufret-Vincenty, R., Li, X., Olson, E. N. and Wang, S. (2011). Regulation of angiogenesis and choroidal neovascularization by members of microRNA-23~27~24 clusters. *Proc Natl Acad Sci U S A* 108, 8287-92.

8   Abbreviations

4xCBF1	4 tandem CBF1 binding elements
ALK1	activin receptor-like kinase 1, ACVRL1
ALK5	activin receptor-like kinase 5, TGF-βR1, TβR-1
ANG	Angiopoietin
ASRGL1	asparaginase like 1
B3GAT2	β-1,3-glucuronyltransferase 2
bp	base pair
Cdkn1b	cyclin dependent kinase inhibitor 1b
Ch	chromosome
COL9A2	collagen, type IX, alpha 2
CTGF	connective tissue growth factor
CTPS	CTP synthase
cv	cardinal vein
CXCR4	chemokine (C-X-C motif) receptor 4
da	dorsal aorta
DCC	deleted in colorectal cancer
DLAV	dorsal longitudinal anastomotic vessel
Dll4	Delta-like 4
dpf	days post-fertilization
EC	endothelial cell
ECM	extracellular matrix
EFNB2	ephrin B2
EGF	epidermal growth factor
Egfl7	EGF-like domain 7
EGFP	enhanced GFP
eNOS	endothelial nitric oxide synthase

ENU	N-ethyl-N-nitrosourea
EphrinA3	eph-related receptor tyrosine kinase ligand 3
FACS	fluorescence-activated cell sorting
FCS	fetal calf serum
Flk1	Fetal liver kinase 1, VEGFR2, KDR
Flt1	Fms-related tyrosine kinase 1, VEGFR1
Flt4	Fms-related tyrosine kinase 4, VEGFR3
FN3	fibronectin type 3
GFP	green fluorescent protein
Hey2	hairy/enhancer-of-split related with YRPW motif protein 2
HGS	hepatocyte growth factor-regulated tyrosine kinase substrate
HHT	hereditary haemorrhagic teleangiectasia
HIF1α	hypoxia-inducible factor 1-alpha
Hlx1	H2.0-like homeobox-1
hpf	hours post-fertilization
HSPG	heparan sulfate proteoglycan
HUAEC	human umbilical artery endothelial cell
HUVEC	human umbilical vein endothelial cell
Ig	immunoglobulin
IL-8	interleukin-8
ISV	intersegmental vessel
ITGA5	integrin subunit alpha5
Jak1	Janus kinase 1
KCNK9	potassium channel subfamily K member 9
LNA	locked nucleic acid
MAPK	mitogen-activated protein kinase
Mb	mega base pairs
miR	microRNA, miRNA

MMP	matrix metalloprotease
MO	morpholino
mRNA	messenger RNA
nc	notochord
NDRG1	N-myc downstream regulated 1
NFYC	nuclear transcription factor Y, gamma
NICD	Notch intracellular domain
NRARP	Notch-regulated ankyrin repeat-containing protein
Nrp	Neuropilin
nt	nucleotide
nt	neural tube
obd	out-of-bounds, plexinD1 mutation
OGFRL1	opioid growth factor receptor-like 1
PAI	plasminogen activator inhibitor
PBS	phospahate buffered saline
pd	pronephric duct
PDGF	Platelet-derived growth factor
PDGFR	PDGF receptor
PI3K	phosphoinositide 3-kinase
PIK3R1	phosphoinositide-3-kinase regulatory subunit 1
PLCγ	phospholipase C gamma
PlGF	Placental growth factor
RGC	retinal ganglion cell
RIMS3	regulating synaptic membrane exocytosis 3
RISC	RNA-induced silencing complex
Robo	Roundabout
RT-PCR	reverse transcription polymerase chain reaction
SCF	stem cell factor

SDS–PAGE	sodium dodecyl sulfate polyacrylamide gel electrophoresis
Sema	Semaphorin
SIRT1	sirtuin1
SIV	subintestinal vessel
SMAP2	small ArfGAP2
Spred1	Sprouty-related EVH-domain-containing protein 1
ST3GAL1	sialyltransferase 4A
TGF-β	Transforming growth factor-β
TMX	Tamoxifen
TP1	terminal protein 1
TRAPPC9	trafficking protein particle complex 9
TSP1	thrombospondin 1
UNC5	uncoordinated-5
UTR	untranslated region
VCAM1	vascular cell adhesion molecule 1
VE-Cadherin	vascular endothelial-Cadherin
VEGF	vascular endothelial growth factor
VEGFR	VEGF receptor
vSMC	vascular smooth muscle cell
WISP1	WNT1 inducible signaling pathway protein 1
ZFAT	zinc finger protein 406

9   List of figures

10 List of tables

11   Curriculum vitae and publications

2010.7-present   PhD student (under the supervision of Prof. Dr. Ferdinand le Noble)

Max Delbrück Center for Molecular Medicine, Berlin-Buch
& Freie Universität Berlin

2006.9-2010.1   M.S. in Biochemistry and Molecular Biology (Prof. Dr. Houyan Song)

Department of Biochemistry and Molecular Biology, Shanghai
Medical School
& Key Lab of Molecular Medicine, Ministry of Education, Fudan Univ.

2003.7-2006.8   Research Assistant

Department of Biochemistry and Molecular Biology, Fudan Univ.

1999.9-2003.7   B.S. in Aquaculture

College of Aqua-life Science and Technology, Shanghai Ocean Univ.

List of publications

Jiang Q.*, Lagos-Quintana M.*, Liu D., Shi Y., Helker C., Herzog W., le Noble F. (2013). miR-30a regulates endothelial tip cell formation and arteriolar branching. *Hypertension* 62(3):592-598.

Jiang Q.*, Liu D.*, Sun S., Hu J., Tan L., Wang Y., et al. (2010). Critical role of connexin43 in zebrafish late primitive and definitive hematopoiesis. *Fish Physiol Biochem* 36(4):945-951.

Jiang Q.*, Liu D.*, Gong Y., Wang Y., Sun S., Gui Y., et al. (2009). yap is required for the development of brain, eyes, and neural crest in zebrafish. *Biochem Biophys Res Commun* 384 (1): 114-119.

Sun S., Gui Y., **Jiang Q.**, Song H. (2012). Dihydrofolate reductase is required for the development of heart and outflow tract in zebrafish. *Acta Biochim Biophys Sin (Shanghai)* 43(12):957-969.

Chen H., Hu J., Yang J., Wang Y., Xu H., **Jiang Q.**, et al. (2010). Generation of a fluorescent transgenic zebrafish for detection of environmental estrogens. *Aquat Toxicol* 96(1):53-61.

Xu H., Yang J., Wang Y., **Jiang Q.**, Chen H., and Song H. (2008). Exposure to 17alpha-ethynylestradiol impairs reproductive functions of both male and female zebrafish (Danio rerio). *Aquat Toxicol* 88:1-8.

Wang Y., Qian L., Liu D., Yao L., **Jiang Q.**, Yu Z., et al. (2007). Bone morphogenetic protein-2 acts upstream of myocyte-specific enhancer factor 2a to control embryonic cardiac contractility. *Cardiovasc Res* 74:290-303.

Wang Y., Qian L., Dong Y., **Jiang Q.**, Gui Y., Zhong T., et al. (2006). Myocyte-specific enhancer factor 2A is essential for zebrafish posterior somite development. *Mech Dev* 123:783-791.

Zhang L., Zhong T., Wang Y., **Jiang Q.**, Song H., and Gui Y. (2006). TBX1, a DiGeorge syndrome candidate gene, is inhibited by retinoic acid. *Int J Dev Biol* 50:55-61.

Wang Y., Zhong T., Qian L., Dong Y., **Jiang Q.**, Tan L., et al. (2005). Wortmannin induces zebrafish cardia bifida through a mechanism independent of phosphoinositide 3-kinase and myosin light chain kinase. *Biochem Biophys Res Commun* 331 (1): 303-308.

Wang Y., Qian L., Yu Z., **Jiang Q.**, Dong Y., Liu X., et al. (2005). Requirements of myocyte-specific enhancer factor 2A in zebrafish cardiac contractility. *Febs Letters* 579 (21): 4843-4850.

* Equal contribution